

where z_2 and z_1 are the liquid levels on the inside and outside respectively, referred to some arbitrary point. The difference in the vacuum capacitance, and the (small) vertical offset, are contained in the factor $\Delta C(0)$, which is the capacitance difference measured while the outside and inside are in equilibrium.

The vapor inside the capacitor was assumed to be at the temperature of the liquid. This was obviously true for the inside capacitor, and was assured for the outside capacitor by placing it inside a copper tube whose lower end was immersed in the liquid. Any residual radiation leak to the capacitor could be absorbed by the high conductivity of the superfluid helium film.

The capacitance difference was measured directly by the use of the system shown in Fig. 9, which incorporates the use of a commercial capacitance bridge of the ratio-transformer type. The outside capacitor was connected to the "unknown" ports of the bridge, and the inside capacitor was connected to the "external standard" ports of the bridge. With the appropriate settings, the indicated capacitance at balance is equal to the difference of these two capacitors.

In order to maintain a fixed level difference between the inside and the outside, the desired capacitance difference was set on the bridge, then the corresponding level difference was approximated by manual adjustment of the vertical level of the vacuum can, and then the level control feedback system indicated in Fig. 9 was activated. The signal conditioner produced a signal derived from the error signal and its time integral. This was combined with a large manually controlled offset signal to form the velocity command for the motor-controller system. A digital volt-meter at this point served to monitor the vertical speed of the vacuum can. A gain-of-one amplifier (not shown) was used to float the velocity command voltage so as to meet the input requirement of the motor-controller. When running smoothly, the system was capable of maintaining a set capacitance difference within 30-50 ppm. The main trouble encountered was rough movement in the pulley used to counterbalance the weight of the moving system. It was quite obvious when the system became stuck, and so the data could be retaken.

The configuration of Fig. 9 was altered slightly for the equilibrium data points. First, as mentioned earlier, the inside heater was turned off, then the controls on the bridge changed so that the off-balance signal was determined by the difference of C_0 from a set value, and then the control system was activated. This had the effect of maintaining the outside level fixed relative to the vacuum can. When transients had died away, this allowed measurement of several parameters with the inside and outside at complete equilibrium, i.e., no mass or heat flow, no temperature or pressure difference. As mentioned earlier, the temperatures were recorded as a check on their stability. Also measured was the small downward velocity necessary to maintain a fixed outside level, because this allowed determination of the evaporation rate of the outside He bath. Then the velocity was fixed at this value, and the bridge controls changed back so that $\Delta C(0)$ could be measured.

The dielectric constants were at first computed from the Clausius-Mossotti equation and polarizability found in NBS Technical Note 631 [26], the liquid densities taken from

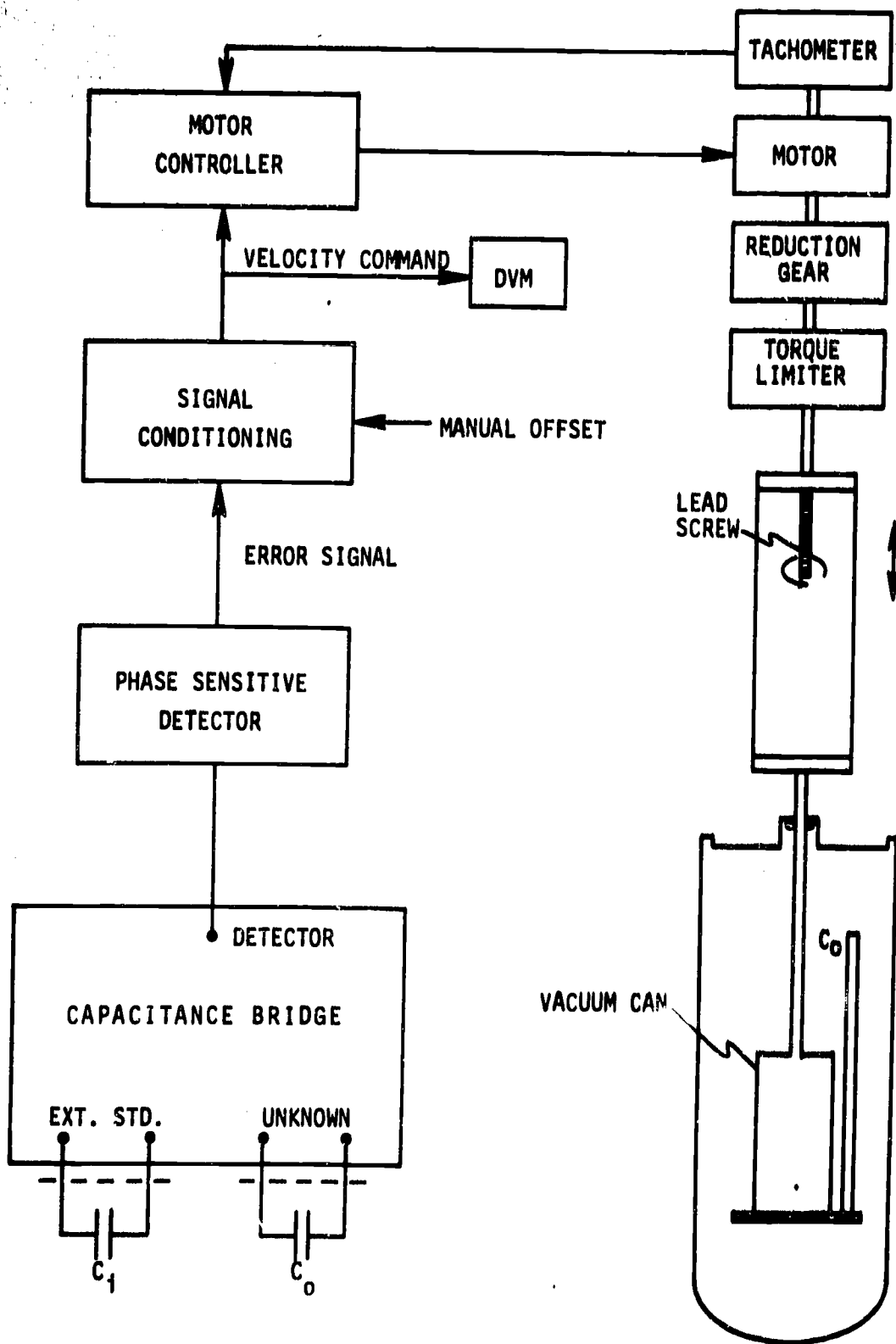


Figure 9. A schematic drawing of the system used to maintain a constant difference between the inside and outside levels.

the text of Donnelly [7], and the vapor densities from the ideal gas equation of state. They could also be derived from full vs. empty measurements, which were found not to agree with the calculations. The reason was found to be inconsistent units in the Clausius-Mossotti equation as found in the above reference, which had the effect of making the polarizability too small by a factor of $4\pi/3M \approx 1.047$ (M = molecular weight). With this correction, the agreement was excellent between the calculated value of ϵ at 1.92 K of 1.05736 and the measured value of 1.05740. It was found that while the values of ϵ and ϵ' varied significantly with temperature, their difference was constant to within a part per thousand over our temperature range. Therefore, the calculated value of $\epsilon - \epsilon' = 0.05714$, appropriate for the highest temperature, where other results depend most sensitively on its value, was used for all temperatures. C_v/ℓ was taken to be 0.5599 pF/cm, the average of the values measured for the two capacitors. Combining all these factors leads to the expression for $z_2 - z_1$ actually used in equation (21),

$$z_2 - z_1 = -31.27 \frac{\text{cm}}{\text{pF}} \left(\Delta C(z_2 - z_1) - \Delta C(0) \right) \quad (25)$$

where $\Delta C(0)$ was slightly different for the different temperatures.

This single simple calibration served for the entire long run, because the capacitors proved to have excellent stability and linearity, as determined by the regular measurement of $\Delta C(0)$. By varying the point at which the outside level was fixed during an equilibrium point, the two capacitors could be compared with each other over a significant fraction of their lengths. It was desirable to keep equilibration times short, so that equilibrium points were taken only where the inside level was still in the narrow section, thus limiting the comparison to the lower 2/3 of the inside capacitor and the lower 1/3 of the outside capacitor. Within this range, $\Delta C(0)$ was found to be essentially independent of height and time. Expressed as a height difference, via equation (25), the standard deviation of $\Delta C(0)$ for all the equilibrium points was 0.01 cm. It is thought that the good stability and linearity of the capacitors is due in part to several design features arrived at by trial and error. They are: (1) a mounting for the inside tube that allows some small axial movement, which prevents compression and bowing of this long slender column, and (2) the rather wide gap, whose proportions appear to be about the optimum compromise between sensitivity to level change and insensitivity to dimensional errors, particularly lack of coaxiality.

A remark should be made about the limitations that the experimental method placed on the pressure difference measurements. They are due to the vapor pressure difference caused by the temperature difference between the inside helium vessel and outside bath [the first term in eq (21)]. If this term was large, then the liquid level difference had to be large and of opposite sign for those flow regimes in which the total pressure difference was small (essentially flows for which V was small). For an extreme example, at $T = 1.92$ K with $\Delta T = 0.047$ K and $V = 0$, the inside level z_2 was 25 cm below the outside level, z_1 .

3.5 Mass Flow Rate

The volumetric flow rate through the flow tube was determined from the geometry of the apparatus and from the vertical speed of the vacuum can that was necessary to maintain a fixed level difference between the inside and the outside helium spaces.

The functional relation between these quantities was determined by application of the mass conservation relation to the geometry sketched in Fig. 10. The upward velocities of the outside liquid surface, the inside liquid surface, and the vacuum can (all with respect to some fixed point in the laboratory), are designated by V_o , V_i and V_b respectively. The areas of the inside liquid surface, the outside liquid surface, and the dewar are designated as A_i , A_o and A_d .

The small amounts of mass entering or leaving the vapor phase can be ignored, so that mass conservation can be expressed in terms of the liquid volumes as

$$\begin{aligned} &\text{volume added outside} + \text{volume added inside} \\ &+ \text{volume evaporated} = 0 \end{aligned}$$

During the small time interval dt , the volume added inside is $(V_i - V_b)A_i dt$. If we designate $V_e (< 0)$ as the velocity of the vacuum can during an equilibrium data point, and assume that the evaporation rate is not time dependent, then the volume evaporated in time dt is $-V_e A_d dt$. (The correct area is A_d and not A_o because the volume displaced by the vacuum can remains constant during the equilibrium point.) The volume added outside has two contributions: the added volume on the surface area of $V_o A_o dt$, and the volume that has been vacated by the movement of the can $= V_b(A_d - A_o)dt$. The result is

$$V_o A_o + V_b(A_d - A_o) + (V_i - V_b)A_i - V_e A_d = 0 \quad (26)$$

But under the conditions of the experiment, the level difference between the inside and the outside remains constant, therefore

$$V_i = V_o \quad (27)$$

The average velocity of net fluid flow through the flow tube (V) is expressed as

$$V = (V_i - V_b)A_i / A_x \quad (28)$$

where A_x is the cross-sectional area of the tube. Combining the above equations gives

$$V = - \frac{A_i A_d}{A_x (A_o + A_i)} (V_b - V_e) \quad (29)$$

As defined, V is positive for flow toward the inside.

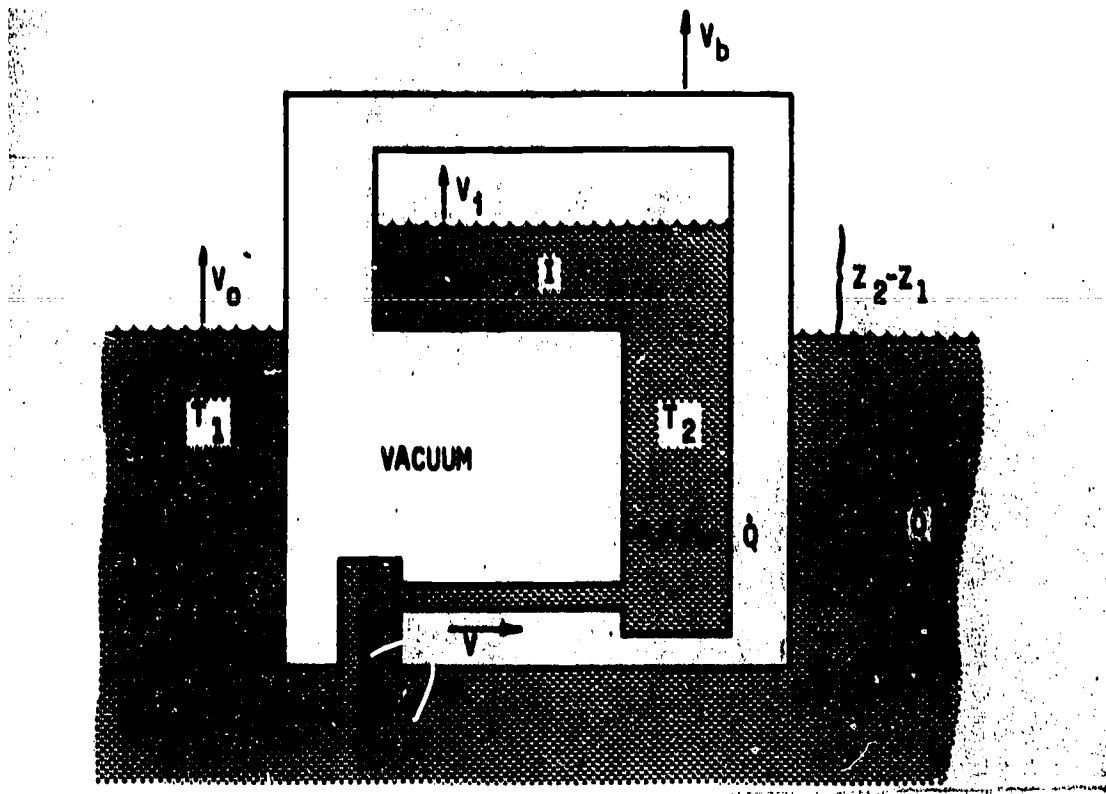


Figure 10. A schematic diagram of the main variables of the experiment.

In order to cover a wider range in flow rates, the inside helium space was constructed with a wide cross-section for the top one-third of the inside capacitor, and a narrow cross-section for the bottom two-thirds. In order to allow large level differences for inflow it was often necessary to have the outside level well above the top of the wide section of the inside space, hence well above the top of the vacuum can. In all then, there were four different combinations of inside and outside surface areas for which data could be taken; the parameters, and the "mode" identification numbers used on the data sheets, are listed in Table 1.

3. (i) The Flow Tube

The flow tube used in this experiment was a commercial quality stainless steel tube with an o.d. = 0.160 cm, and an i.d. determined to be 0.1149 ± 0.0006 cm. It had a length (l.) of 60 cm and was wound in two turns of 10 cm diameter. The inside end was mounted about 3.5 cm above the outside end. The ends were cut off square.

The inside diameter was determined by room temperature gas flow measurements performed after the experiment, but while the tube was undisturbed in its mounting on the apparatus. The results seemed inconsistent until it was realized that, in laminar flow, even the rather small curvature of the tube could have large effects on the gas flow. Helium gas and nitrogen gas were used to cover a range in Reynolds' number (Re) from 55 to 1930. The volumetric flow rate of gas was measured by a wet test meter whose calibration against a bell prover had a standard deviation of 0.6%. The pressure drop (ΔP) across the flow tube was measured by the commercial capacitance manometer used in the experiment. The volumetric flow rate was multiplied by the factor $(1 - P_s/P_0)$ to correct for the water vapor added by the wet test meter (where P_0 is the ambient pressure, and P_s is the vapor pressure of water at the ambient temperature). The ideal gas equation of state was used, the temperature taken to be ambient, and the density of the gas taken to be the mean of the values calculated for the ends of the tube. The fractional pressure drop never exceeded 0.18. Thus we obtain the equivalent volumetric flow rate Ω of dry gas.

The data were analyzed by using the laminar flow equation for a straight tube applied to the lowest Re data to deduce a diameter D . This was then used to calculate the (Fanning) friction factor f as a function of Re . The equations used were

$$f = \frac{\pi^2}{32} \frac{D^5}{\Omega^2} \frac{\Delta P}{L} \left(1 + \frac{\Delta P}{2P_0} \right) \quad (30)$$

$$Re = \frac{4P_0\Omega}{\pi D\eta}$$

where P_0 is the mass density of dry gas at ambient temperature and pressure. The viscosity η was taken from [26] and [27]. We have plotted in Fig. 11 the experimental friction factor divided by the expected values for a straight tube in laminar flow; the solid line

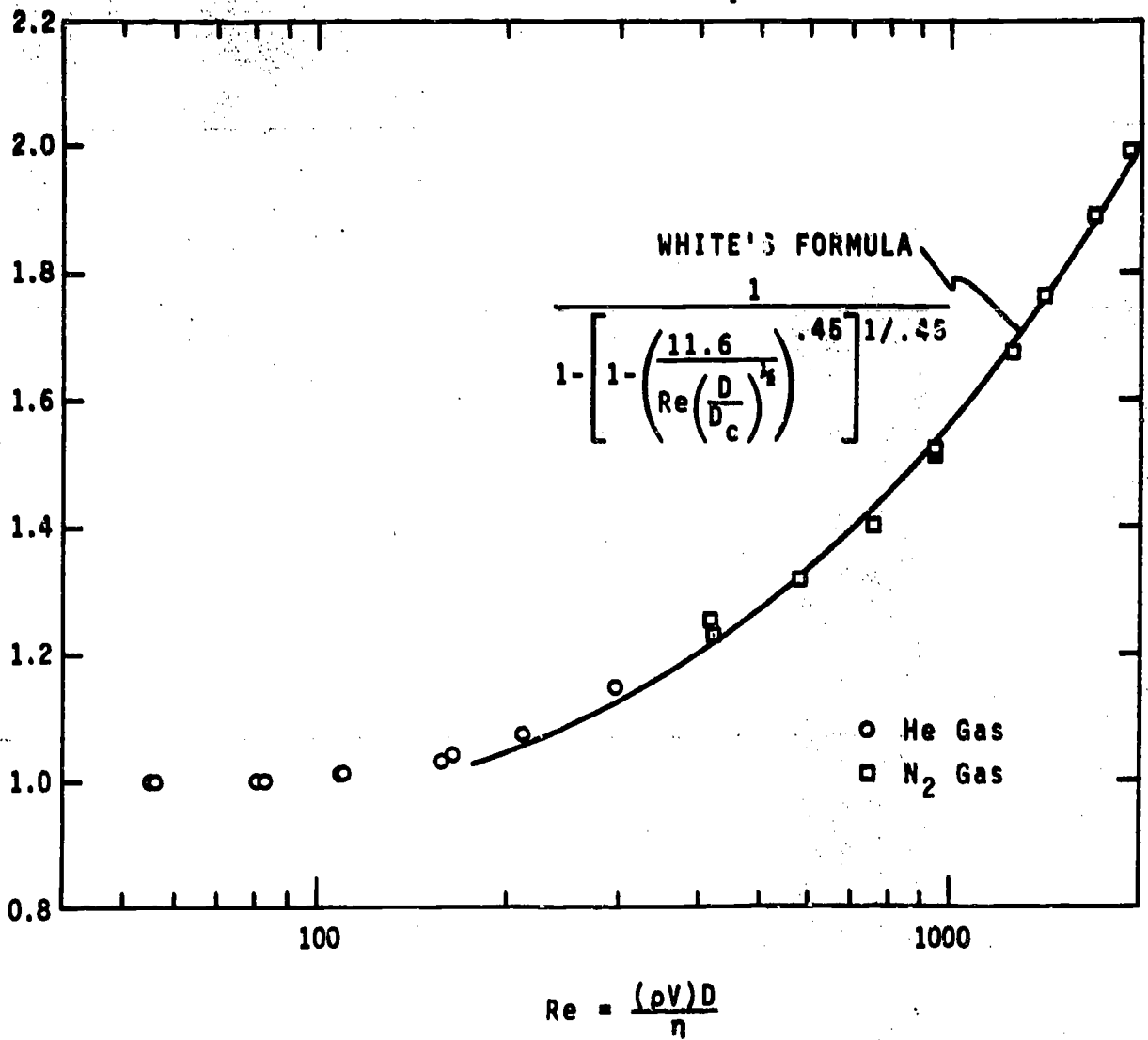


Figure 11. The results of the room temperature gas flow measurements on the flow tube.

Table 1.

	Mode Number	Inside Interface Location	
		Narrow	Wide
Outside Interface Location	Vacuum Can	1	3
	Support Tube	2	4
	A_1 (narrow)	=	4.96 cm^2
	A_1 (wide)	=	78.4 cm^2
	A_0 (VC)	=	$A_{\text{dewar}} - 105.2 \text{ cm}^2$
	A_0 (ST)	=	$A_{\text{dewar}} - 2.8 \text{ cm}^2$
	A_{dewar}	=	219.4 cm^2

is the formula of White [28] for curved tubes calculated for our diameter of curvature D_c . The good agreement makes us confident that the correct value of the diameter has been found. The principle uncertainty in its measurement is the uncertainty in the volumetric flow measurement and its corrections. The deviations from the calculated values over the entire range of the measurement indicate a standard deviation for D of about 0.3%.

Precautions were taken to prevent or reduce any effects on the flow due to the presence of frozen air. The first was the protected location of the outside end of the flow tube; it was in a chamber which was recessed about one inch into the bottom of the base plate (see Fig. 7.). Such a location appears inaccessible to condensing air or falling air particles. Of course, only helium gas was allowed to be present in the dewar during the cooldown. Another precaution was the addition of a filter (which used ordinary chemical filter paper) onto the transfer line used to fill the helium dewar, in an effort to reduce buildup of frozen air during the long run.

The only problem which could not be definitely eliminated was a cumulative buildup of those particles small enough to remain in suspension in the liquid helium; they might be expected to accumulate from air introduced during the insertion of the transfer tube, etc. There was no way to measure their concentration, nor are we aware of any data on the sizes of particles that might be expected to remain in suspension. However, the lack of any significant cumulative shifts in data points that were repeated during the 35-day run, we take to be good evidence that suspended solid particles were not a significant problem. See, for example, the good reproducibility ($\sim 1\%$) of the $T = 1.39$, $\Delta T = 0.019$ data taken at the very beginning and end of the long run (e.g., data points 9 422 and 10 515).

That evidence is reinforced by a mishap that took place early on October 1. A technician working nearby accidentally knocked off a large rubber vacuum hose used to pump on the helium dewar. At the time, the liquid helium was probably warm enough to be at a vapor pressure above atmospheric pressure, but still, in the 30-60 seconds it took him to replace the hose, we would guess that more air should have been introduced than during all the previous activities. Again, no significant changes in the repeated data can be seen following that date.

3.7 The Energy Flow Measurement

The inside helium vessel and the flow tube were surrounded by an insulating vacuum. Thus the energy flow through the tube could be determined from an energy balance calculation. The essential elements of the situation are shown in Fig. 10. The unusual feature of this calculation turns out to be the large influence of the vapor that is present.

The energy balance is done in two parts; first we calculate the change in total energy of the helium in the inside vessel (the control volume) from thermodynamics applied to a small change in its mass. The conditions of the change are that the temperature, and hence the vapor pressure, remain fixed and that the total volume is fixed, even though the total mass is changing. Designating the specific volumes of the liquid and vapor as v and v' (not to be confused with the velocities v_n , v_s , V), and the specific internal energies as u and u' , we find that the increases of total mass M , of total volume, and of total energy U are given by

$$\begin{aligned}
 dM &= dm + dm' \\
 d(\text{Vol})|_{T,P} &= v \, dm + v' \, dm' = 0 \\
 dU|_{T,P,\text{Vol}} &= u \, dm + u' \, dm' \qquad (31)
 \end{aligned}$$

where dm and dm' are the increases in the liquid and vapor masses. Combining these equations gives

$$dU|_{T,P,\text{Vol}} = \frac{v'u - vu'}{v' - v} dM \qquad (32)$$

We can use the definition of the chemical potential, eq (16), and the well known fact that the chemical potentials of the liquid and vapor are equal in equilibrium, to find that

$$u' = u - P(v' - v) + T(s' - s) \quad (33)$$

Substituting into the previous equation and using the Clausius-Clapeyron equation for the slope of the vapor pressure curve $\left(\frac{\partial P}{\partial T}\right)_{svp}$ and the definition of dM in terms of the tube cross-section and the average velocity

$$dM = \rho V A_x dt \quad (34)$$

we find

$$dU|_{T,P,V_01} = [\rho v h - VT \left(\frac{\partial P}{\partial T}\right)_{svp}] A_x dt \quad (35)$$

In the second part of the energy balance calculation we express dU in terms of the external sources of energy, i.e., in terms of the energy that flows through the boundaries of the control volume. They are the heating rate \dot{Q} of the internal heater and the energy flux $j_U A_x dt$ that enters through the flow tube. As discussed in section 2, this energy flux can be expressed in terms of the enthalpy flux and the heat current \dot{q} , using equations (18b) and (19). Equating this to the previous equation gives

$$\dot{Q} + (\rho v h + \dot{q})_{ent} A_x = [\rho v h_2 - VT_2 \left(\frac{\partial P}{\partial T}\right)_{svp,T_2}] A_x \quad (36)$$

The energy flux on the left hand side is to be evaluated at the entrance of the flow tube to the inside helium vessel. The energy change on the right hand side is to be evaluated at the temperature and pressure that prevail within the inside vessel, whose values are indicated by the subscript 2. Let us define the heat flux density \dot{q}_2 by

$$\dot{q}_2 = - \frac{\dot{Q}}{A_x} - VT_2 \left(\frac{\partial P}{\partial T}\right)_{svp,T_2} \quad (37)$$

If the temperature and pressure are essentially continuous at the entrance, which we expect to be true in most cases, we have $h_{ent} = h_2$, and so $\dot{q}_{ent} = \dot{q}_2$. In any case, by application of eq. (20), we can find $\dot{q}(x)$ at some location x , if we know \dot{q}_2 and the temperature and pressure at x . For our case the relation is

$$\dot{q}(x) = \dot{q}_2 + \rho v (h_2 - h(x)) \quad (38)$$

We shall quote all our results for the energy transport as values of \dot{q}_2 . As defined, the

sign convention of \dot{q}_2 is consistent with the one for V [eq. (29)], so that heat flow away from the (higher temperature) inside vessel has a negative sign.

The second term of eq (37) is readily interpreted as the heat of condensation (or evaporation) that must be absorbed by the liquid in order to change the volume of vapor. Its presence is due to the particular configuration used to perform the experiment. At the higher temperatures of this experiment, it becomes nearly as large as \dot{Q}/A_x for the larger values of V , and thus its presence causes a significant deterioration in the measurement accuracy of \dot{q}_2 . It is the quantity \dot{q}_2 that is most significant (not \dot{Q}/A_x) because it is the quantity to be compared to the \dot{Q}/A_x of section 2.

This heat of condensation also introduced an extra limitation in the range of velocities for which data could be taken. For fixed ΔT , it was often found that for inflow ($V > 0$), when this term acts like an extra heat source, that its magnitude increased more rapidly with V than the heat conducted out (\dot{q}_2). Therefore, it was not possible for eq (37) to be satisfied with positive values of \dot{Q} if V was greater than some particular value. When encountered, this limiting value of V is indicated on the graphs of \dot{q}_2 vs. V (figs. 22-25) by a vertical bar.

We have neglected the kinetic energy terms in the total energy balance because they can be shown to be quite small for all the conditions encountered in this experiment. We have also left out gravitational potential energy terms, because a careful accounting of them found that they just cancelled the work done on the fluid by the movement of the container. In Appendix 2, we rederive eq (36) with a full accounting of potential energy terms and the work done on the fluid in raising or lowering the vessel.

3.8 Extraneous Heat Flows

The energy balance equations that have been given for determining the heat flow are correct only if we have accounted for all the energy exchanges, i.e., only if there are no extraneous heat flows between the inside and the outside helium vessels. Below are explained the precautions taken and the tests made to ensure that these extraneous heat flows were small.

The poor thermal conductivity of the stainless steel walls of the vacuum can dictated that it be surrounded by a heat shield, HS of Fig. 5. This took the form of a thin (0.04 cm) copper sheet fitted to surround the sides and top of the vacuum can. Its lower end was always immersed in the liquid, and its upper end was soldered to the support tube ~ 10 cm above the top of the vacuum can, thus intercepting the heat conducted down the support tube. On the inside of the support tube, the lower 10 cm was stuffed with coarse brass wool to act as a radiation shield.

The inside helium space was supported by three long, thin-wall stainless steel legs that attached to the bottom (or base plate) of the vacuum can. The rather close fit suggested the precaution of mounting three sharpened nylon screws on the legs just below the wide section of the inside space; they could be extended so as to maintain a fixed spacing between the inside space and the vacuum can. All electrical leads that went to the inside

space were first thermally "tempered" to the base-plate and were of low thermal conductivity wire.

It was not practical to maintain a good vacuum at all times in the vacuum space, because this prevented the inside helium space from ever cooling down enough to fill with liquid. Therefore the inside space was filled before cool-down with hydrogen gas at a pressure of a few Torr.* This acted as a thermal exchange gas, as long as the vacuum can remained above ~ 10 K. Once the vacuum can was cooled below ~ 3 K, the hydrogen gas was frozen to the walls or adsorbed onto about 3 cm^3 of "molecular sieve" that was present. After the first transfer was completed and the vacuum gauge outgassed, the seals were checked by monitoring the vacuum space for several hours with a He leak detector; it was checked again several days later. The vacuum was monitored throughout the long run by a Phillips-type vacuum gauge mounted on the top of the support tube. It registered $2-5 \times 10^{-5}$ Torr during data taking, except for jumps of an order of magnitude (which lasted 1-2 minutes) that were caused by the sudden withdrawals of a good fraction of the vacuum can from the liquid; this was almost certainly due to slight desorption of hydrogen from the suddenly warmer walls.

The thermal isolation was checked directly at the beginning of the run by measuring the total thermal conductance between the inside and the outside at temperatures above the lambda point. This was done by maintaining a fixed outside temperature $T_2 = 2.31$ K, providing a small heat input with the inside heater, and waiting 1-2 hours for the temperature to equilibrate at a value 0.5-1.5 K higher than the outside temperature. The vacuum can was completely immersed for these measurements, but the higher temperature of the inside prevented liquid from entering. (It was found that this type of test can be very misleading if there exist any pockets on the inside that can trap liquid; the relatively large latent heat of the liquid that is being evaporated on the inside and condensed on the outside can cause a large and long-lived false conductivity).

Assuming that the thermal conductance linking the inside and the outside is temperature independent, the three data points that were taken yielded a value for the thermal conductance of 1.5×10^{-3} W/K. This value is about 1 1/2 orders of magnitude larger than was calculated for conduction through the legs, electrical leads, etc. It was found that conduction through the low pressure hydrogen gas could account for the conductance, if the indicated pressures at the Phillips gauge were taken at face value. Still, this value for the conductance was low enough so that we could choose to ignore the unexpected persistence of unchanged indicated pressures ($2 - 5 \times 10^{-5}$ Torr) at the lower temperatures, where the calculated vapor pressure of hydrogen should be considerably smaller.

These same measurements indicated that a heat input of 2×10^{-4} W remained at $\Delta T = 0$. This could represent a real heat leak (e.g., incomplete radiation shielding), or it could reflect a small temperature dependence in the thermal conductivity. This heat leak, if real, would require that all values of \dot{q}_2 be corrected by the addition of -0.019 W/cm^2 . Since data could not be taken at low enough ΔT 's to distinguish between the two alternatives, we have not made this correction to the data, and instead view this as an upper limit to the possible systematic error in \dot{q}_2 .

*1.0 Torr - 133.3 Pa.

3.9 Error Estimates

The errors of this data are not always as small, nor as accurately known, as might be wished, primarily because of the exploratory nature of the experiment. The method was new, the results could be only crudely anticipated, and it seemed more desirable to emphasize a broad range for the measurements rather than concentrate on their accuracy. Given these conditions, they seem satisfactory. The errors for quantities given in Appendix 1 vary, depending on the conditions, and are summarized in Table 2.

A part of the random error in the temperature and pressure difference measurements could be evaluated quite reliably from the variation of the equilibrium point data. This variation should include the effect of electronic noise, intrinsic sensor resolution, drift in the sensor characteristics, and inaccuracies in the data reduction. Including all the equilibrium point data, we find that the temperature difference had a standard deviation of $(4, 3, 2, \text{ and } 4) \times 10^{-5}$ K at the four temperatures of 2.10, 1.92, 1.65 and 1.39 K respectively. The standard deviations for the height difference were 0.016, 0.012, 0.009 and 0.011 cm respectively. Through eq (21), these figures imply a standard deviation for the pressure difference of 0.4, 0.2, 0.1 and 0.1 Pa respectively.

For the regular data points there may exist an extra source of random error that is not included in the figures given above; it is the fluctuations that might be introduced by the control systems that are used to maintain a "constant" temperature and pressure difference. The short term fluctuations in the altitude and temperature differences (time constants of a few seconds) were judged by the error signals of the feedback systems to be rarely more than 0.02 cm and 0.0001 K. However, because it is the time-average values that count, it is the longer term fluctuations (the drift during the 3-5 minutes it took to record the data) that determine the real error. For the altitude difference, we estimate that this source of error was negligible. Unfortunately, the temperature sensors of the control system (but not the temperature measuring system) were found to drift. On bad days, these drifts caused progressive shifts in the measured ΔT of 2-3% over the course of the day. In the worst cases, the rate of drift suggests that ΔT should change by an amount somewhat less than the errors given above. Somewhat arbitrarily then, we increase the error estimates of ΔT by 50%. Our final estimate of the random error (one standard deviation) in ΔT is $(6, 4, 3 \text{ and } 6) \times 10^{-5}$ K, and in ΔP is 0.6, 0.3, 0.2 and 0.1 Pa, respectively, for the four mean temperatures.

The systematic error in temperature difference is determined by the systematic error in the pressure measurement during calibration as discussed below. This leads to a systematic error in temperature difference of between 0.5% and 0.7%.

The pressure difference is subject to systematic error, due to uncertainties in the capacitance-to-altitude conversion. Estimated at 2 parts per thousand, it implies a possible systematic error of $\sim 2.8 \times 10^{-2} \times (z_2 - z_1)$ Pa, where z is expressed in centimeters. This error becomes significant only for the large ΔT , small V , data at the higher temperatures.

The errors in the mean temperature are determined by the errors in the vapor pressure measurements used to calibrate the thermometers. We could evaluate the random errors in

Table 2. Estimated Errors

Random Error (1σ)

Systematic Error

Measured Quantity (Units)	Temperature			
	2.100	1.919	1.650	1.395
T (K)	0.2 mK	0.2 mK	0.3 mK	0.4 mK
	1.1 mK	1.1 mK	1.1 mK	0.8 mK
ΔT (K)	0.06 mK	0.04 mK	0.03 mK	0.06 mK
	0.005 ΔT	0.006 ΔT	0.006 ΔT	0.007 ΔT
Δz (cm)	0.01 cm	0.01 cm	0.01 cm	0.01 cm
	0.002 Δz (cm)	0.002 Δz	0.002 Δz	0.002 Δz
ΔP (Pa)	0.6 Pa	0.3 Pa	0.2 Pa	0.1 Pa
	0.03 Δz (cm)	0.03 Δz	0.03 Δz	0.03 Δz
V (cm/s)	0.02 V	0.02 V	0.02 V	0.02 V
	0.02 V	0.02 V	0.02 V	0.02 V
\dot{q}_2 (W/cm ²)	0.01($\dot{q}_2+0.047$ V)	0.01($\dot{q}_2+0.030$ V)	0.01($\dot{q}_2+0.013$ V)	0.01($\dot{q}_2+0.004$ V)
	0.01($\dot{q}_2+0.047$ V)	0.01($\dot{q}_2+0.030$ V)	0.01($\dot{q}_2+0.013$ V)	0.01($\dot{q}_2+0.004$ V)

the calibrations at 1.92 and 1.39 K, from the standard deviations for data taken on several different occasions; they were 0.2 and 0.4 mK respectively. A few simple tests indicated that systematic errors due to placement of the pressure probe could not be too much larger than this. The absolute calibration of the pressure gauge could not be confirmed in the region of interest; if we take the manufacturer's estimate and increase it by a factor of three, we arrive at a systematic error in pressure of about 0.3%. This implies a systematic error of about 1 mK in mean temperature on the T_{58} scale.

The random error in V is determined from the standard deviation in the voltage-to-speed conversion (1.5%), the estimated accuracy to which the voltage fluctuations could be averaged by eye, (1%), and the non-uniformity in the geometry (1%). Combined in quadrature, this gives a random error of 2%. An estimate of the error in geometry suggests that each mode might have a systematic error as large as 2% of V .

The relative error in \dot{q}_2 (both random and systematic) depended rather strongly on the conditions of the measurement, because of the sometime large value for the vapor's latent heat correction (second term of eq (37)). Assuming an error in V of 2%, we find that the error in \dot{q}_2 is given by αV (V in cm/s), where α has the values of (4.8, 3.0, 1.3 and 0.4) $\times 10^{-4}$ W/cm² for the temperatures of 2.10, 1.92, 1.65 and 1.39 K respectively. At the most extreme value of V (70 cm/s), this corresponds to errors of 0.033, 0.020, 0.009 and 0.003 W/cm². When V is small, and \dot{q}_2 is large, this error is not too significant, and we must include the estimated random and systematic errors of the first term in eq (37) of 1% and 1% respectively.

4. RESULTS AND DISCUSSION

Data were collected at four values of the mean of the outside and the inside temperature. Using the formulas given in section 3, each data point was reduced to give values for the actual pressure and temperature differences between the ends of the flow tube and the resulting steady state values for the net fluid velocity V and the heat flux density \dot{q}_2 . These results are presented in tabular form in Appendix 1, along with some other data and derived quantities of interest.

4.1 The Net Fluid Velocity

Nearly all the results for the net fluid velocity V (the actual mass flow rate divided by the total density and the flow tube cross-sectional area) are shown in Figs. 12-15. The absolute values of V have been graphed there as a function of the absolute value of the pressure difference, so that data for both directions of flow are superimposed. The value of the nominal temperature difference is indicated by the symbols; the measured temperature differences may differ from the nominal by as much as 3%, due to the drifts discussed earlier.

More than half of the results might be summarized in a very simple statement: they are largely indistinguishable from those of an ordinary fluid in fully developed turbulent flow. This statement applies for those flows at the larger velocities or Reynolds numbers, which are the ones most likely to be of interest for applications.

These graphs of $|\Delta P|$ vs $|V|$ reveal quite distinctly one of the important results of this experiment: V depends primarily on ΔP -- its dependence on ΔT is significant only at the lower velocities. This result is only to be expected for an ordinary (single-phase) fluid, because the temperature gradient does not appear in the equation of motion of the fluid (we are excluding indirect effects due to buoyancy forces). In contrast, the temperature gradient appears explicitly in the (simple) superfluid equation of motion, eq (6), as part of the chemical potential gradient. Even though that simple equation for v_s is not expected to remain valid for our conditions, it suggests the possibility that v_s might be a function mainly of $\Delta\mu$; this would make V also a function of $\Delta\mu$, at least if ρ_s/ρ is not too small. This possibility is completely excluded (for our conditions) by the weak dependence of V on ΔT . To make a numerical comparison, we can use the expression

$$\rho\Delta\mu = \Delta P - \rho s\Delta T$$

which we have included in the data listing in Appendix 1. We find that under most conditions, the temperature difference dominates the chemical potential difference, and that neither one has much influence on the net mass flow. As a typical example, we can examine the data for $T = 1.92$, $\Delta T = 0.019$; not until ΔP is about 50 times smaller than $\rho s\Delta T$ (~ 2150 Pa) do we see much effect of the latter on V .

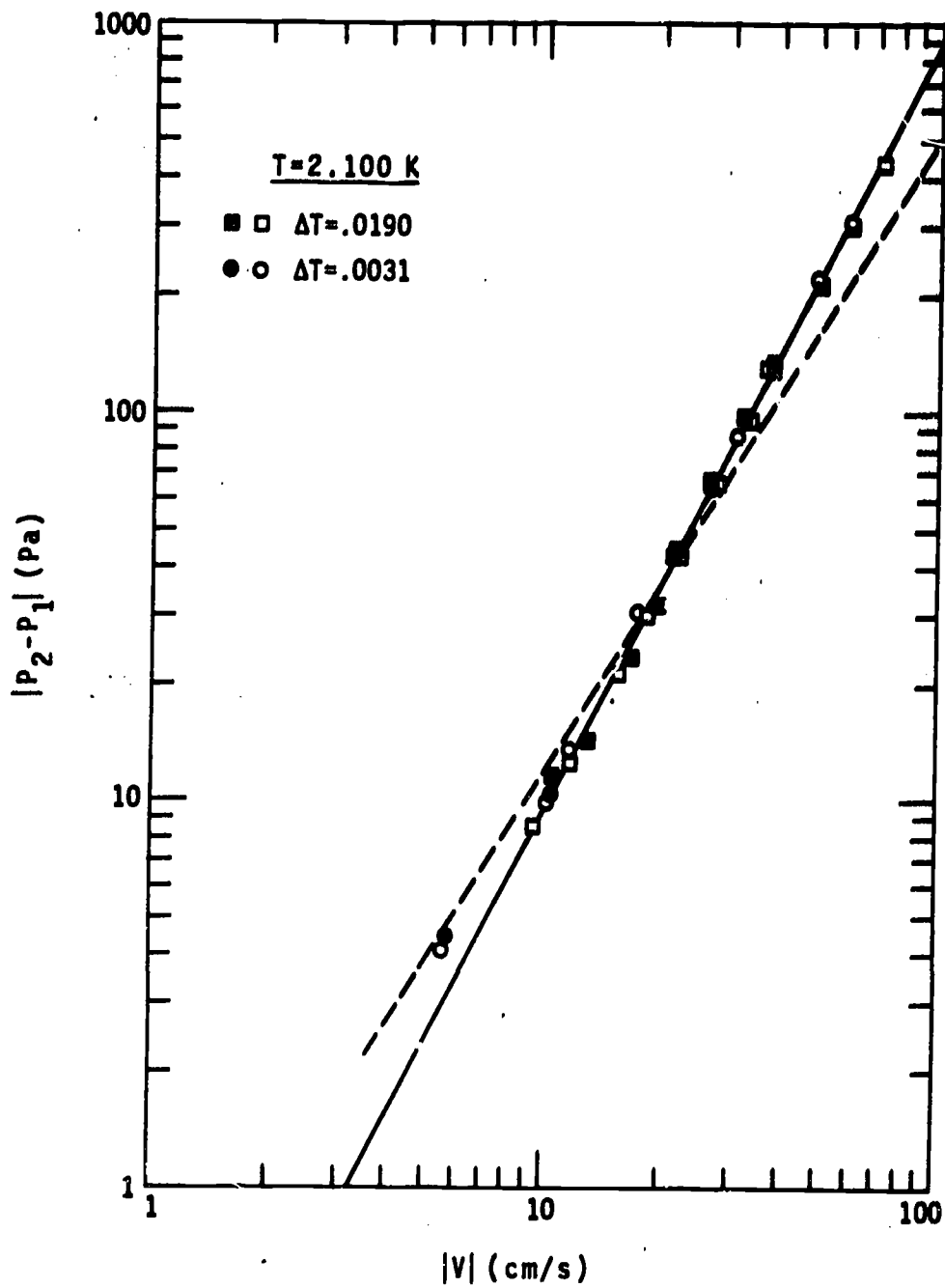


Figure 12. The pressure difference vs the net fluid velocity at 2.100 K. The dashed [solid] line is eq (41) [(42)].

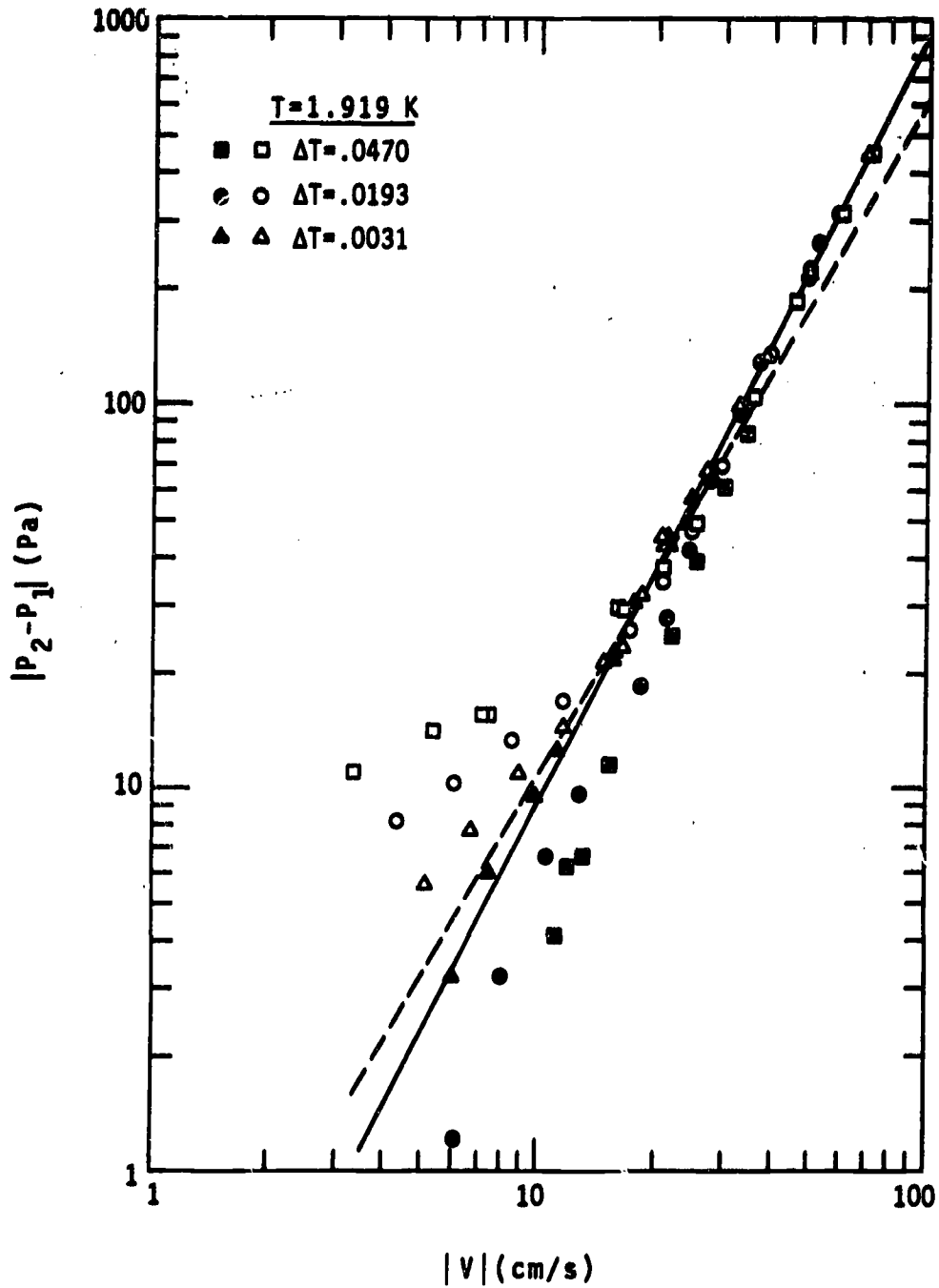


Figure 13. The pressure difference vs the net fluid velocity at 1.919 K. The dashed [solid] line is eq (41) [(42)].

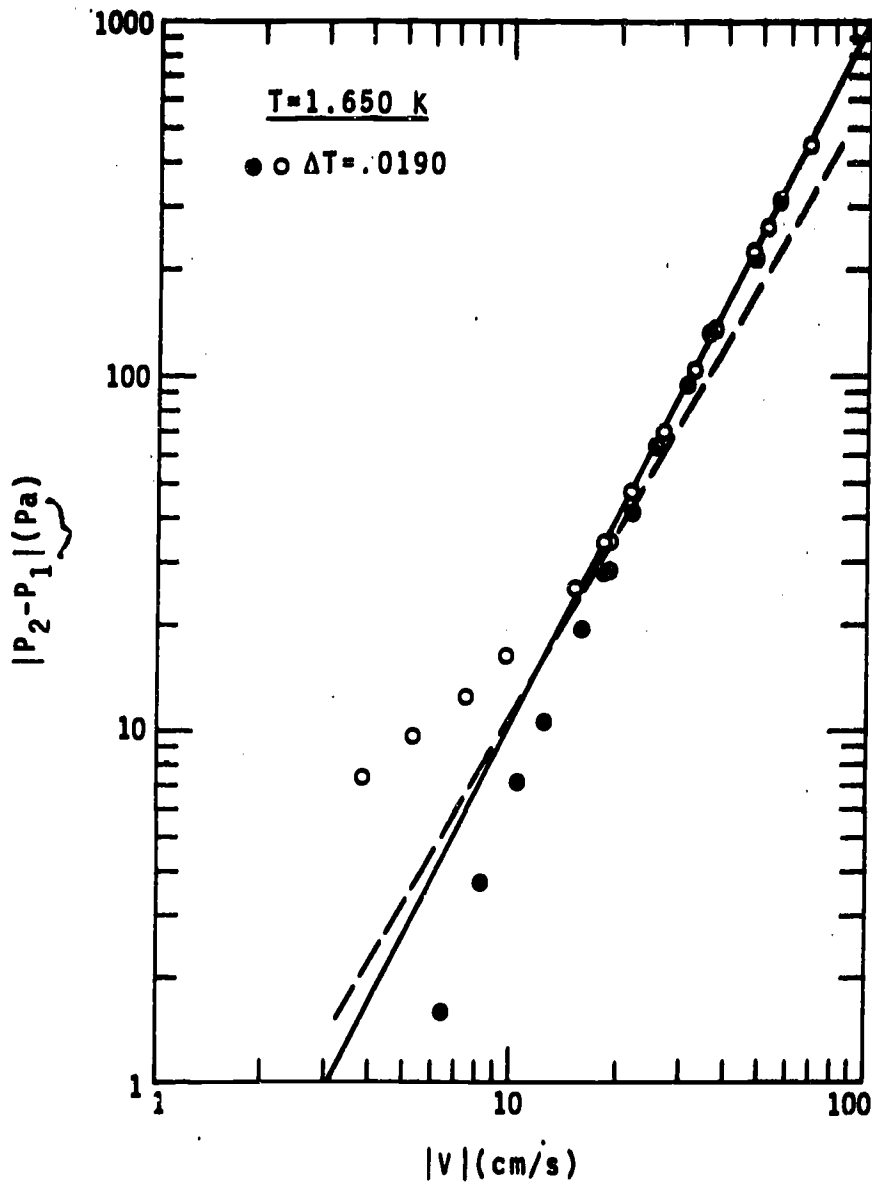


Figure 14. The pressure difference vs the net fluid velocity at 1.650 K. The dashed [solid] line is eq (41) [(42)].

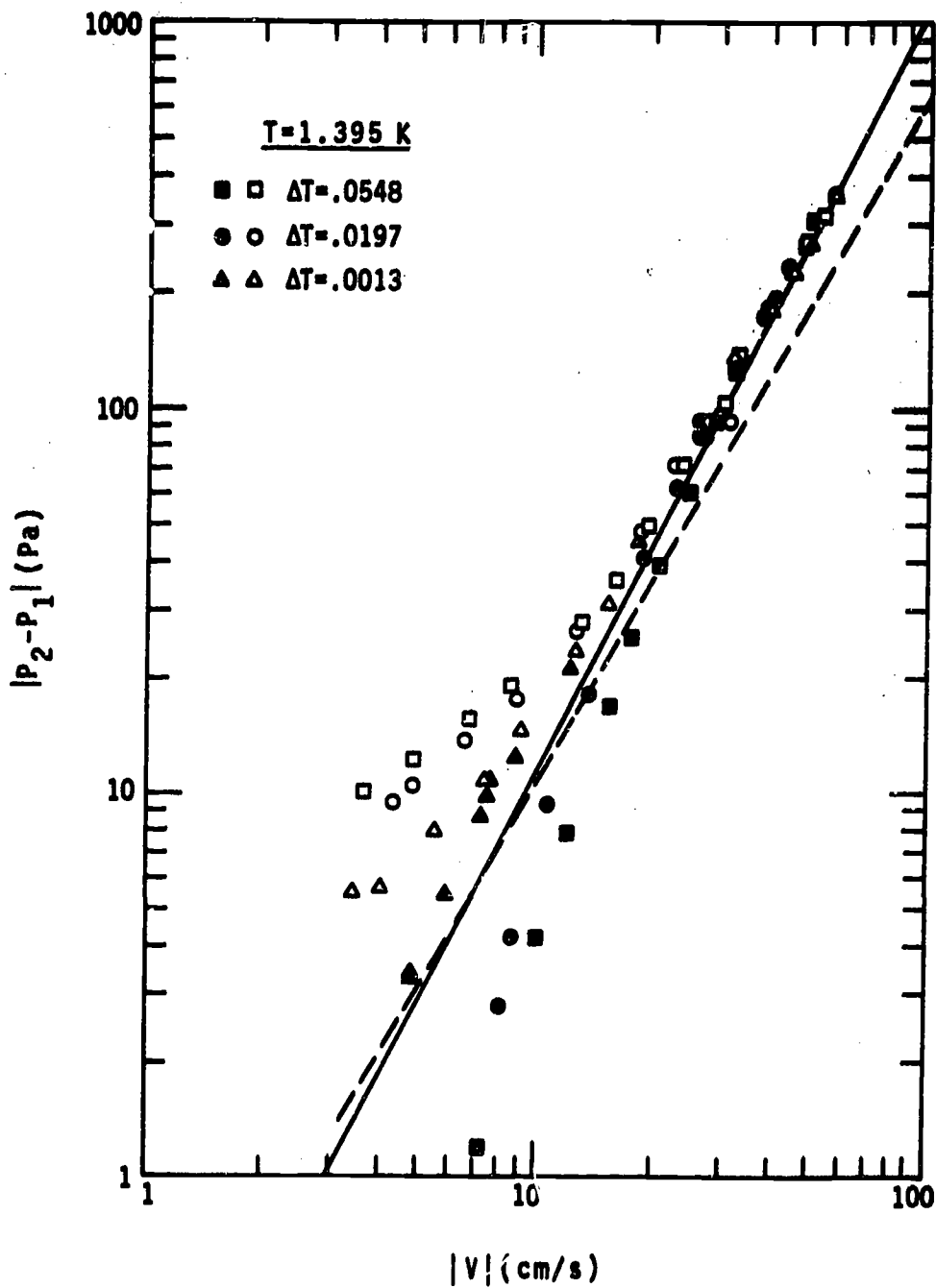


Figure 15. The pressure difference vs the net fluid velocity at 1.395 K. The dashed [solid] line is eq (41) [(42)].

A related, but not-equivalent, observation is that neither v_s nor v_n becomes solely a function of ΔP in this same limit. This comparison is not quite as clear-cut as for V vs ΔP , because v_s and v_n (unlike V) can vary significantly along the flow tube, as can be seen from the expressions obtained from eqs (1, 2, and 19).

$$v_n = V + \frac{\dot{q}}{\rho_s T} \quad v_s = V - \frac{\rho_n}{\rho_s} \frac{\dot{q}}{\rho_s T} \quad (39)$$

The variation of both \dot{q} and T can cause substantial changes in v_n and v_s . Nevertheless, the average of the velocities at the ends of the flow tube, plotted against the overall pressure difference, ought to give a good indication of whether or not the local value of velocity is solely a function of ΔP . Such plots of the two worst cases of correlation between v_n or v_s and P are shown in Fig. 16 and 17. The data for a particular ΔT fall on two lines, whose difference is correlated with the sign of ΔT (relative to ΔP). These worst cases are also the cases where v_n and v_s differ the most from V . In those cases where there is a good correlation of v_n or v_s with ΔP (e.g., v_n at $T = 2.10$, v_s at $T = 1.39$, or all the small ΔT data) then it is also true that these velocities do not differ significantly from V .

The final major observation to make is that the numerical results for V vs P are largely indistinguishable from what we would expect for an ordinary fluid at these velocities. For an ordinary fluid, the flow is known to be turbulent for Reynolds numbers greater than $2 - 4 \times 10^3$. The most reasonable choice (but not the only one!) of a counterpart for He II might be the "total" Reynolds number, defined by

$$Re = \frac{\rho V D}{\eta_n} \quad (40)$$

For all our conditions, this is equal (to within 15%) to $1.15 \times 10^3 V$, for V expressed in cm/s. Then the range in velocities that we could cover corresponded to a range in Re of $5 - 85 \times 10^3$, all apparently above the threshold for classical turbulent flow. If the inside surface of the flow tube were smooth enough, we know that the pressure drop for an ordinary fluid should be given by the "Blasius Formula"

$$\Delta P_B = 0.079 Re^{-(1/4)} \frac{4L}{D} [(1/2)\rho V^2] \quad (41)$$

This formula is shown on each of the graphs (Figures 12-15) as a dashed line. We see that the main trend of the data is reproduced. In the high velocity region, the formula underestimates the pressure drop, but for an ordinary fluid, a rather modest surface roughness would be capable of making up the difference. We have no data on the surface roughness of our flow tube, so that we are not able to determine if this accounts quantitatively for the difference.

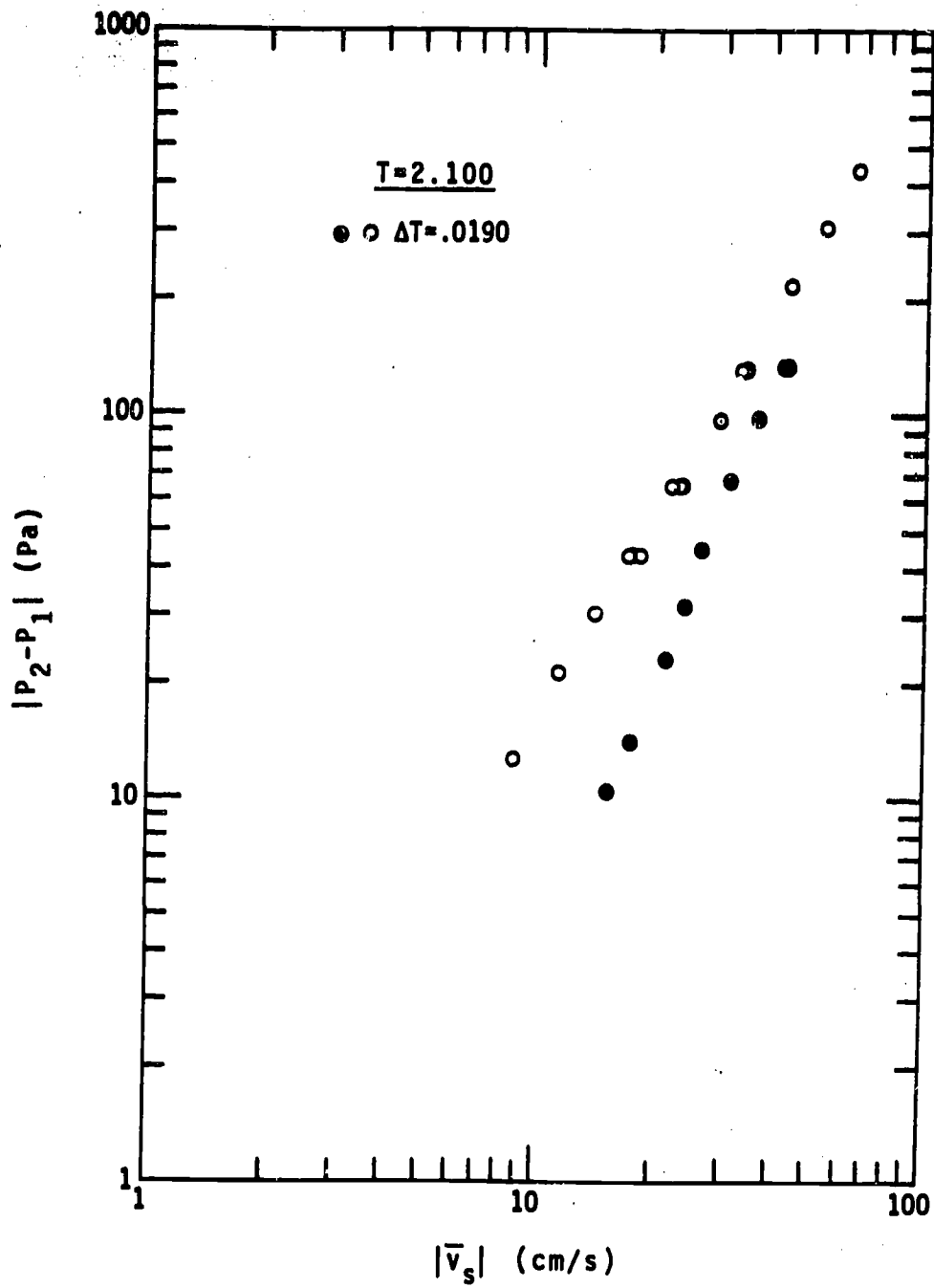


Figure 16. The pressure difference vs the average superfluid velocity at 2.100 K. Cf. Fig. 12.

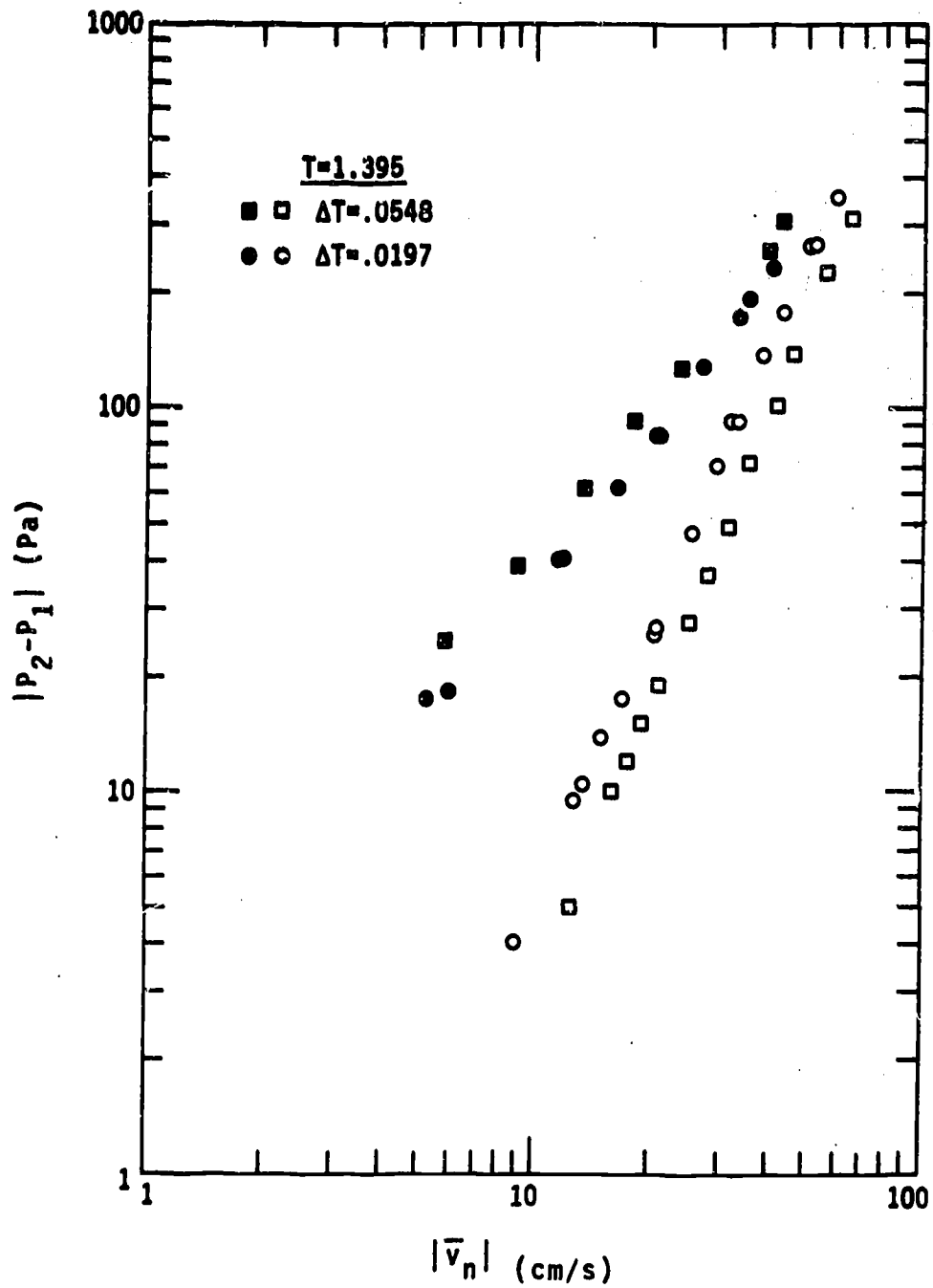


Figure 17. The pressure difference vs the average normal fluid velocity at 1.395 K. Cf. Fig. 15.

This result is very appealing, because it suggests that the two-fluid dynamics reduces to ordinary fluid dynamics in some limiting cases. It suggests, even if only further experiment can prove, that the pressure drop should change with L and D in the same way as the ordinary fluid results eq (41). It might be suggested that the superfluid fraction has been reduced to zero by the large flow velocities but that can be ruled out on a number of grounds, including the results reported in the next section, which would display no heat transport above the "enthalpy rise" value if the heat current were only the thermal conduction of He I. Actually, it presents a difficult problem, because there is no obvious way to derive such results from the current versions of two-fluid hydrodynamics.

For the purpose of a more sensitive comparison of the data, we have made a rough fit to a constant friction factor formula, defined by

$$\Delta P_c = f \frac{4L}{D} [(1/2)\rho V^2] \quad (42)$$

where f has the values 0.0062, 0.0062, 0.0067 and 0.0075 for the temperatures 2.10, 1.92, 1.65 and 1.39 K respectively. This formula is plotted as the solid line in figures 12-15. The fractional deviations of the data from this formula have been plotted in Figs. 18-21. This plot gives a more exact impression of the data coverage, scatter and departure from a simple behavior.

We have not yet found any simple correlation for the lower velocity data, nor have we been able to specify what condition it is that determines just where that region starts. However, in all the conditions encountered in this experiment, this ignorance is in regions where the pressure drop is small enough so that it may be mainly of academic interest.

No correction was made for end effects, because we have no experience that indicates that they should be made. If such an extra pressure drop were present, of about the same size as for ordinary fluid flow (say $1/2 \rho V^2$), then it would represent about a 6% correction to the data.

If the change due to the curvature of the flow tube were about the same for He II as for an ordinary fluid in turbulent flow, then there would be about 1% extra pressure drop at 10 cm/s, and about 12% extra pressure drop at $V = 70$ cm/s [29].

4.2 The Heat Current Density

We have shown in sections 2 and 3 that the quantity \dot{q}_2 represents the useful heat (per channel cross-sectional area) that can be removed from a heat source by the fluid in a cooling channel. We showed that for a heat source which is a small heated section in the middle of a cooling channel of length $2L$, assuming the other conditions are matched, our experimental result for $\dot{q}_2(V)$, $V > 0$, would represent the heat absorbed by the incoming fluid, and that the result for $\dot{q}_2(V)$, $V < 0$ would represent an additional heat conducted away by the departing fluid.

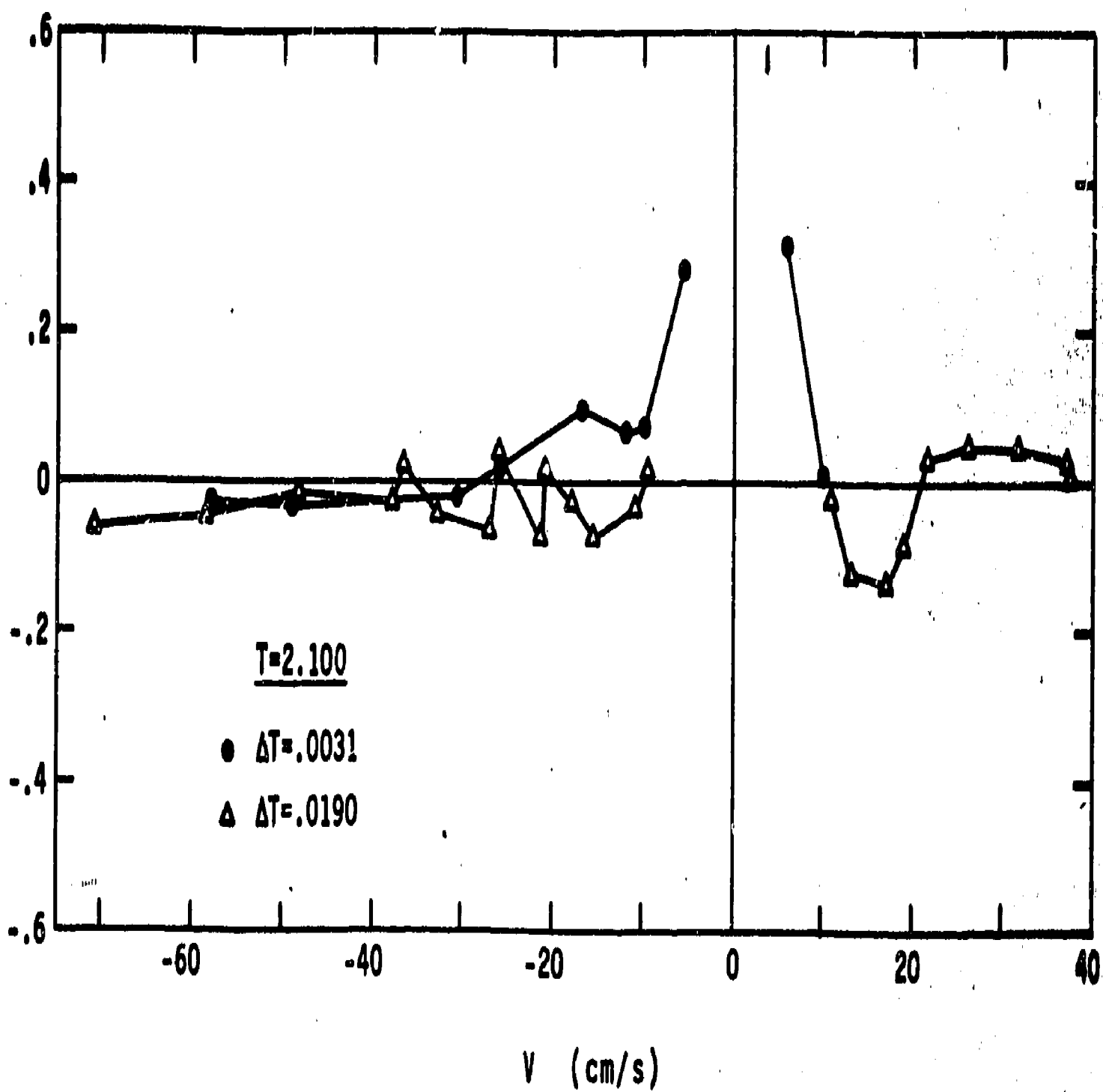


Figure 18. The data of Fig. 12, plotted as deviations from eq (42).

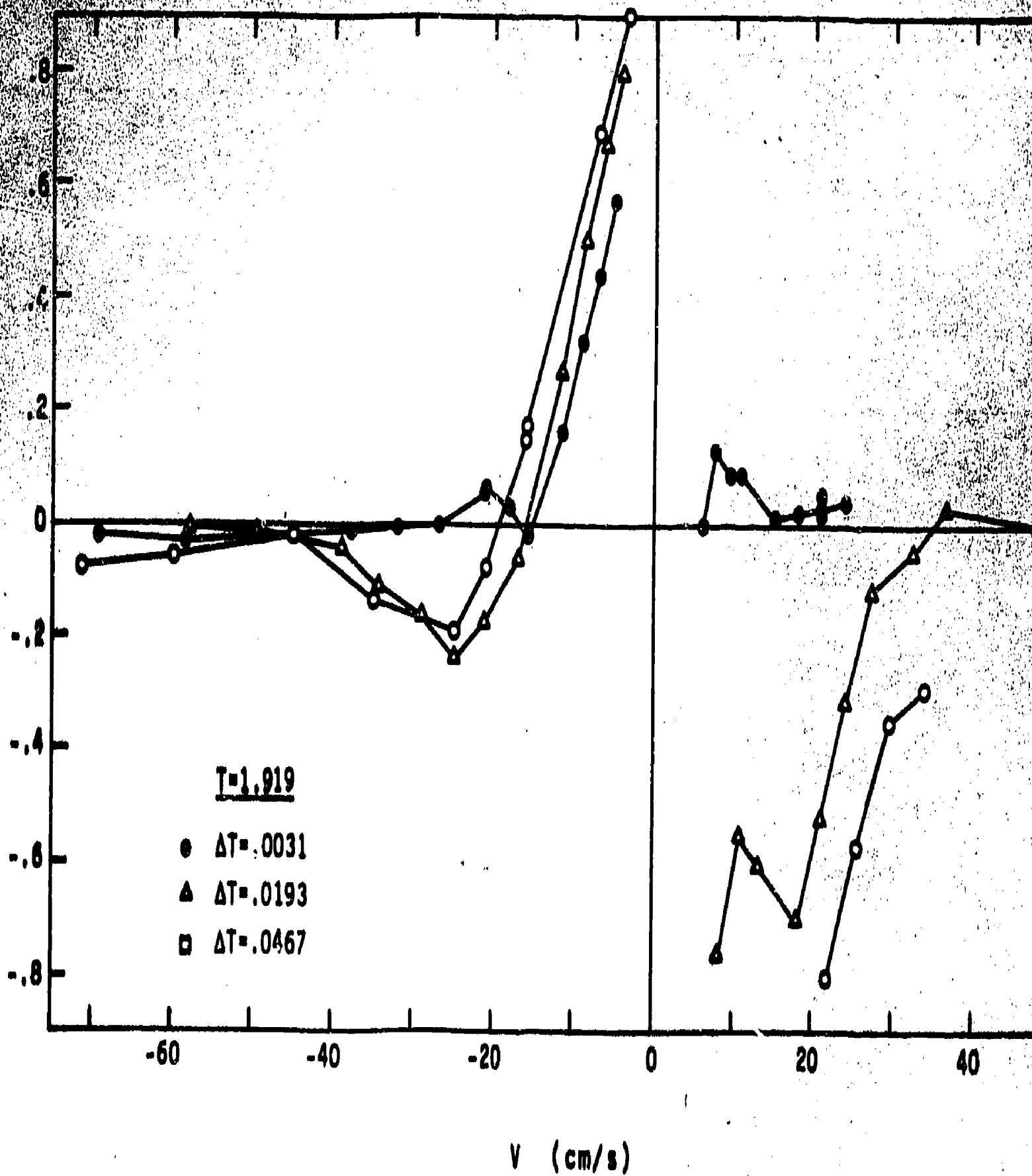


Figure 19. The data of Fig. 13, plotted as deviations from eq (42).

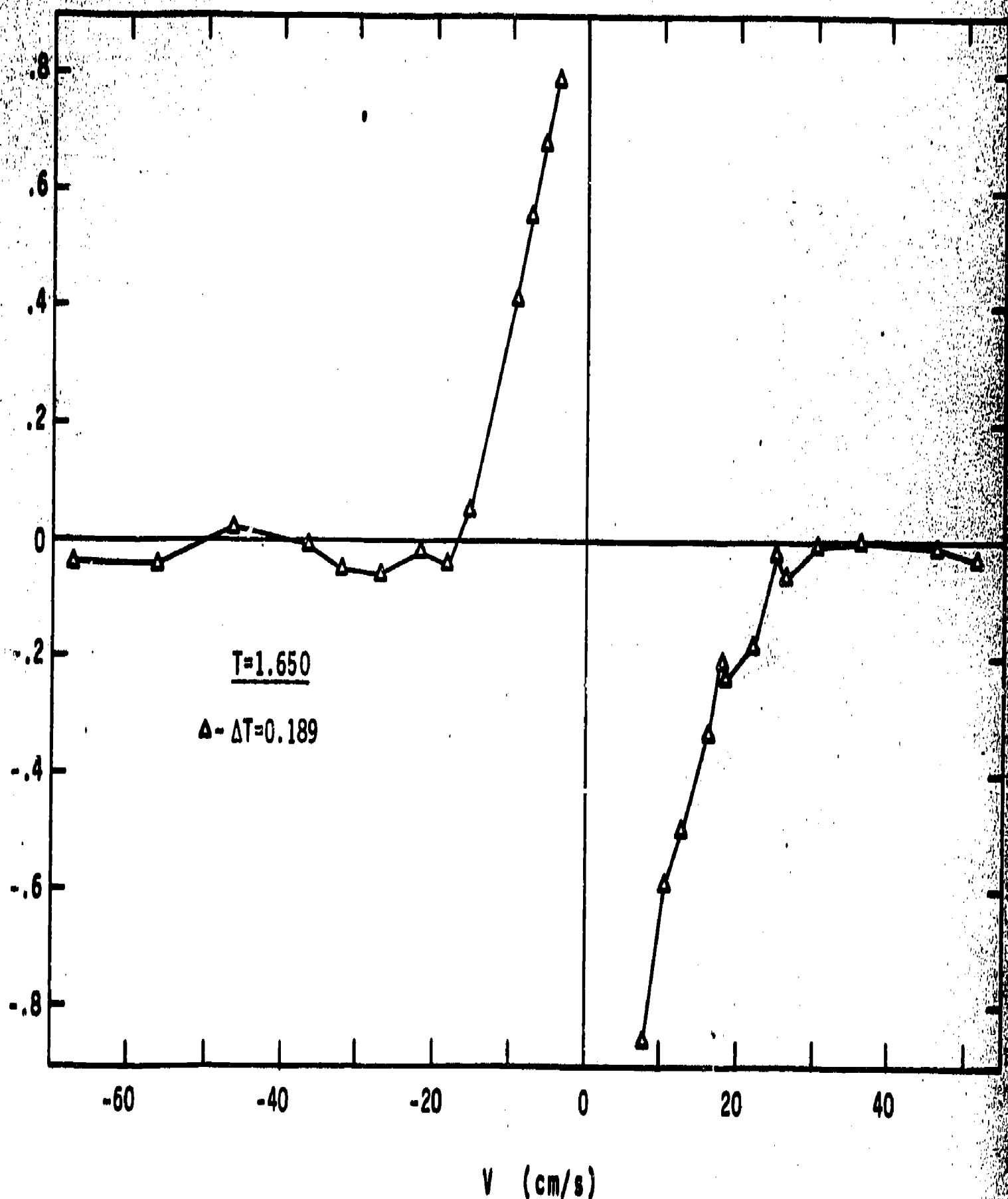


Figure 20. The data of Fig. 14, plotted as deviations from eq (42).

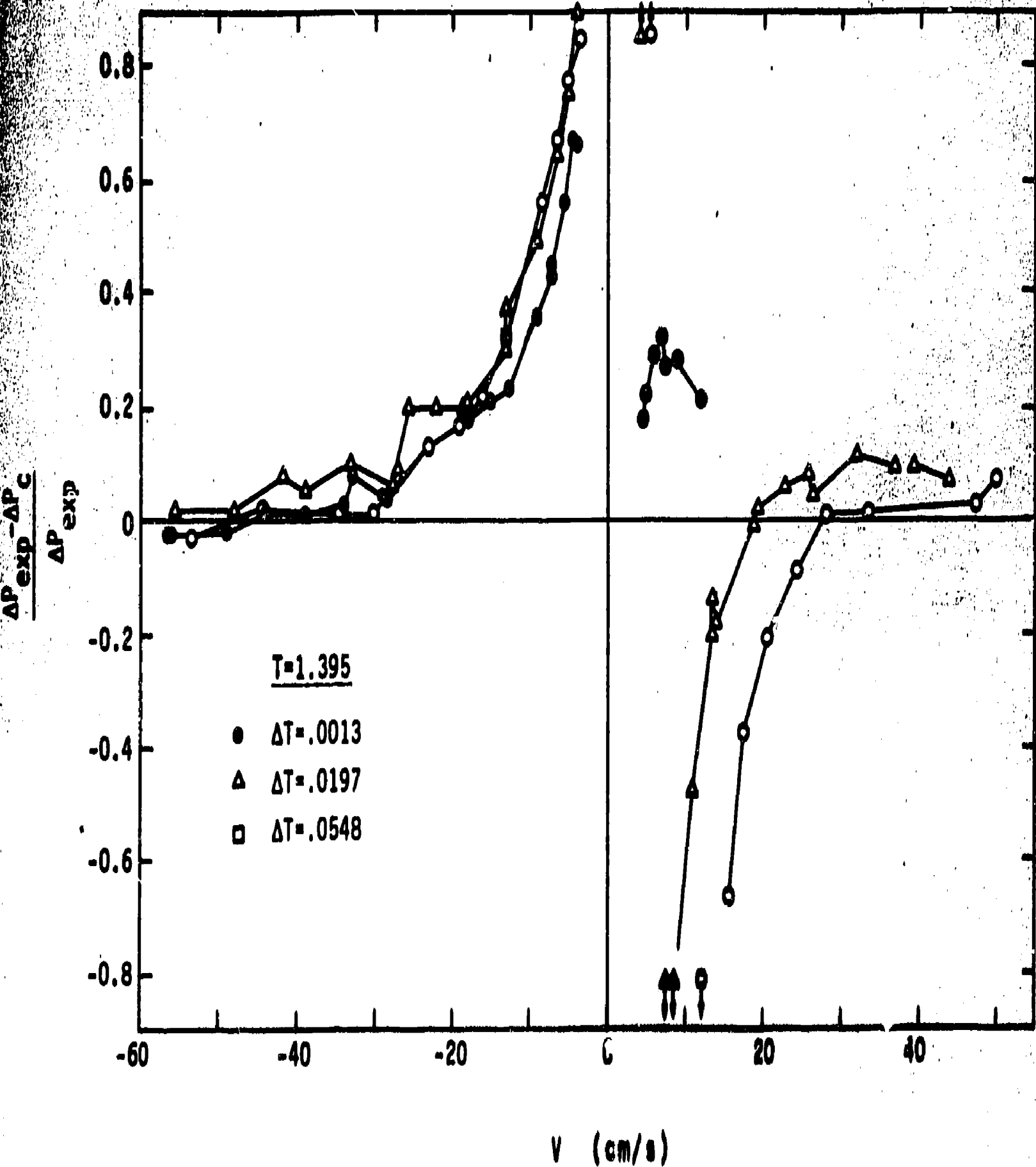


Figure 21. The data of Fig. 15, plotted as deviations from eq (42).

The results for \dot{q}_2 are shown in Figs. 22-25, where they are plotted as a function of V . The symbols indicate the nominal values for ΔT , but the explicit dependence on ΔP is not indicated; it can be inferred from the value of V .

Constructing a correlation for the data is not so straightforward as for the net fluid velocity. In that case, mass conservation required that V be a constant, so that once it was found that ΔP is mainly a function of V , we can infer that the local and average pressure gradients are nearly the same. In this case, the temperature gradient and the heat current density can turn out to be strong functions of position along the tube.

We proceed in a manner similar to that found in section 2.2. The one-dimensional energy equation [eq (20)] gives us an expression that relates $\dot{q}(x)$ to $T(x)$, and to the velocity and the local pressure; the latter two quantities can be taken directly from experiment. The model building comes in trying to devise a successful second equation that will allow solution for the unknowns \dot{q} and T .

The most natural choice we have come up with so far is to set the chemical potential gradient equal to one of the mutual friction expressions using eq (10) with $\partial v_s / \partial t = 0$. This amounts to setting \dot{q} equal to some simple function of $\nabla \mu$.

We used Vinen's expression [9],

$$\nu_s \frac{d\mu}{dx} = A \rho_s \rho_n \left(|v_n - v_s| - v_c \right)^2 (v_n - v_s) \quad (43)$$

and took the values for A from his graph. The value of v_c (not very influential in the calculation) was arbitrarily fixed at 0.5 cm/s, a value near his.

The equations were integrated numerically, the T at x_2 fixed at T_2 , and \dot{q} given various starting values, until the temperature at the other end matched. The resulting values of \dot{q}_2 are displayed as the solid lines on the graphs of \dot{q} vs V , Fig. 22-25.

The calculations do reproduce some features of the data. First, they do a reasonable job of doing what they were originally designed to do, i.e., predict the $V = 0$ data, the poor spots being $T = 1.395$ and $T = 2.100$, where the calculated values are all about 10% high. Second, for the higher T 's they do a reasonable job of predicting the slope of \dot{q}_2 , near $V = 0$. Finally, one curve (Fig. 25) does go through zero (albeit much more steeply) about where the data reverses sign, at the lowest T and ΔT . This last feature, and the other sharp drop at negative V , are found only for the conditions in which ΔP becomes large enough to cause $\Delta \mu$ to reverse sign; we have the interesting possibility of a heat current flowing toward higher temperatures. Unfortunately, the experimental evidence for this current reversal is not quite compelling. The data had a small scatter, and were reproducible, but the possibility of a systematic error (an extraneous heat input) of about the size needed to cancel the effect, cannot be excluded.

Overall, though, this simple theory does not work very well, the most striking result being that for both $V = 0$ and $V > 0$ the observed \dot{q}_2 is less than expected. As originally formulated, Vinen's arguments that lead to eq (43) clearly suggest that the equation should remain valid when $V \neq 0$. These results lead us to conclude otherwise.

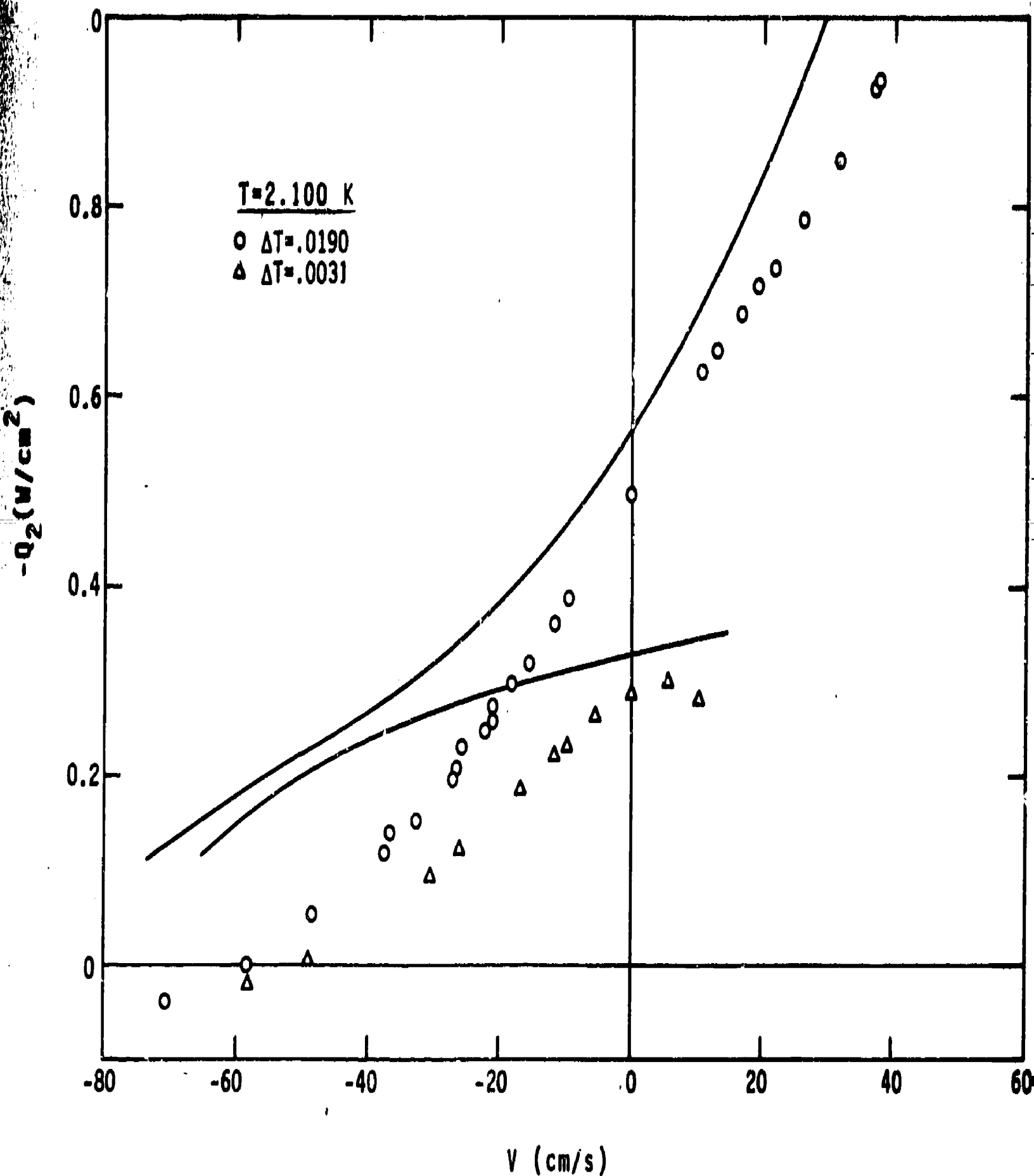


Figure 22. The useful heat current density vs the net fluid velocity at 2.100 K. The solid lines are the calculations that assume mutual friction is unaltered by the net fluid flow.

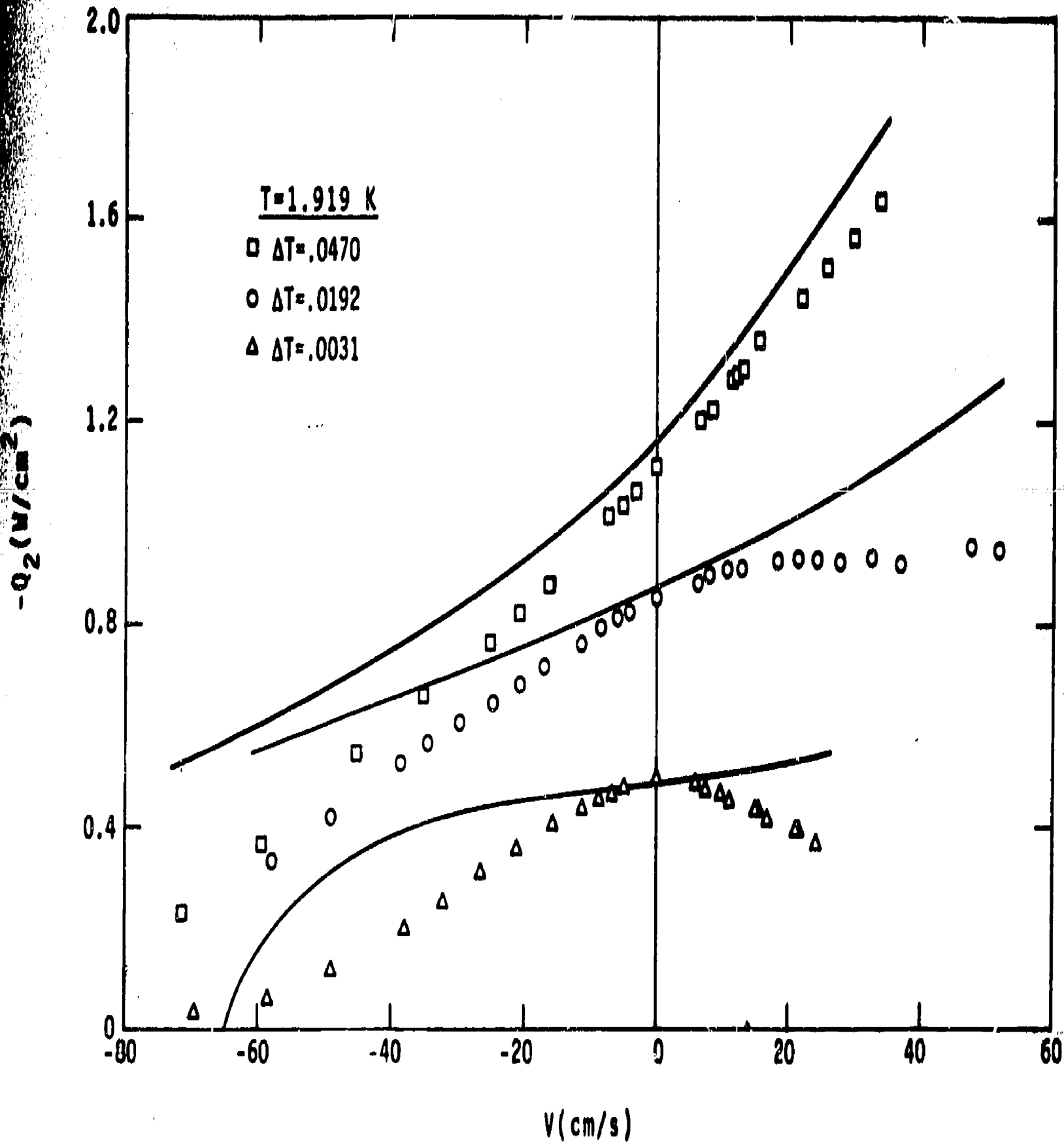


Figure 23. The useful heat current density vs the net fluid velocity at 1.919 K. The solid lines are the calculations that assume mutual friction is unaltered by the net fluid flow.

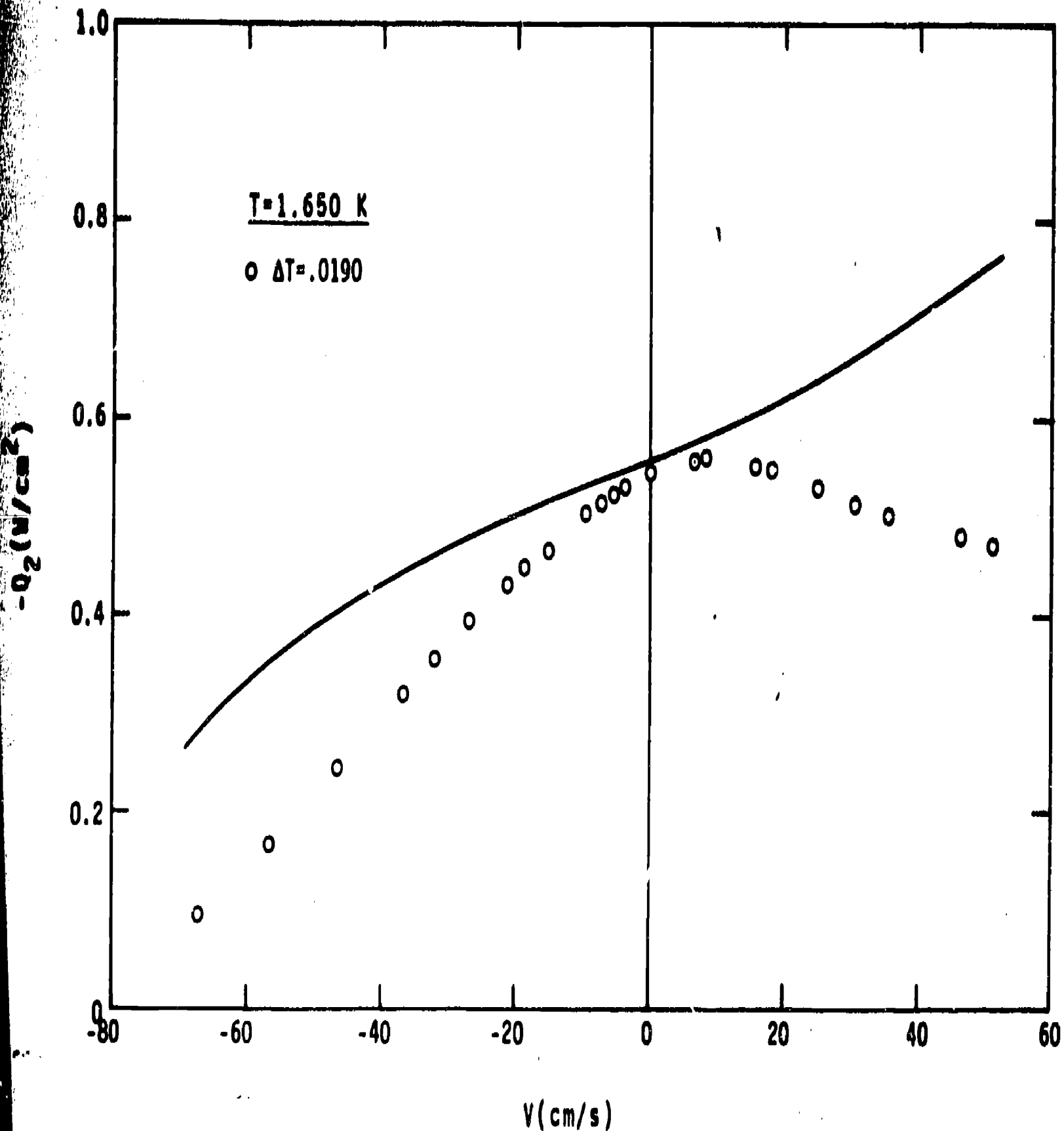


Figure 24. The useful heat current density vs the net fluid velocity at 1.650 K. The solid line is the calculation that assumes mutual friction is unaltered by the net fluid flow.

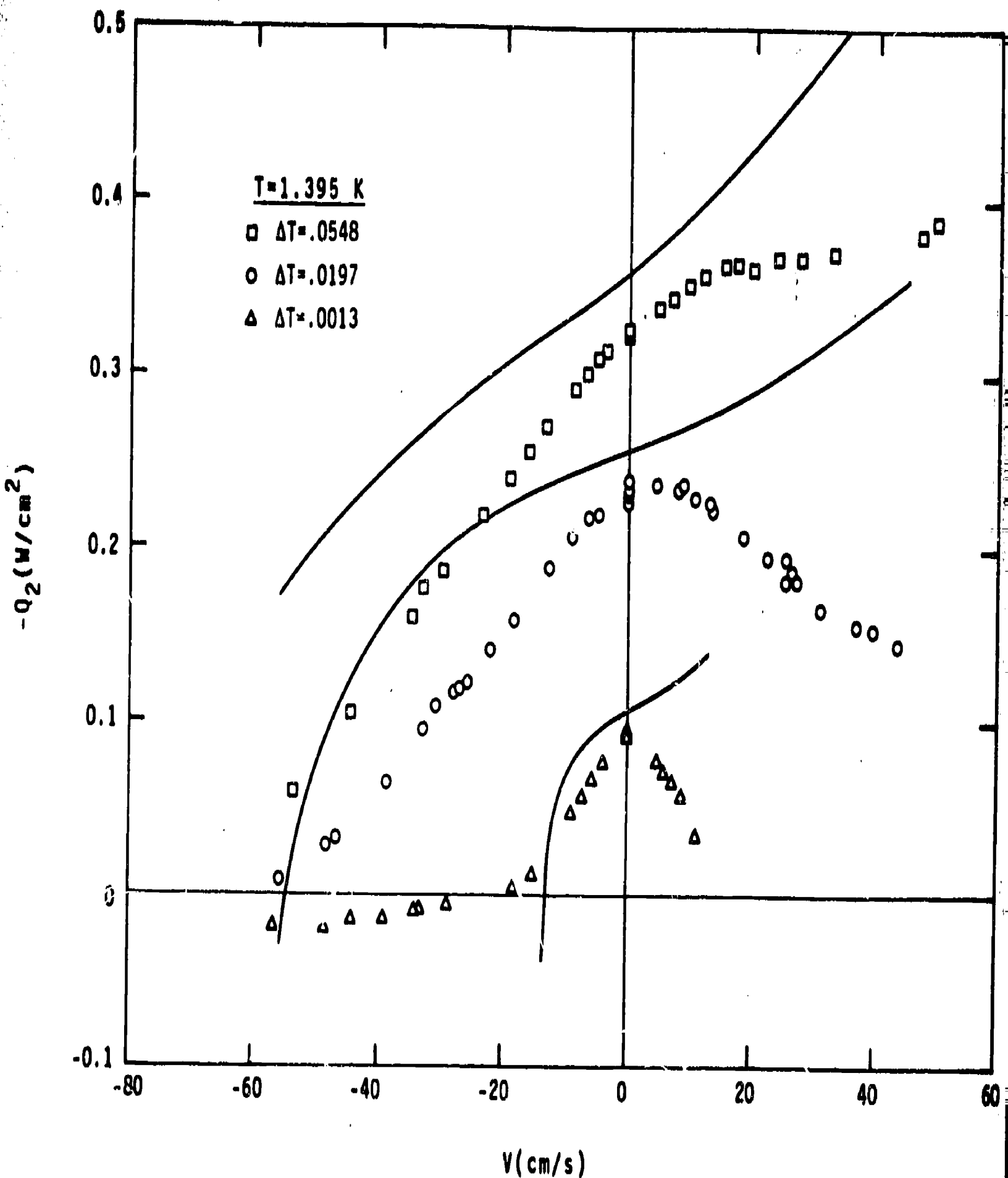


Figure 25. The useful heat current density vs the net fluid velocity at 1.395 K. The solid lines are the calculations that assume mutual friction is unaltered by the net fluid flow.

These results seem to be suggesting that we might retain Vinen's identification of the source of mutual friction with the presence of vorticity in the superfluid fraction, if we now suppose that the net fluid flow is capable of generating superfluid vorticity, in amounts over and above that generated by the mean counterflow of the two components.

5. ENHANCEMENT OF HEAT TRANSPORT BY FORCED CONVECTION

Without understanding quantitatively how mutual friction is increased by mass flow we can still draw some qualitative conclusions which indicate that in some circumstances at least, much more heat can be transported by forced convection than by "natural" convection.

Our reasoning is based again on investigating the limit as the heat current goes to zero everywhere except near the heater. The energy equation for He II also integrates immediately to give the now familiar result that the total heat absorbed by the fluid is equal to the enthalpy difference times the flow rate. For the incoming fluid ($V > 0$), we get $\dot{q}_2 = \rho V C_p \Delta T$; for the departing fluid ($V < 0$), we get $\dot{q}_2 = 0$. The positive velocity portion of the enthalpy-rise-heat-current is given on the graphs (Figs. 26-29) of \dot{q}_2 vs V . This value should, and does, act as a lower bound for the useful heat that can be rejected by the heat source. If the extra mutual friction caused by the mass flow has not "killed off" the heat current, then we can expect an extra contribution.

Now let us consider a comparison of "natural" to forced convection. Suppose we want to use the flow tube from these experiments to cool some localized heat source. First, let us estimate the best that we can do at 1.8 K with pure counterflow, with two tubes connected to the source, but no forcing of circulation around the loop. We suppose that we have a pressurized system so that we can increase the ΔT to 0.300 K. At best, the heat current per tube will increase as the cube root of T , and since $\dot{q}_2(T = 1.92, \Delta T = 0.047, V = 0) = -1.11 \text{ W/cm}^2$, the best we can do (ignoring the temperature dependence of the proportionality constant in equation (8)) is

$$(1.11) \times 2 \times \left(\frac{0.300}{0.047} \right)^{1/3} = 4.1 \text{ W/cm}^2$$

Second, how well can we do with forced convection? The enthalpy-difference-heat-current (the lower limit) for the same ΔT is

$$\rho V \int_{1.8}^{2.1} C_p dT = V \times (0.21 \text{ J/cm}^3)$$

If we have enough head (2.5 m) to force the flow at 200 cm/s, we get

$$42 \text{ W/cm}^2$$

60

which is 10 times larger. The pump work divided by the heat transported is

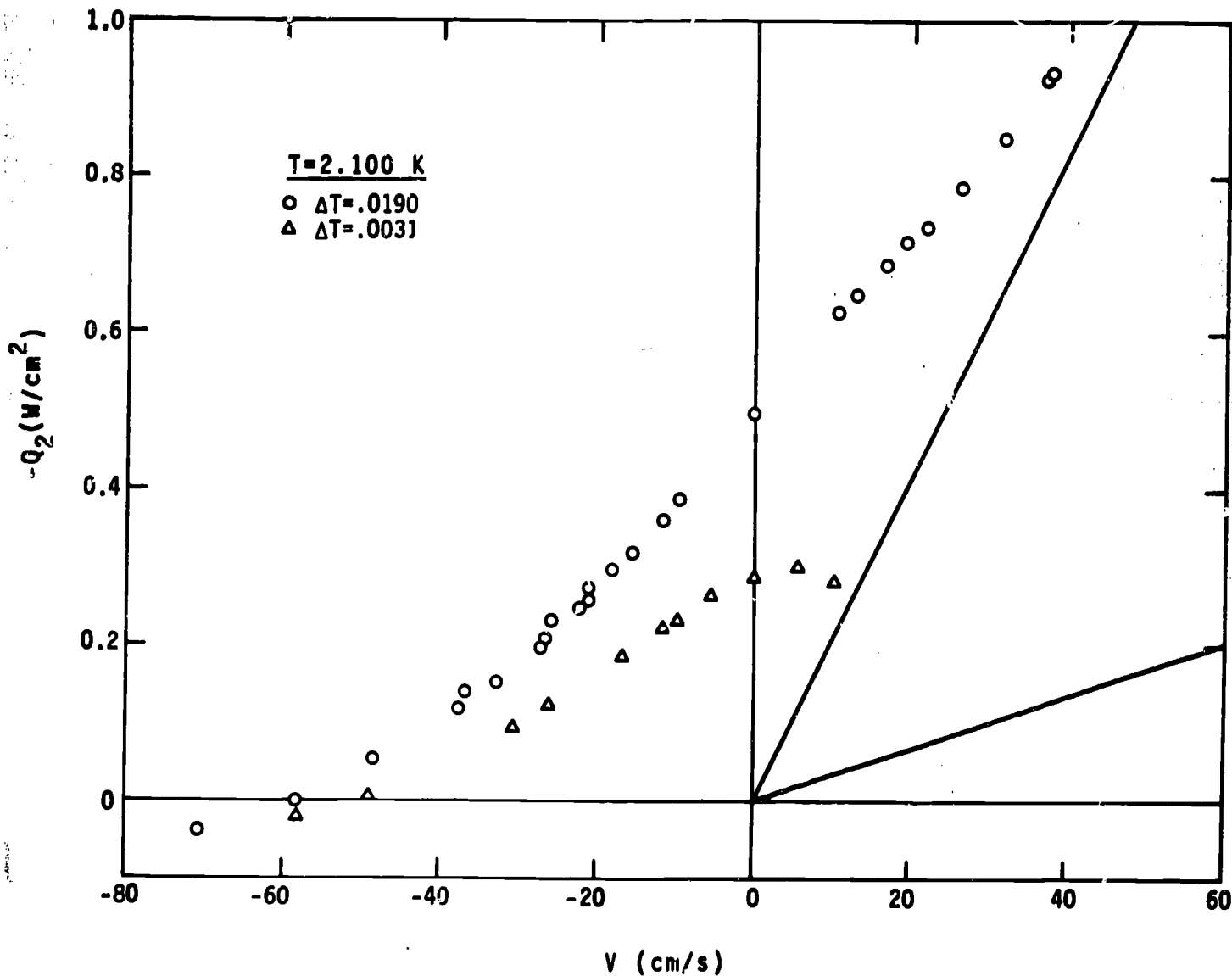


Figure 26. The data of Fig. 22. The lines are the enthalpy rise values for the different ΔT 's.

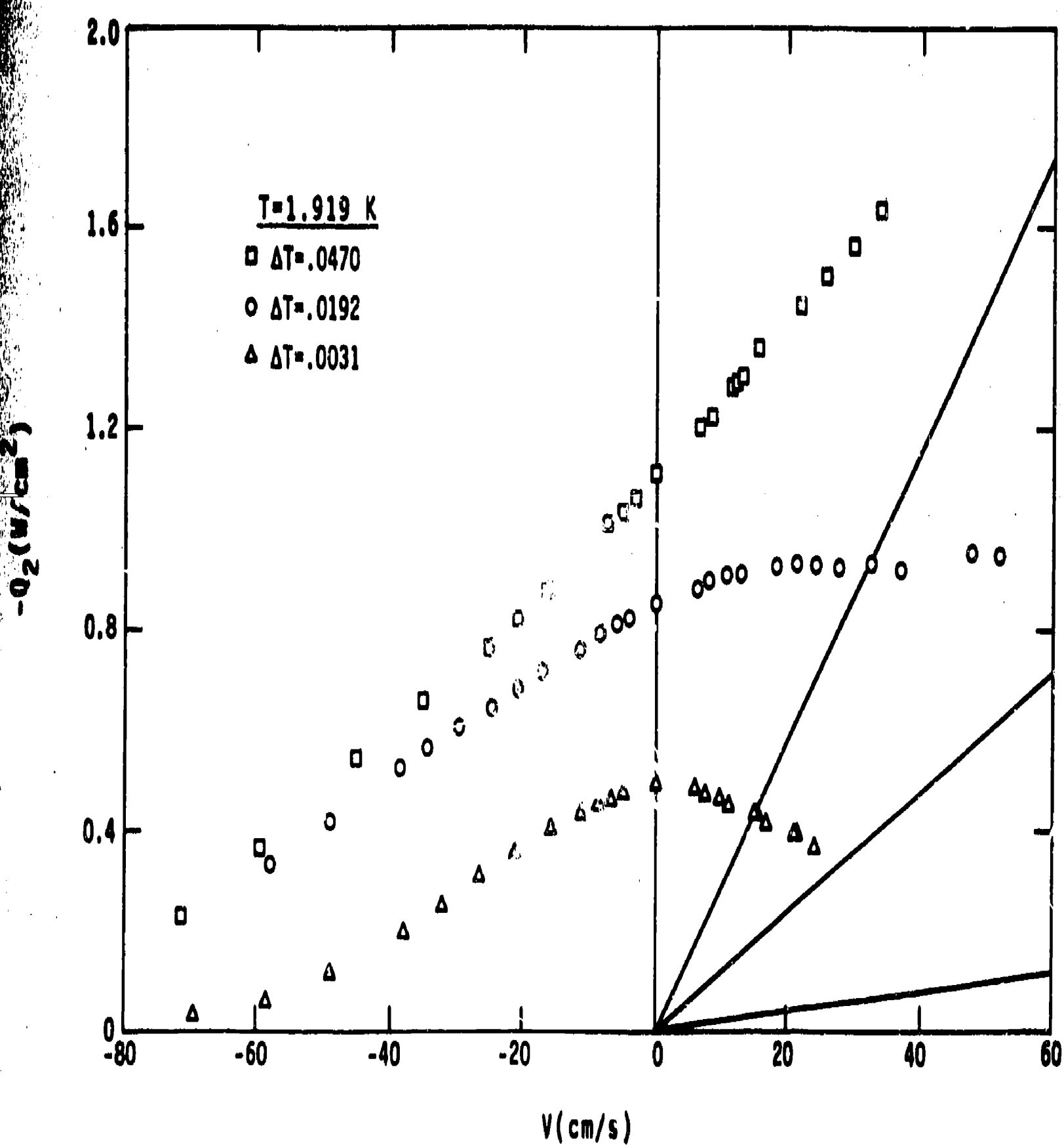


Figure 27. The data of Fig. 23. The lines are the enthalpy rise values for the different ΔT 's.

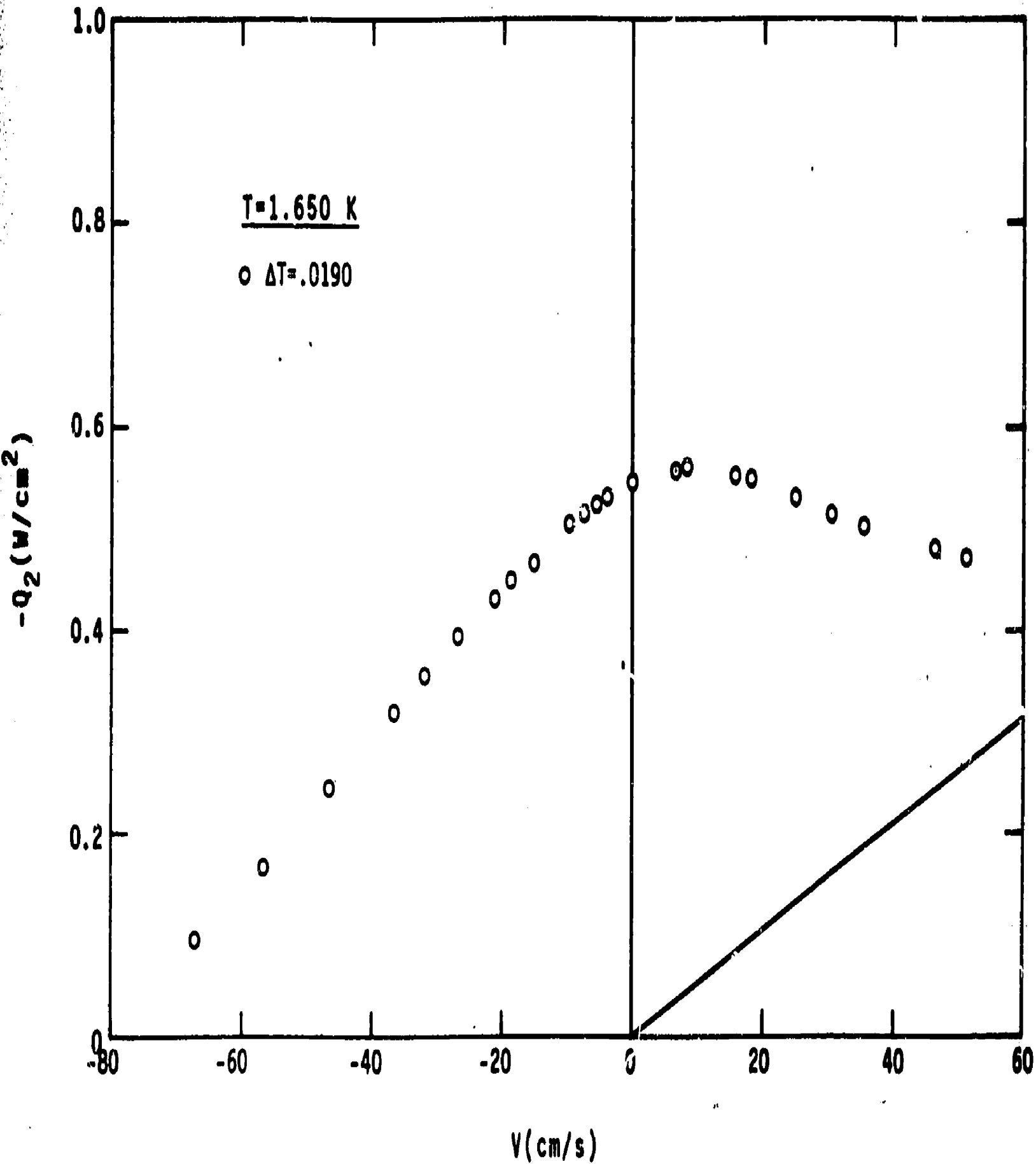


Figure 28. The data of Fig. 24. The lines are the enthalpy rise values for the different ΔT 's.

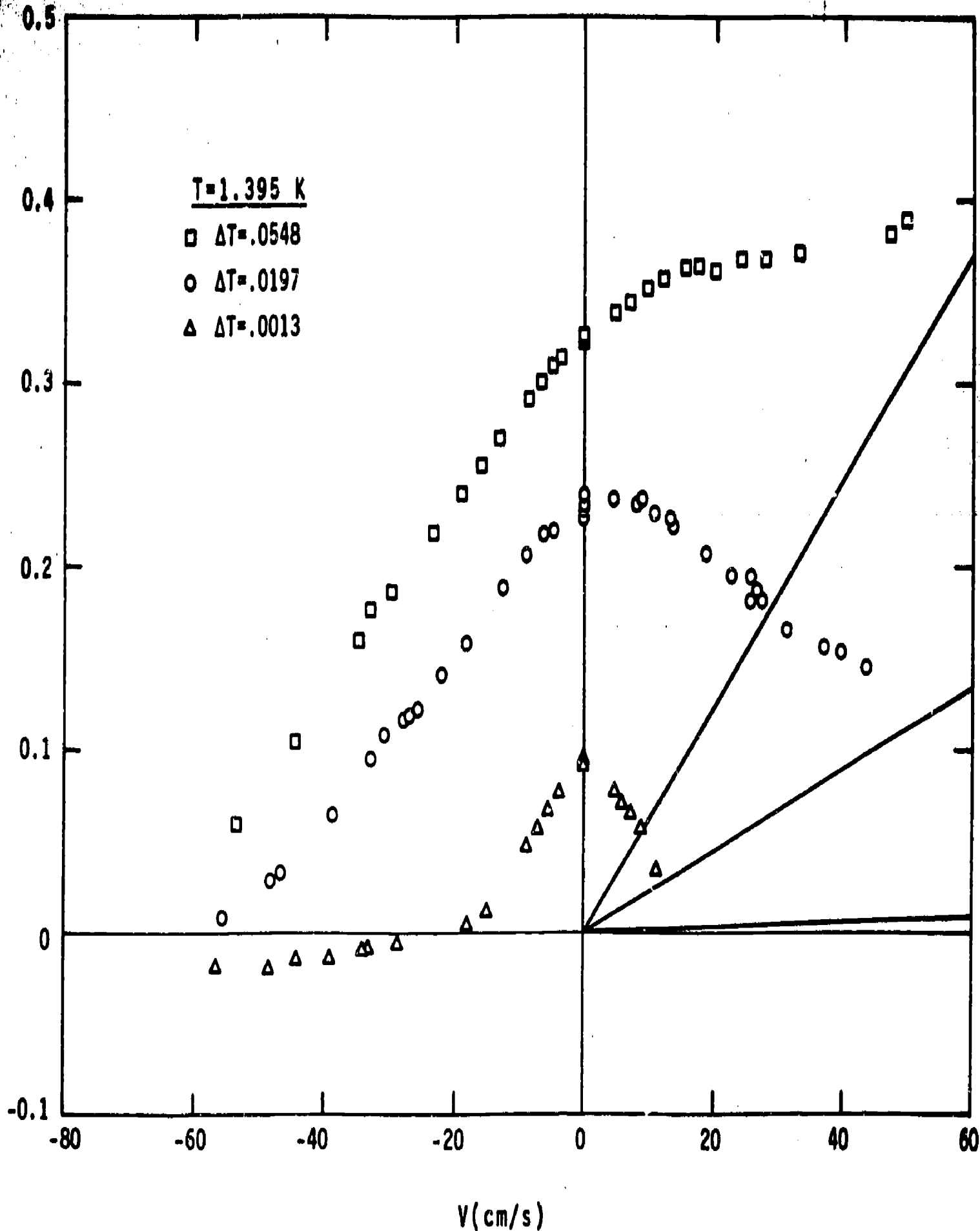


Figure 29. The data of Fig. 25. The lines are the enthalpy rise values for the different ΔT 's.

$$\frac{\Delta P \cdot V}{\rho V f C \frac{dT}{p}} \approx \frac{3.6 \times 10^3 \text{ Pa}}{0.21 \text{ J/cm}^3} \approx \frac{3.6 \times 10^3}{2.1 \times 10^5} \approx 1.7\%$$

If 17% pumpwork were acceptable, then another factor of 3 increase in heat absorbed is possible.

While this example may not be typical of any prospective application, it does illustrate how in some situations forced cooling might be of interest.

These experimental results for \dot{q}_2 show the transition from this purely classical and predictable heat transport to the more or less predictable values for zero mass flow -- the pure counterflow regime.

6. CONCLUSIONS

This experimental study enables the following generalizations to be made regarding combined heat and mass flow in Helium II.

1. Velocity of flow is primarily a function of pressure gradient. Towards the higher velocities encountered in these experiments, the relationship between velocity and pressure gradient is independent of the temperature gradient and strongly resembles a classical fluid. At lower velocities a complex relationship exists between V, ΔT and ΔP , which needs further clarification.
2. At zero velocity, axial heat transport typical of the "mutual friction" regime is again confirmed. Either positive or negative velocities reduce this heat transport below what would be calculated from the Vinen theory, and, as the magnitude of the velocity increases, classical forced convection heat transport is approached. For strongly negative velocities there is some evidence that a reversal in the direction of the heat current takes place as predicted from the Vinen theory. More definitive experiments would be required to confirm this.
3. In practical situations, axial heat transport far in excess of the usual pure counterflow values may be achieved by imposing mass flow or forced convection with the usual classical pressure drop.

7. ACKNOWLEDGEMENTS

Vincent Arp played a vital role in initiating and encouraging this project, and in defining the problems which it addresses. Jim Siegwarth generously loaned experimental equipment and expertise. One of us (W.J.) would like to acknowledge support provided through the National Bureau of Standards Postdoctoral Research Associateship Program in association with the National Research Council.

8. REFERENCES

- [1] G.v.d. Heijden, W.J.P. de Voogt, and H.C. Kramers, "Forces in the Flow of Liquid Helium II, I" *Physica* 59, 473 (1972).
- [2] G.v.d. Heijden, A.G.M.v.d. Boog and H.C. Kramers, "Forces in the Flow of Liquid He II, III," *Physica* 77, 487 (1974)
- [3] W. de Haas, A. Hartoog, H.v. Beelen, R. de Bruyn Ouboter and K.W. Taconis, "Dissipation in the Flow of He II," *Physica* 75, 311 (1974).
- [4] W. de Haas and H. van Beelen, " A Synthesis of Flow Phenomena in He II," *Physica* 83B, 129-146 (1976).
- [5] J. Wilks, The Properties of Liquid and Solid Helium, Oxford University Press (1967).
- [6] W.E. Keller, Helium-3 and Helium-4, Plenum Press (1969).
- [7] R.J. Donnelly, W.I. Glaberson and P.E. Parks, Experimental Superfluidity, University of Chicago (1967).
- [8] S.J. Putterman, Superfluid Hydrodynamics, North-Holland (1974).
- [9] W.F. Vinen, "Mutual Friction in a Heat Current in Liquid Helium-II," I - Proc. Roy. Soc. A240, 114 (1957); II - Proc. Roy. Soc. A240, 128 (1957); III - Proc. Roy. Soc. A242, 493 (1957); IV - Proc. Roy. Soc. A243, 400 (1958).
- [10] R.K. Childers and J.T. Tough, "Helium II Thermal Counterflow: Temperature -and Pressure - Difference Data and Analysis in Terms of the Vinen Theory," *Physical Rev.* B13, 1040 (1976).
- [11] D.R. Ladner, R.K. Childers and J.T. Tough, "He II Thermal Counterflow at Large Heat Currents," *Phys. Rev.* B13, 2919 (1976).
- [12] V. Arp, "Heat Transport Through Helium II," *Cryogenics* 10, 96 (1970).
- [13] C. Linnet and T.H.K. Frederking, "Thermal Conditions at the Gorter-Mellink Counterflow Limit Between 0.01 and 3 Bar," *J. Low Temp. Phys.* 21, 447, (1975).
- [14] G. Krafft, "Kühlung Langer Rohrsysteme mit Superfluidem Helium," Kern Forschungszentrum Karlsruhe Report KFK1786, (1973).
- [15] R.K. Childers and J.T. Tough, "Superheating in He II," *Low Temp. Phys.* LT13, 1, 359 (1972).
- [16] R. Eaton III, W.D. Lee and F.J. Agee, "High-Heat Flux Regime of Superfluid Cooling in Vertical Channels," *Phys. Rev.* A5, 1342 (1972).
- [17] L.D. Landau and E.M. Lifshitz, Fluid Mechanics, Pergamon Press (1959).
- [18] R.B. Bird, W.E. Stewart and E.N. Lightfoot, Transport Phenomena, John Wiley (1960).
- [19] S.R. de Groot, Thermodynamics of Irreversible Processes, North-Holland (1951).
- [20] E.F. Hammel and W.E. Keller, "Dissipation and Critical Velocities in Superfluid Helium," International Conference of Low Temperature Physics - LT10, Moscow, Vol I, p. 30 (1967).
- [21] P.H. Roberts and R.J. Donnelly, "Superfluid Mechanics," *Ann. Rev. of Fluid Mech.* 6, 179 (1974).
- [22] R. Meservey, "Superfluid Flow in a Venturi Tube," *Phys. of Fluids* 8, 1209 (1965).

- [23] P.M. McConnell, "Liquid Helium Pumps," (U.S.) National Bureau of Standards Internal Report NBSIR-73-316 (1973).
- [24] F.G. Brickwedde, H.v. Dijk, M. Durieux, J.R. Clement and J.K. Logan, "The 1958 He⁴ Scale of Temperatures," J. of Res. NBS 64A, 1 (1960).
- [25] S.G. Sydorak and R.H. Sherman, "The 1962 He³ Scale of Temperatures I," J. of Res. 68A, 547 (1974).
- [26] R.D. McCarty, "Thermophysical Properties of Helium-4 from 2 to 1500 K with Pressures to 1000 Atmospheres," (U.S.) National Bureau of Standards Tech. Note 631 (1972).
- [27] H.J.M. Hanley and J. Ely, "The Viscosity and Thermal Conductivity Coefficients of Dilute Nitrogen and Oxygen," J. Phys. Chem. Ref. Data 2, 735 (1973).
- [28] C.M. White, "Streamline Flow Through Curved Pipes," Proc. Roy. Soc. A123, 645 (1929).
- [29] H. Ito, "Friction Factors for Turbulent Flow in Curved Pipes," Trans. ASME, J. of Basic. Eng., June 1959, p 123.

9. NOMENCLATURE

English

A	Gorter-Mellink constant
A_d, A_i, A_o	horizontal cross-sectional area
A_x	cross-sectional area of the flow tube
C_p	isobaric heat capacity per unit mass
C, C_v, C_1, C_2	capacitance
D	diameter of the flow tube
E	total energy of the helium
g	gravitational constant
h, h_1, h_2, h_{ent}	enthalpy per unit mass
$j_u (j_e)$	the energy (total energy) current density
l	active capacitor length
L	flow tube length
L_o	length of quantized vortex line per unit volume
$M (m, m')$	the total (liquid, vapor) mass of helium within the inner vessel
P, P_1, P_2, P_{sv}	pressure
P_o, P_s	(for gas flow measurements) the ambient pressure, the partial pressure of water vapor
\dot{Q}	heat current or rate of heat addition
$\dot{q}, \dot{q}_1, \dot{q}_2, \dot{q}_{ent}$	heat current density
Re	Reynolds' number
s, s', s_1, s_2	entropy per unit mass
T, T_1, T_2, T_{ent}	temperature
U	total internal energy of the helium within the inner vessel
u, u', u_1, u_2, u_{ent}	internal energy density per unit mass
v, v'	volume per unit mass
v_n, v_s	normal and super component velocities (cross-sectional average)
V	net fluid velocity (cross-sectional average)
V_b, V_e, V_i, V_o	vertical velocities
x	axial coordinate
z_1, z_2, z_b, z_{ent}	altitudes

Greek

Δ	(indicates the difference of two values)
ϵ, ϵ'	dielectric constant
η, η_n	coefficient of viscosity
ρ, ρ_n, ρ_s	mass per unit volume
μ	Gibbs potential per unit mass (chemical potential)
w	vorticity
Ω	volumetric flow rate

Subscripts

$1 (2)$	} for the outside helium bath (inner vessel)
or	
$o (i)$	
$e, (b, d)$	for evaporation measurements (the vacuum can, the dewar)
ent	at the entrance of the flow tube to the inner vessel
SV, svp	along the liquid-vapor coexistence line
$u (e)$	associated with the internal (total) energy density

Superscripts

primed and unprimed quantities distinguish between the vapor and the liquid, respectively

APPENDIX 1

The following tables give the important results for almost every data point taken during the long run. Listed are the average and the difference of the temperatures of the inside and the outside helium vessels (TMEAN,DT), the altitude difference calculated from the preceding two quantities (DP), the velocity of net fluid flow through the flow tube (V), and the nominal heat current density at the inside end of the flow tube (Q2).

The sign convention is determined by taking the positive direction to run from the outside toward the inside. Therefore positive temperature differences indicate that the inside was hotter than the outside; a positive pressure difference, that the inside end of the flow tube is at a higher pressure than the outside end. The negative values of Q2 indicate that heat is flowing towards the (cooler) outside, etc.

All temperatures are given in kelvins (measured on the $T_{58} \text{He}^4$ vapor pressure scale), the pressure difference is given in pascals ($= 1 \text{ newton/meter}^2 = 10 \text{ dyne/centimeter}^2$), the altitude difference in centimeters, and the velocities are given in centimeters/second. The reader should be alert to a practice that is commonly found in the He II literature and this paper, and that is the mixing of MKS and cgs units. Therefore, when various quantities are multiplied together, further multiplication by powers of ten may be necessary to maintain consistent units.

Each data point is identified by numbers found in the ninth column of the table; the month and day on which a data-taking session was started is indicated by the numbers under DATE, the sequence number for that data point is indicated under $\#N$, and the mode number that indicates the location of the liquid interfaces is given under MO (see Table 1). The data points have been sorted: first by TMEAN, then by whether they are regular data points or equilibrium points ($Q2 = 0$) and finally by chronological order.

In columns 7 and 8 are given the results for the two auxiliary thermometers TIB and TOB. They were intended to measure the temperatures near, but not at, the inside and outside ends respectively. (See the text for an account of the relatively large uncertainties in this particular measurement). The temperature of the outside helium bath was subtracted from the indicated temperature at each location to give the listed values of DTIB and DTOB.

Several other quantities of possible interest can be calculated from the experimental results by using known values for some thermodynamic properties and some formulas from section 2 and 3. We have listed RDMU, the density times the difference in the chemical potential, which is given by $\Delta P - \rho \bar{s} \Delta T$. Also tabulated is Q1, ($Q1 \equiv \dot{q}_1$), the nominal heat flux density at the outside end of the flow tube, defined by $Q1 \equiv Q2 + (z_2 - z_1) \rho V$. Finally, we have tabulated the nominal values for the normal- and super-fluid velocities at the two ends from the formulas

$$VN1 = v + \frac{Q1}{\rho s_1 T_1} ,$$

$$VS1 = - \frac{\rho_n}{\rho_s} \frac{Q1}{s_1 T_1} , \text{ etc.}$$

The thermodynamic properties were taken from a power-law interpolation of tables A and E of Putterman [8].

Appendix I. Experimental Data.

MEAN (K)	OT (K)	CZ (CM)	JP (PA)	V (CM/S)	Q2 (M/CM2)	DT08 (K)	DT18 (K)	DATENMO	ROMU (PA)	Q1 (M/CM2)	VN2 (CM/S)	VN1 (CM/S)	V52 (CM/S)	V51 (CM/S)
2.10033	.11913	-14.96	-.1	0.00	-.497	.00095	.01677	917 7 1	-3542.4	-.497	-1.24	-1.32	4.87	3.68
2.10034	.11911	-24.34	-134.3	37.55	-.533	-.00030	.01212	917 4 4	-3673.7	-.164	35.22	37.11	46.69	38.76
2.10032	.11997	-5.58	132.1	-37.81	-.118	.00402	.01731	917 9 3	-3380.3	-.896	-38.10	-40.18	-36.65	-31.16
2.10029	.01897	-14.85	-.3	0.00	-.498	.00030	.01704	91710 1	-3513.3	-.498	-1.24	-1.32	4.87	3.69
2.10038	.11867	14.30	442.5	-70.72	.034	.01053	.01952	91713 3	-3015.8	-1.417	-70.62	-74.47	-71.09	-60.19
2.10034	.01870	6.42	305.4	-59.47	-.601	.00304	.01677	91714 3	-3164.6	-1.201	-58.48	-61.66	-58.47	-49.56
2.10036	.01874	.67	210.9	-48.50	-.654	.00623	.01832	91715 3	-3250.7	-1.046	-48.70	-51.34	-48.03	-40.80
2.10027	.01493	-14.76	-.4	0.00	-.499	.00076	.01795	91716 1	-3503.8	-.499	-1.24	-1.32	4.87	3.70
2.10052	.01412	-14.94	-.2	0.00	-.494	.00151	.02021	920 3 1	-3542.5	-.494	-1.23	-1.31	4.86	3.56
2.10054	.01305	-21.01	-30.0	31.67	-.850	-.00040	.01262	920 4 4	-3629.2	-.202	29.55	31.13	40.03	33.17
2.10053	.01401	-4.00	17.2	-32.42	-.154	.00340	.01762	920 5 3	-3424.2	-.430	-33.21	-35.02	-31.31	-26.66
2.10059	.01333	-19.03	-07.0	20.15	-.789	-.00038	.01346	920 6 4	-3594.5	-.253	24.18	25.48	33.91	28.03
2.10051	.01303	-16.20	00.2	-27.20	-.199	.00306	.01885	920 7 3	-3460.0	-.762	-27.78	-29.30	-25.32	-21.63
2.10054	.01907	-10.00	-45.0	21.58	-.736	-.00010	.01472	920 8 4	-3579.9	-.293	19.75	20.81	28.84	23.75
2.10061	.01903	-10.20	50.2	-25.34	-.230	.00306	.01885	920 9 4	-3460.0	-.766	-26.57	-28.02	-23.73	-20.31
2.10061	.01303	-10.00	00.2	-26.93	-.208	.00306	.01885	92010 3	-3460.0	-.763	-27.45	-28.95	-24.89	-21.27
2.10065	.01894	-11.81	43.5	-21.24	-.272	.00221	.01825	92011 4	-3476.2	-.708	-21.91	-23.11	-18.56	-15.98
2.10065	.01693	-11.00	43.5	-22.21	-.248	.00221	.01825	92012 3	-3476.2	-.705	-22.83	-24.08	-19.77	-16.97
2.10060	.01494	-11.81	43.5	-21.36	-.259	.00221	.01825	92013 1	-3476.2	-.698	-22.01	-23.21	-18.81	-16.18
2.10072	.01306	-14.94	-.4	0.00	-.497	.00106	.01908	92014 1	-3534.1	-.497	-1.24	-1.31	4.91	3.69
2.10036	.01411	-14.03	-.7	0.00	-.496	.00015	.01644	92110 1	-3538.4	-.496	-1.23	-1.31	4.86	3.67
2.10044	.01497	-10.00	-23.3	10.73	-.687	-.00028	.01470	92111 1	-3536.4	-.345	15.02	15.82	23.48	19.29
2.10044	.01497	-13.33	21.0	-15.50	-.319	.00084	.01686	92112 1	-3491.8	-.638	-16.38	-17.27	-12.45	-10.85
2.10045	.01497	-17.04	-32.2	19.27	-.717	-.00000	.01438	92113 1	-3545.6	-.323	17.49	18.41	26.30	21.66
2.10046	.01897	-12.76	30.4	-20.12	-.297	.00136	.01698	92114 1	-3483.0	-.668	-18.85	-19.89	-15.20	-13.16
2.10044	.01895	-14.80	-.7	0.00	-.496	.00004	.01629	92115 1	-3511.4	-.496	-1.24	-1.31	4.86	3.68
2.10044	.01945	-15.00	-14.1	12.93	-.649	-.00021	.01510	92116 1	-3524.8	-.384	11.32	11.91	19.29	15.78
2.10045	.01895	-13.93	10.7	-11.78	-.360	.00071	.01682	92117 1	-3497.8	-.601	-12.68	-13.37	-8.25	-7.32
2.10045	.01895	-15.55	-10.5	10.67	-.627	-.00023	.01527	92118 1	-3521.0	-.409	9.10	9.58	16.82	13.70
2.10045	.01490	-14.10	0.6	-9.46	-.388	.00052	.01674	92119 1	-3492.9	-.581	-10.42	-11.00	-5.65	-5.14
2.10045	.01890	-14.80	-1.1	0.00	-.497	.00061	.01624	92120 1	-3502.6	-.497	-1.24	-1.32	4.87	3.69
2.10037	.01313	-15.30	-.8	0.00	-.497	.00065	.01648	10 2 3 1	-3542.8	-.497	-1.24	-1.32	4.87	3.68
2.10033	.01966	-24.38	-135.0	37.32	-.926	-.00052	.01170	10 2 4 4	-3665.2	-.163	35.01	36.88	46.39	38.53
2.10036	.01893	-5.03	131.1	-36.99	-.140	.00394	.01714	10 2 5 3	-3374.8	-.901	-37.34	-39.38	-35.62	-30.31
2.10073	.00332	-2.00	-.0	0.00	-.288	-.00036	.00224	10 210 1	-616.1	-.288	-.74	-.74	2.41	2.28
2.10069	.00336	-1.00	13.0	-11.69	-.222	-.00045	.00193	10 211 1	-609.0	-.265	-12.25	-12.37	-9.83	-9.59
2.10074	.00329	-3.29	-10.2	10.38	-.282	-.00047	.00182	10 212 1	-620.0	-.245	9.66	9.74	12.73	12.32
2.10069	.00334	-1.91	10.1	-9.95	-.232	-.00047	.00173	10 213 1	-609.9	-.268	-10.55	-10.65	-8.02	-7.83
2.10071	.00326	-2.56	-.1	0.00	-.289	-.00044	.00205	10 214 1	-604.5	-.289	-.74	-.75	2.41	2.29
2.10075	.00327	-2.67	-4.5	5.71	-.298	-.00054	.00172	10 215 1	-611.1	-.278	4.95	4.99	8.19	7.91
2.10074	.00324	-2.20	4.1	-5.54	-.265	-.00057	.00164	10 216 1	-598.8	-.284	-6.27	-6.32	-3.38	-3.34
2.10071	.00303	3.69	07.2	-30.69	-.094	-.00053	.00143	10 217 3	-404.0	-.199	-30.93	-31.21	-29.91	-29.12
2.10067	.00307	19.32	310.4	-39.40	.021	.00022	.00285	10 218 3	-258.5	-.191	-58.39	-58.84	-58.62	-58.93
2.10066	.00352	13.07	220.0	-49.12	-.605	-.00034	.00170	10 219 3	-335.4	-.176	-49.13	-49.57	-49.07	-47.72
2.10065	.00314	2.13	51.5	-20.18	-.124	-.00044	.00156	10 220 3	-515.8	-.215	-26.49	-26.73	-25.14	-24.48
2.10072	.00306	-2.43	-.4	0.00	-.286	-.00058	.00149	10 221 1	-568.4	-.286	-.73	-.74	2.38	2.27
2.10073	.00307	-.24	30.9	-17.10	-.184	-.00062	.00264	10 222 1	-537.4	-.242	-17.62	-17.77	-15.61	-15.24

Appendix i (continued). Experimental Data.

TMEAN (K)	DT (K)	Z (CM)	UP (PA)	V (CM/S)	Q2 (W/CM2)	DT00 (K)	DT18 (K)	DATENNMO	ROMU (PA)	Q1 (W/CM2)	VN2 (CM/S)	VN1 (CM/S)	V52 (CM/S)	V51 (CM/S)
2.16989	-0.00005	-0.01	-0.7	0.00	0.000	.JJ071	-0.14057	917 1 1	9.0	0.000	0.00	0.00	0.00	0.00
2.16995	.00004	-0.01	.2	0.00	0.000	.JJ067	.00255	917 2 1	-6.8	0.000	0.00	0.00	0.00	0.00
2.16995	.00002	-0.00	.2	0.00	0.000	.JJ083	.00294	917 3 1	-3.2	0.000	0.00	0.00	0.00	0.00
2.09573	.00000	-0.01	-0.0	0.00	0.000	.JJ069	.00253	917 4 1	-0.2	0.000	0.00	0.00	0.00	0.00
2.09074	.00000	-0.01	-0.0	0.00	0.000	.JJ065	.00233	917 5 1	-9.3	0.000	0.00	0.00	0.00	0.00
2.09084	-0.00004	-0.03	-0.7	0.00	0.000	.JJ026	.00123	917 6 1	5.6	0.000	0.00	0.00	0.00	0.00
2.09082	.00003	530.19	760.12	0.00	0.000	.JJ011	.00066	91711 1	7697.8	0.000	0.00	0.00	0.00	0.00
2.09083	.00003	-0.02	-0.0	0.00	0.000	.JJ006	.00054	91712 1	-5.1	0.000	0.00	0.00	0.00	0.00
2.09087	-0.00001	.01	-0.9	0.00	0.000	.JJ024	.00129	91717 1	1.6	0.000	0.00	0.00	0.00	0.00
2.09071	.00006	-0.00	.6	0.00	0.000	.JJ014	.00078	918 1 1	-9.8	0.000	0.00	0.00	0.00	0.00
2.09071	-0.00001	-0.00	-0.1	0.00	0.000	-0.0012	.00008	918 2 1	1.5	0.000	0.00	0.00	0.00	0.00
2.09094	.00002	.03	.6	0.00	0.000	.00122	.00426	920 1 1	-3.1	0.000	0.00	0.00	0.00	0.00
2.09098	.00004	.03	.6	0.00	0.000	.00090	.00339	920 2 1	-1.7	0.000	0.00	0.00	0.00	0.00
2.09113	.00003	.01	.5	0.00	0.000	.00025	.00126	92015 1	-4.1	0.000	0.00	0.00	0.00	0.00
2.16100	-0.00001	530.19	760.17	0.00	0.000	.JJ052	.00237	921 1 1	7665.1	0.000	0.00	0.00	0.00	0.00
2.16111	-0.00004	-0.01	-0.0	0.00	0.000	-0.00074	-0.00158	921 2 1	6.9	0.000	0.00	0.00	0.00	0.00
2.16130	-0.00001	-0.01	-0.3	0.00	0.000	-0.00074	-0.00156	921 3 1	2.0	0.000	0.00	0.00	0.00	0.00
2.16154	-0.00001	-0.01	-0.3	0.00	0.000	-0.00072	-0.00156	921 4 1	1.4	0.000	0.00	0.00	0.00	0.00
2.16111	-0.00001	-0.01	-0.2	0.00	0.000	-0.00073	-0.00158	921 5 1	1.1	0.000	0.00	0.00	0.00	0.00
2.09149	.00001	-0.01	-0.1	0.00	0.000	-0.00072	-0.00157	921 6 1	-1.0	0.000	0.00	0.00	0.00	0.00
2.09149	.00003	-0.02	.0	0.00	0.000	-0.00069	-0.00151	921 7 1	-5.0	0.000	0.00	0.00	0.00	0.00
2.09124	.00000	-0.01	-0.1	0.00	0.000	-0.00067	-0.00153	921 8 1	-0.6	0.000	0.00	0.00	0.00	0.00
2.09092	.00002	-0.01	.1	0.00	0.000	-0.00065	-0.00151	921 9 1	-3.4	0.000	0.00	0.00	0.00	0.00
2.16033	-0.00004	.01	-0.4	0.00	0.000	-0.00074	-0.00155	10 2 1 1	7.5	0.000	0.00	0.00	0.00	0.00
2.09075	-0.00003	.01	-0.2	0.00	0.000	-0.00075	-0.00157	10 2 2 1	5.2	0.000	0.00	0.00	0.00	0.00
2.16167	-0.00002	.01	-0.1	0.00	0.000	-0.00074	-0.00155	10 2 6 1	2.9	0.000	0.00	0.00	0.00	0.00
2.09094	-0.00001	.01	-0.1	0.00	0.000	-0.00075	-0.00156	10 2 7 1	2.4	0.000	0.00	0.00	0.00	0.00
2.16246	-0.00011	.03	-0.9	0.00	0.000	-0.00060	-0.00129	10 2 8 1	20.2	0.000	0.00	0.00	0.00	0.00
2.09062	-0.00005	.03	-0.2	0.00	0.000	-0.00052	-0.00098	10 2 9 1	9.9	0.000	0.00	0.00	0.00	0.00
2.09093	-0.00003	530.19	760.15	0.00	0.000	.JJ000	.00050	10 223 1	7668.7	0.000	0.00	0.00	0.00	0.00
1.92308	.02003	-15.53	0.2	0.00	-0.961	.JJ139	.02605	9 2 2 1	-3276.8	-0.961	-4.18	-4.60	3.78	3.98
1.92414	.02008	-15.67	0.1	0.00	-0.961	.JJ137	.02702	9 2 3 1	-3296.5	-0.961	-4.18	-4.60	3.78	3.98
1.92414	.02901	-18.00	-39.2	24.70	-1.161	.JJ117	.02572	9 2 4 1	-3344.7	-0.720	19.65	21.25	29.26	27.38
1.92407	.02867	-12.55	44.2	-24.14	-0.709	.JJ257	.02728	9 2 5 1	-3214.9	-1.138	-27.28	-29.63	-21.40	-19.98
1.91935	.04728	-25.53	0.7	0.00	-1.108	.JJ231	.04438	910 1 1	-5309.7	-1.108	-4.75	-5.56	4.48	4.00
1.91942	.04721	-20.79	-11.0	15.28	-1.361	.JJ136	.04242	910 2 4	-5321.8	-0.922	9.45	10.66	20.60	18.61
1.91941	.04714	-27.72	-25.1	21.94	-1.448	.00120	.04142	910 3 4	-5332.5	-0.818	15.73	17.84	27.64	24.98
1.91941	.04711	-12.71	144.1	-45.23	-0.545	.01011	.04565	910 4 4	-5110.4	-1.850	-47.57	-54.51	-43.07	-38.59
1.91948	.04710	-31.78	-83.7	33.87	-1.635	.JJ099	.03940	910 5 4	-5382.3	-0.667	26.86	30.53	40.37	36.28
1.91944	.04709	-30.22	-01.5	24.74	-1.569	.JJ100	.04002	910 6 4	-5358.9	-0.718	23.02	26.15	35.98	32.34
1.91953	.04706	-28.66	-34.4	25.65	-1.508	.JJ109	.04074	910 7 4	-5334.1	-0.774	19.19	21.77	31.64	28.45
1.91952	.04702	-15.65	132.1	-15.21	-0.660	.JJ0767	.04950	910 8 4	-5187.5	-1.671	-38.03	-43.58	-32.59	-29.17
1.91969	.04684	-26.22	-0.2	11.93	-1.249	.00136	.04264	910 9 2	-5278.6	-0.959	6.36	7.13	17.09	15.48
1.91954	.04693	-25.37	0.4	0.00	-1.109	.JJ226	.04412	91010 1	-5279.0	-1.109	-4.75	-5.55	4.48	4.01
1.91946	.04694	-29.37	0.7	0.00	-1.108	.00226	.04410	911 1 2	-5277.4	-1.108	-4.75	-5.55	4.48	4.00
1.91943	.04687	-24.09	15.6	-7.13	-1.014	.00298	.04455	911 2 2	-5256.3	-1.217	-11.47	-13.22	-3.18	-2.73
1.91943	.04687	-24.09	15.6	-7.20	-1.013	.00298	.04455	911 3 1	-5256.3	-1.218	-11.54	-13.30	-3.18	-2.80
1.91943	.04686	-26.66	-4.1	11.07	-1.286	.00161	.04276	911 4 1	-5274.8	-0.970	5.56	6.22	16.18	14.58
1.91943	.04686	-26.66	-4.1	10.99	-1.282	.00161	.04276	911 5 2	-5274.8	-0.968	5.49	6.14	16.08	14.49

Appendix I (continued). Experimental Data.

TIME#	DT	LZ	JP	V	QZ	DT00	DT10	DATENMO	RCHU	Q1	VN2	VN1	VS2	VS1
(K)	(K)	(CM)	(PA)	(CM/S)	(W/CH2)	(K)	(K)		(PA)	(W/CH2)	(CM/S)	(CM/S)	(CM/S)	(CM/S)
1.91941	.04684	-25.23	6.7	0.30	-1.106	.00224	.04395	911 6 7	-5261.0	-1.104	-4.75	-5.55	4.40	4.00
1.91939	.04682	-24.98	11.0	-3.30	-1.463	.00259	.04321	911 7 2	-5255.0	-1.157	-7.66	-9.09	.93	.86
1.91941	.04679	-25.61	1.7	6.53	-1.205	.00175	.04324	911 8 2	-5260.6	-1.079	1.36	1.43	11.31	10.81
1.91939	.04674	-25.25	6.4	0.00	-1.108	.00221	.04385	911 9 2	-5230.5	-1.108	-4.75	-5.55	4.40	4.00
1.91934	.04664	6.4	451.1	-71.50	-.273	.01954	.04530	91110 3	-4793.3	-2.297	-72.56	-83.07	-70.64	-63.27
1.91933	.04658	-3.38	317.6	-54.76	-.366	.01200	.04522	91111 3	-4920.7	-2.000	-61.34	-70.18	-58.30	-52.24
1.91934	.04644	-25.13	0.2	0.33	-1.105	.00222	.04353	91112 2	-5215.2	-1.105	-4.74	-5.53	4.30	3.99
1.91925	.04631	-21.48	49.7	-25.04	-.763	.00543	.04463	91113 1	-5156.9	-1.472	-28.37	-32.46	-22.87	-19.78
1.91922	.04622	-24.37	6.3	0.80	-1.104	.00220	.04336	91114 2	-5189.5	-1.104	-4.74	-5.53	4.30	3.99
1.91922	.04623	-22.79	37.0	-20.77	-.924	.00463	.04447	91115 1	-5159.4	-1.409	-24.31	-27.63	-17.50	-15.60
1.91925	.04627	-25.41	-0.6	13.06	-1.309	.00149	.04199	91116 1	-5208.1	-.942	7.44	8.35	16.26	16.46
1.91925	.04627	-25.41	-6.0	13.04	-1.309	.00149	.04199	91117 2	-5208.1	-.942	7.38	8.29	16.19	16.41
1.91920	.04628	-23.46	29.0	-15.90	-.886	.00405	.04437	91118 2	-5172.6	-1.334	-19.70	-22.58	-12.39	-11.00
1.91920	.04624	-23.43	23.0	-16.21	-.381	.00405	.04437	91119 1	-5172.6	-1.338	-20.00	-22.91	-12.72	-11.30
1.91923	.04619	-24.94	6.5	0.00	-1.104	.00224	.04335	91120 1	-5185.6	-1.104	-4.74	-5.53	4.30	3.99
1.91923	.04620	-25.41	-0.0	4.19	-1.227	.00164	.04253	91121 1	-5193.8	-.997	2.92	3.20	13.06	11.79
1.91922	.04614	-24.47	13.1	-5.26	-1.036	.00270	.04373	91122 1	-5177.6	-1.144	-9.73	-11.21	-1.10	-1.00
1.92384	.02466	-15.47	0.5	0.00	-.954	.00144	.02670	914 4 1	-3259.7	-.958	-4.17	-4.58	3.76	3.55
1.92380	.02457	-12.35	30.2	-25.05	-.703	.00263	.02718	914 5 1	-3203.3	-1.146	-29.12	-30.54	-22.29	-20.01
1.91942	.00315	-1.49	.9	0.00	-.496	.00023	.00273	928 9 1	-353.3	-.496	-2.29	-2.31	1.88	1.87
1.91942	.00315	-4.30	-1.34	20.99	-.395	.00014	.00247	92810 1	-397.8	-.356	19.17	19.34	22.49	22.33
1.91942	.00315	1.45	45.4	-21.22	-.364	.00022	.00248	92811 1	-303.7	-.406	-22.90	-23.11	-19.04	-19.69
1.91943	.00315	-4.83	-43.8	21.23	-.396	.00031	.00276	92812 1	-338.0	-.357	19.40	19.57	22.73	22.97
1.91943	.00315	1.43	45.4	-21.26	-.359	.00024	.00243	92813 1	-308.9	-.401	-22.93	-23.14	-19.92	-19.77
1.91936	.00317	-4.50	-43.0	21.35	-.395	.00030	.00253	92814 1	-339.6	-.354	19.53	19.70	22.84	22.68
1.91934	.00313	.51	31.8	-16.15	-.385	.00034	.00265	92815 1	-320.0	-.420	-19.92	-20.10	-16.69	-16.57
1.91933	.00313	-3.45	-30.6	17.86	-.416	.00041	.00310	92816 1	-382.3	-.383	15.94	16.38	19.44	19.38
1.91938	.00313	-.11	22.9	-15.73	-.405	.00038	.00276	92817 1	-329.0	-.435	-17.68	-17.76	-14.28	-14.18
1.91962	.00304	-3.24	-21.9	15.21	-.437	.00035	.00304	92818 1	-369.5	-.408	13.28	13.31	16.46	16.75
1.91937	.00314	-1.64	1.3	0.00	-.496	.00026	.00268	92819 1	-352.0	-.496	-2.29	-2.31	1.88	1.87
1.91935	.00312	-.79	14.5	-11.40	-.436	.00049	.00307	92820 1	-336.4	-.460	-13.42	-13.54	-9.74	-9.67
1.91939	.00307	-2.98	-12.7	11.05	-.453	.00036	.00310	92821 1	-357.9	-.433	6.96	9.03	12.76	12.68
1.91933	.00313	-.45	11.0	-8.90	-.457	.00030	.00267	92822 1	-340.8	-.474	-11.00	-11.18	-7.17	-7.11
1.91945	.00303	-2.33	-9.4	9.50	-.464	.00043	.00325	92823 1	-350.2	-.446	7.42	7.48	11.31	11.24
1.91937	.00311	-1.17	7.7	-6.78	-.406	.00034	.00282	92824 1	-341.7	-.479	-8.93	-9.01	-5.01	-4.98
1.91943	.00307	-2.11	-6.0	7.47	-.473	.00043	.00333	92825 1	-350.9	-.459	5.29	5.33	9.26	9.20
1.91943	.00313	-1.33	5.8	-5.09	-.474	.00040	.00303	92826 1	-346.8	-.484	-7.28	-7.34	-3.30	-3.27
1.91936	.00312	-1.45	-3.4	5.97	-.488	.00040	.00302	92827 1	-354.1	-.477	3.72	3.75	7.82	7.76
1.91936	.00313	-1.43	1.3	0.00	-.495	.00033	.00284	92828 1	-350.7	-.495	-2.28	-2.30	1.87	1.86
1.91946	.00322	-1.09	1.2	0.00	-.498	.00019	.00250	929 4 1	-361.6	-.498	-2.30	-2.32	1.89	1.88
1.91953	.00316	-5.75	-57.3	24.17	-.370	.00016	.00243	929 5 3	-412.9	-.325	22.46	22.65	25.57	25.39
1.91950	.00316	3.00	67.5	-26.82	-.309	.00019	.00242	929 6 3	-288.3	-.362	-28.24	-28.50	-25.65	-25.46
1.91947	.01428	-10.34	3.4	0.00	-.850	.00094	.01780	929 9 1	-2164.6	-.850	-3.82	-4.07	3.28	3.15
1.91947	.01931	-25.47	-218.8	44.20	-.456	.00059	.01664	92910 4	-2391.0	-.399	43.97	46.35	51.94	49.74
1.91953	.01924	5.23	226.3	-49.36	-.420	.00219	.01808	92911 3	-1938.2	-1.010	-51.26	-54.21	-47.76	-45.64
1.91953	.01923	-29.63	-264.0	51.59	-.944	.00055	.01641	92912 4	-2427.2	-.351	47.64	50.20	55.51	53.17
1.91951	.01925	-.45	137.3	-38.89	-.527	.00190	.01607	92913 3	-2028.6	-.988	-41.25	-43.61	-36.86	-35.22
1.91955	.01926	-19.72	-130.0	36.65	-.929	.00062	.01893	92914 4	-2297.2	-.504	32.49	34.24	40.23	38.52
1.91955	.01322	11.54	315.3	-58.13	-.333	.00247	.01807	92915 3	-1846.8	-1.031	-59.62	-63.05	-56.84	-54.30
1.91953	.01931	-10.35	3.4	0.00	-.952	.00096	.01792	92916 1	-2168.5	-.852	-3.82	-4.07	3.28	3.16
1.91966	.01929	-10.38	3.4	0.00	-.851	.00092	.01778	930 3 1	-2167.9	-.951	-3.82	-4.07	3.28	3.15

74

Appendix I (continued). Experimental Data.

TMEAN (K)	DT (K)	DZ (CM)	DP (PA)	V (CM/S)	Q2 (M/CM2)	DT0B (K)	DT1B (K)	DATENMO	RDHU (PA)	Q1 (M/CM2)	VN2 (CM/S)	VN1 (CM/S)	VS2 (CM/S)	VS1 (CM/S)
1.91963	.01224	-17.25	-34.7	32.47	-.935	.00064	.01707	930 4 4	-2265.9	-.956	28.27	29.81	36.87	34.93
1.91962	.01925	-3.50	161.1	-34.51	-.564	.00176	.01803	930 5 3	-2065.0	-.972	-37.04	-39.16	-32.34	-30.91
1.91959	.01921	-15.07	-64.1	27.52	-.927	.00066	.01711	930 6 4	-2226.2	-.605	23.46	24.72	31.10	29.06
1.91961	.01919	-5.69	69.4	-25.27	-.612	.00159	.01795	930 7 3	-2190.1	-.956	-32.01	-33.84	-26.91	-25.72
1.91962	.01914	-13.35	-42.1	24.15	-.932	.00067	.01715	930 8 4	-2200.3	-.651	28.01	21.88	27.78	24.88
1.91958	.01918	-7.25	47.0	-24.89	-.648	.00152	.01794	930 9 3	-2111.1	-.940	-27.80	-29.39	-22.40	-21.41
1.91962	.01919	-10.31	3.5	0.00	-.851	.00092	.01768	93010 1	-2156.0	-.851	-3.82	-4.87	3.28	3.15
1.91949	.00318	-1.08	1.0	0.00	-.498	.00015	.00246	10 1 4 1	-356.7	-.498	-2.29	-2.32	1.89	1.87
1.91944	.00316	-3.24	-21.5	14.94	-.439	.00017	.00241	10 1 5 1	-376.7	-.410	12.92	13.03	16.61	16.69
1.91944	.00317	-.12	23.2	-16.24	-.405	.00019	.00243	10 1 6 1	-333.5	-.437	-18.10	-18.27	-14.78	-14.59
1.91942	.01927	-16.35	3.0	6.00	-.851	.00093	.01775	10 3 4 1	-2165.0	-.851	-3.82	-4.87	3.28	3.15
1.91942	.01925	-12.54	-27.3	21.14	-.933	.00067	.01733	10 3 5 1	-2193.8	-.686	16.95	17.86	24.73	23.68
1.91953	.01928	-4.16	34.4	-24.87	-.684	.00142	.01803	10 3 6 1	-2135.0	-.930	-23.94	-25.31	-18.23	-17.82
1.91965	.01924	-11.31	-14.5	14.27	-.930	.00078	.01745	10 3 7 1	-2189.7	-.715	14.11	14.86	21.85	20.92
1.91963	.01928	-9.79	26.3	-17.38	-.715	.00134	.01801	10 3 8 1	-2143.9	-.916	-20.29	-21.46	-14.33	-13.89
1.91965	.01927	-10.35	3.5	6.00	-.853	.00094	.01778	10 3 9 1	-2165.1	-.853	-3.82	-4.87	3.28	3.16
1.91971	.01333	-11.23	-9.0	12.77	-.916	.00076	.01757	10 310 1	-2182.2	-.766	8.66	9.11	16.38	15.88
1.91970	.01321	-9.42	17.1	-11.53	-.767	.00119	.01795	10 311 1	-2154.3	-.932	-14.93	-15.81	-8.54	-8.16
1.91974	.01923	-11.04	-0.6	16.41	-.912	.00073	.01756	10 312 1	-2171.5	-.790	6.32	6.64	13.93	13.34
1.91973	.01924	-9.67	13.4	-8.46	-.794	.00072	.01792	10 313 1	-2156.6	-.894	-12.02	-12.73	-5.40	-5.14
1.91974	.01923	-10.83	-3.4	8.03	-.900	.00078	.01761	10 314 1	-2168.3	-.886	3.99	4.19	11.49	11.81
1.91973	.01924	-9.83	10.3	-6.34	-.816	.00085	.01789	10 315 1	-2159.8	-.887	-9.70	-10.28	-2.90	-2.76
1.91973	.01931	-10.37	3.7	0.00	-.853	.00097	.01781	10 316 1	-2170.3	-.853	-3.92	-4.87	3.29	3.16
1.91974	.01325	-10.89	-1.2	6.09	-.886	.00081	.01758	10 317 1	-2168.7	-.814	2.11	2.19	9.49	9.18
1.91976	.01931	-10.35	6.2	-4.36	-.828	.00104	.01788	10 318 1	-2165.8	-.879	-8.01	-8.49	-1.10	-1.04
1.91951	.00317	-1.63	.8	0.00	-.496	.00017	.00244	10 321 1	-396.3	-.496	-2.29	-2.31	1.88	1.87
1.91954	.00310	29.57	445.8	-09.64	-.031	.00026	.00243	10 322 3	96.9	-.194	-69.78	-70.94	-64.52	-68.91
1.91953	.00310	26.13	312.6	-58.56	-.059	.00026	.00244	10 323 3	-43.8	-.190	-58.83	-59.45	-58.34	-57.88
1.91955	.00316	13.94	223.5	-49.23	-.114	.00024	.00242	10 324 3	-131.9	-.219	-49.76	-50.26	-48.88	-48.41
1.91958	.00311	7.63	134.0	-38.01	-.201	.00016	.00237	10 325 3	-211.9	-.278	-38.94	-39.31	-37.23	-36.98
1.91959	.00314	5.19	98.6	-32.33	-.254	.00018	.00238	10 326 3	-259.1	-.319	-33.58	-33.81	-31.36	-31.13
1.91960	.00317	-1.63	.8	0.00	-.499	.00016	.00241	10 327 1	-355.4	-.499	-2.30	-2.32	1.89	1.88
1.90935	-.00003	.03	-.2	6.00	0.000	.00004	-.00052	9 2 1 1	3.1	0.000	0.00	0.00	0.00	0.00
1.90964	-.00001	.01	.1	0.00	0.000	.00005	-.00051	9 3 1 1	1.2	0.000	0.00	0.00	0.00	0.00
1.90961	.00003	.01	.3	0.00	0.000	.00008	-.00044	91123 1	-2.5	0.000	0.00	0.00	0.00	0.00
1.90953	.00003	-.00	.2	0.00	0.000	.00008	-.00050	91124 1	-2.6	0.000	0.00	0.00	0.00	0.00
1.91368	.00001	-.01	.0	0.00	0.000	.00004	-.00053	91125 1	-1.5	0.000	0.00	0.00	0.00	0.00
1.92223	.00002	-.01	.0	0.00	0.000	.00004	-.00058	91126 1	-2.0	0.000	0.00	0.00	0.00	0.00
1.93152	.00005	-.01	.2	0.00	0.000	.00002	-.00060	91127 1	-5.1	0.000	0.00	0.00	0.00	0.00
1.93971	.00002	-.01	-.1	0.00	0.000	-.00001	-.00066	91128 1	-1.9	0.000	0.00	0.00	0.00	0.00
1.94237	.00003	-.01	.1	0.00	0.000	-.00003	-.00068	91129 1	-3.5	0.000	0.00	0.00	0.00	0.00

Appendix 1 (continued). Experimental Data.

TIMEAN (K)	DT (K)	GZ (CM)	DP (PA)	V (CM/S)	QZ (M/CMZ)	DT08 (K)	DT18 (K)	DATENNMO	RONU (PA)	Q1 (M/CMZ)	VN2 (CM/S)	VN1 (CM/S)	VSE (CM/S)	VSI (CM/S)
1.91272	0.0002	0.01	0.1	0.00	0.000	0.0009	0.0046	914 1 1	-2.7	0.000	0.00	0.00	0.00	0.00
1.91304	0.0001	0.01	0.0	0.00	0.000	0.0010	0.0044	914 2 1	-1.5	0.000	0.00	0.00	0.00	0.00
1.91349	0.0003	0.01	0.1	0.00	0.000	0.0009	0.0046	914 3 1	-3.5	0.000	0.00	0.00	0.00	0.00
1.91367	-0.0003	0.02	0.0	0.00	0.000	0.00076	0.00151	920 1 1	3.4	0.000	0.00	0.00	0.00	0.00
1.91396	-0.0001	0.02	0.2	0.00	0.000	0.00056	0.00089	920 2 1	1.1	0.000	0.00	0.00	0.00	0.00
1.91440	0.0001	0.01	0.2	0.00	0.000	0.00041	0.00040	920 3 1	-0.7	0.000	0.00	0.00	0.00	0.00
1.91702	0.0001	0.01	0.1	0.00	0.000	0.00024	0.00002	920 4 1	-0.6	0.000	0.00	0.00	0.00	0.00
1.91910	-0.0001	0.01	-0.0	0.00	0.000	0.00009	0.00041	920 5 1	1.7	0.000	0.00	0.00	0.00	0.00
1.92114	-0.0002	0.00	-0.1	0.00	0.000	0.00000	0.00042	920 6 1	2.5	0.000	0.00	0.00	0.00	0.00
1.92234	0.0001	0.00	0.1	0.00	0.000	0.00009	0.00041	920 7 1	-0.8	0.000	0.00	0.00	0.00	0.00
1.91702	-0.0003	0.02	0.1	0.00	0.000	0.00016	0.00014	92029 1	3.3	0.000	0.00	0.00	0.00	0.00
1.91776	0.0000	0.00	0.1	0.00	0.000	0.00003	0.00056	929 1 1	0.0	0.000	0.00	0.00	0.00	0.00
1.91913	-0.0001	0.00	-0.0	0.00	0.000	0.00002	0.00057	929 2 1	0.7	0.000	0.00	0.00	0.00	0.00
1.92119	-0.0001	0.00	0.0	0.00	0.000	0.00001	0.00050	929 3 1	0.5	0.000	0.00	0.00	0.00	0.00
1.92402	-0.0006	0.00	0.0	0.00	0.000	0.00000	0.00062	929 7 1	0.2	0.000	0.00	0.00	0.00	0.00
1.90481	-0.0007	0.01	-0.3	0.00	0.000	-0.00000	0.00055	929 8 1	7.2	0.000	0.00	0.00	0.00	0.00
1.92914	-0.0006	0.02	-0.0	0.00	0.000	-0.00001	0.00064	930 1 1	3.0	0.000	0.00	0.00	0.00	0.00
1.90991	-0.0003	0.01	-0.1	0.00	0.000	0.00005	0.00053	930 2 1	0.2	0.000	0.00	0.00	0.00	0.00
1.91702	0.0001	0.00	0.1	0.00	0.000	-0.00069	0.00057	10 1 3 1	-0.7	0.000	0.00	0.00	0.00	0.00
1.90963	-0.0001	536.12	7642.3	0.00	0.000	-0.00010	0.00107	10 3 1 4	7643.0	0.000	0.00	0.00	0.00	0.00
1.92910	-0.0004	0.02	-0.5	0.00	0.000	-0.00004	0.00070	10 3 2 1	4.1	0.000	0.00	0.00	0.00	0.00
1.91903	-0.0002	0.01	-0.3	0.00	0.000	0.00005	0.00053	10 3 3 1	2.1	0.000	0.00	0.00	0.00	0.00
1.91702	-0.0002	0.02	-0.4	0.00	0.000	0.00002	0.00060	10 319 1	2.2	0.000	0.00	0.00	0.00	0.00
1.92104	-0.0002	0.02	-0.4	0.00	0.000	-0.00001	0.00062	10 320 1	1.6	0.000	0.00	0.00	0.00	0.00
1.66706	0.2941	-0.25	2.4	0.00	-0.660	0.00161	0.02040	9 2 7 1	-1326.5	-0.660	-7.19	-0.07	1.90	1.96
1.66709	0.2930	-0.13	0.0	-22.62	-0.517	0.00237	0.02066	9 2 8 1	-1479.3	-0.710	-20.25	-31.30	-21.07	-20.52
1.66790	0.2940	-11.30	-42.1	21.65	-0.708	0.00125	0.02702	9 2 9 1	-1370.4	-0.525	13.93	15.23	23.77	23.20
1.64977	0.1802	-4.42	3.2	0.00	-0.544	0.00096	0.01037	925 6 1	-927.1	-0.544	-6.49	-7.00	1.62	1.61
1.64976	0.1897	-14.30	-130.4	35.70	-0.501	0.00076	0.01705	925 7 4	-1050.1	-0.320	29.00	31.66	37.27	36.71
1.64976	0.1892	4.40	136.3	-36.76	-0.319	0.00151	0.01030	925 8 3	-709.1	-0.515	-40.57	-43.30	-35.01	-35.24
1.64974	0.1891	-11.40	-35.0	30.64	-0.514	0.00070	0.01706	925 9 4	-1019.8	-0.357	24.51	26.04	32.16	31.69
1.64977	0.1807	1.95	130.5	-32.12	-0.354	0.00140	0.01033	92510 3	-822.5	-0.524	-30.35	-30.06	-31.07	-30.50
1.64977	0.1805	-4.30	3.2	0.00	-0.546	0.00094	0.01019	92511 1	-910.9	-0.546	-6.52	-7.02	1.62	1.61
1.64970	0.1895	-4.41	3.1	0.00	-0.545	0.00094	0.01030	92515 1	-923.7	-0.545	-6.51	-7.02	1.62	1.61
1.64970	0.1893	-7.10	-20.1	10.27	-0.540	0.00075	0.01005	92517 1	-954.7	-0.454	11.73	12.43	19.90	19.61
1.64975	0.1894	-2.73	34.2	-10.70	-0.440	0.00122	0.01039	92510 1	-892.0	-0.546	-24.04	-25.72	-17.37	-17.00
1.64975	0.1894	-7.10	-20.1	10.42	-0.549	0.00070	0.01004	92519 1	-954.3	-0.453	11.07	12.50	20.05	19.76
1.64973	0.1804	-2.73	34.0	-10.50	-0.449	0.00120	0.01035	92520 1	-809.3	-0.546	-23.94	-25.60	-17.24	-16.96
1.64973	0.1806	-7.10	-20.3	10.57	-0.551	0.00070	0.01001	92521 1	-951.6	-0.455	11.99	12.71	20.20	19.91
1.64974	0.1807	-4.40	3.0	0.00	-0.545	0.00093	0.01022	92522 1	-919.9	-0.545	-6.51	-7.02	1.62	1.61
1.64973	0.1800	-0.45	-19.2	15.02	-0.554	0.00086	0.01005	92524 1	-941.9	-0.473	9.21	9.74	17.47	17.22
1.64973	0.1806	-3.30	25.2	-15.36	-0.467	0.00119	0.01031	92525 1	-897.4	-0.547	-20.94	-22.40	-13.97	-13.74
1.64977	0.1801	-0.04	-10.6	12.51	-0.550	0.00085	0.01005	92526 1	-930.6	-0.494	5.05	6.16	14.17	13.97
1.64977	0.1801	-3.45	16.1	-9.60	-0.503	0.00107	0.01022	92527 1	-903.9	-0.553	-15.61	-16.72	-8.11	-7.97
1.64979	0.1806	-0.04	-10.7	12.54	-0.559	0.00079	0.01799	92528 1	-920.4	-0.494	5.00	6.19	14.20	14.00
1.64977	0.1806	-4.21	12.4	-7.40	-0.514	0.00099	0.01010	92529 1	-905.3	-0.552	-13.54	-14.50	-5.87	-5.77
1.64979	0.1804	-0.59	-7.3	10.64	-0.562	0.00080	0.01001	92530 1	-923.7	-0.507	3.93	4.11	12.31	12.14
1.64979	0.1804	-4.07	3.0	0.00	-0.545	0.00091	0.01010	92531 1	-914.1	-0.545	-6.50	-7.01	1.62	1.61

Appendix 1 (continued). Experimental Data.

MEAN (K)	DT (K)	OZ (CM)	OP (PI)	V (CM/S)	OZ (W/GM2)	UTOB (K)	DTIB (K)	DATENHGO	ROMU (PA)	Q1 (W/GM2)	VN2 (CM/S)	VN1 (CM/S)	VS2 (CM/S)	VS1 (CM/S)
1.64976	.01874	-4.43	9.0	-5.53	-.524	.00100	.01818	92532 1	-906.9	-.552	-11.78	-12.63	-3.98	-3.98
1.64976	.01874	-5.34	-3.7	8.24	-.560	.00086	.01802	92533 1	-920.2	-.518	1.55	1.58	9.90	9.77
1.64977	.01872	-4.55	7.4	-3.88	-.532	.00095	.01814	92534 1	-908.5	-.552	-10.23	-10.98	-2.30	-2.25
1.64977	.01870	-5.18	-1.0	6.48	-.556	.00083	.01798	92535 1	-916.3	-.523	-.16	-.25	8.13	8.03
1.64977	.01869	-4.43	3.0	0.00	-.544	.00092	.01805	92536 1	-911.4	-.544	-6.50	-7.00	1.62	1.61
1.64983	.01904	-4.43	3.1	0.00	-.546	.00114	.01892	927 4 1	-931.1	-.546	-6.51	-7.02	1.62	1.61
1.64983	.01911	-23.71	-203.7	51.55	-.471	.00075	.01800	927 5 4	-1198.4	-.214	45.93	48.80	52.95	52.19
1.64983	.01911	16.43	314.5	-28.61	-.166	.00219	.01920	927 6 3	-620.3	-.481	-58.59	-62.80	-56.12	-55.19
1.64973	.01911	16.01	225.5	-48.55	-.244	.00196	.01903	927 7 3	-709.2	-.499	-49.46	-52.97	-45.83	-45.00
1.64991	.01908	-24.58	-219.3	46.44	-.479	.00079	.01805	927 8 4	-1152.9	-.246	40.78	43.33	47.91	47.22
1.64991	.01901	-.27	59.6	-28.92	-.394	.00133	.01857	927 9 3	-864.1	-.537	-31.69	-33.81	-25.82	-25.40
1.64993	.01910	-9.04	-63.8	25.74	-.531	.00088	.01820	92710 3	-998.3	-.398	19.40	20.72	27.32	26.92
1.64993	.01910	-4.04	-63.6	25.18	-.529	.00080	.01820	92711 4	-998.3	-.398	18.87	20.05	26.75	26.35
1.64997	.01906	20.31	447.7	-27.54	-.095	.00272	.01993	92712 3	-435.2	-.479	-68.67	-73.70	-67.26	-66.13
1.65001	.01913	-9.04	-41.2	21.86	-.547	.00110	.01894	92713 1	-977.7	-.433	15.34	16.28	23.49	23.14
1.65001	.01913	-1.04	2.3	0.00	-.547	.00104	.01870	92714 1	-933.5	-.547	-6.53	-7.04	1.63	1.62
1.65001	.01913	-1.13	17.8	-21.33	-.430	-.37111	-.37111	92715 1	-888.7	-.546	-27.03	-28.92	-20.62	-20.29
1.65236	.00000	.62	.2	0.00	0.000	.00001	.00014	9 2 6 1	.1	0.000	0.00	0.00	0.00	0.00
1.65392	.00003	.61	.2	0.00	0.000	.00007	-.41417	9 210 1	-1.3	0.000	0.00	0.00	0.00	0.00
1.65924	-.00000	.00	.0	0.00	0.000	-.00001	-.00017	925 1 1	.2	0.000	0.00	0.00	0.00	0.00
1.65963	.00004	.03	.2	0.00	0.000	-.00000	.00016	925 2 1	-1.6	0.000	0.00	0.00	0.00	0.00
1.64993	.00001	.01	.1	0.00	0.000	-.00004	.00015	925 3 1	-.3	0.000	0.00	0.00	0.00	0.00
1.64924	.00001	.01	.1	0.00	0.000	-.00003	.00018	925 4 1	-.4	0.000	0.00	0.00	0.00	0.00
1.64026	.00001	.01	.1	0.00	0.000	-.00005	.00016	925 5 1	-.2	0.000	0.00	0.00	0.00	0.00
1.64024	.00001	.00	.0	0.00	0.000	-.00002	.00023	92512 1	-.4	0.000	0.00	0.00	0.00	0.00
1.64990	-.00001	-.00	-.1	0.00	0.000	-.00002	.00020	92513 1	.2	0.000	0.00	0.00	0.00	0.00
1.65941	.00004	-.61	.1	0.00	0.000	.00004	.00021	92514 1	-1.8	0.000	0.00	0.00	0.00	0.00
1.64020	.00002	-.00	.0	0.00	0.000	-.00004	.00018	92515 1	-.9	0.000	0.00	0.00	0.00	0.00
1.65921	-.00001	.00	-.0	0.00	0.000	.00061	.00170	927 1 1	.7	0.000	0.00	0.00	0.00	0.00
1.64971	-.00002	.06	-.0	0.00	0.000	.00020	.00069	927 2 1	1.0	0.000	0.00	0.00	0.00	0.00
1.64624	-.00003	.61	-.0	0.00	0.000	.00009	.00050	927 3 1	1.2	0.000	0.00	0.00	0.00	0.00
1.63395	-.00002	-.61	-.2	0.00	0.000	-.00009	.00012	10 1 1 1	.7	0.000	0.00	0.00	0.00	0.00
1.63997	-.00001	-.61	-.2	0.00	0.000	-.00011	.00009	10 1 2 1	.4	0.000	0.00	0.00	0.00	0.00
1.39517	.01926	-1.40	3.9	0.00	-.231	.00102	.01785	9 3 8 1	-357.6	-.231	-8.42	-9.25	.69	.69
1.39520	.01926	-4.43	-40.5	18.71	-.208	.00101	.01768	9 3 9 1	-402.0	-.169	11.12	11.93	19.33	19.22
1.39513	.01925	1.33	45.3	-18.25	-.158	.00130	.01786	9 310 1	-312.9	-.198	-24.02	-26.19	-17.78	-17.66
1.39534	.01940	-1.42	3.9	0.00	-.231	.00102	.01804	9 4 2 1	-360.5	-.231	-8.41	-9.25	.69	.69
1.39539	.01949	-8.07	-34.9	26.24	-.182	.00102	.01776	9 4 3 1	-451.1	-.127	19.62	21.14	26.78	26.62
1.39533	.01949	-8.07	-34.3	26.73	-.186	.00102	.01776	9 4 4 3	-451.1	-.130	19.95	21.49	27.25	27.39
1.39539	.01949	-8.07	-34.9	25.97	-.181	.00102	.01776	9 4 5 3	-451.1	-.127	19.37	20.87	26.51	26.35
1.39538	.01954	4.43	32.9	-30.87	-.108	.00144	.01818	9 4 6 3	-274.0	-.178	-34.81	-38.01	-30.55	-30.34
1.39538	.01954	4.43	32.9	-27.20	-.118	.00144	.01818	9 4 7 3	-274.0	-.190	-31.50	-34.40	-26.85	-26.66
1.39538	.01954	4.43	32.9	-25.57	-.122	.00144	.01818	9 4 8 1	-274.0	-.180	-30.01	-32.78	-25.21	-25.03
1.39561	.01983	-14.35	-173.7	37.15	-.154	.00091	.01794	9 4 9 4	-546.4	-.078	31.56	34.01	37.60	37.38
1.39557	.01983	10.65	181.9	-38.86	-.064	.00167	.01858	9 410 3	-190.9	-.157	-41.18	-45.14	-38.67	-38.39
1.39567	.02003	23.16	354.9	-55.62	-.008	.00242	.01906	9 411 3	-16.7	-.152	-55.89	-61.69	-55.60	-55.16

Appendix 1 (continued). Experimental Data.

THEAN (K)	DT (K)	OZ (CM)	JP (PA)	V (CM/S)	OZ (M/CM2)	DT08 (K)	DT18 (K)	DATENMU	ROMU (PA)	G1 (M/CM2)	VN2 (CM/S)	VN1 (CM/S)	VS2 (CM/S)	VS1 (CM/S)
1.39572	.02007	-12.73	-235.5	43.71	-.144	.03076	.01806	9 412 4	-613.0	-.097	38.48	41.43	44.14	43.68
1.39569	.02001	16.91	271.0	-48.12	-.029	.03199	.01846	9 413 3	-109.4	-.150	-49.25	-54.18	-48.18	-47.74
1.39561	.01957	-11.14	-129.0	31.76	-.164	.03096	.01782	9 415 4	-496.7	-.099	25.79	27.78	32.25	32.86
1.39553	.01964	16.45	271.1	-46.67	-.031	.03197	.01852	9 416 3	-90.0	-.145	-47.78	-52.48	-46.58	-46.23
1.39555	.01969	-15.47	-135.4	39.56	-.152	.03086	.01782	9 417 4	-568.6	-.073	34.03	36.63	40.02	39.78
1.39546	.01961	7.57	137.7	-32.97	-.091	.03196	.01828	9 418 3	-230.8	-.167	-36.28	-39.67	-32.78	-32.47
1.39539	.01945	-1.01	4.0	0.00	-.233	.03182	.01804	9 419 1	-361.4	-.233	-8.47	-9.32	.69	.70
1.39531	.01954	-6.53	-62.4	22.73	-.194	.03112	.01791	9 420 1	-430.8	-.146	15.69	16.98	23.38	23.16
1.39523	.01972	-.25	26.7	-12.84	-.188	.03122	.01835	9 421 1	-344.0	-.217	-19.68	-21.52	-12.28	-12.19
1.39517	.01977	-3.39	-17.7	13.28	-.226	.03104	.01824	9 422 1	-389.4	-.197	5.08	5.48	13.95	13.87
1.39514	.01980	2.88	71.2	-22.41	-.140	.03141	.01842	9 423 1	-381.8	-.191	-27.98	-38.87	-21.99	-21.83
1.39513	.01984	-2.44	-4.2	8.63	-.236	.03115	.01835	9 424 1	-377.3	-.217	.86	-.86	9.33	9.28
1.39511	.01992	-1.19	13.7	-6.55	-.216	.03115	.01856	9 425 1	-358.9	-.231	-14.39	-15.79	-5.90	-5.85
1.39509	.02001	-2.13	.5	4.57	-.236	.03108	.01856	9 426 1	-376.8	-.226	-3.98	-4.46	5.27	5.25
1.39574	.02004	-1.20	4.4	-4.13	-.223	.03111	.01868	9 427 1	-367.6	-.233	-12.24	-13.45	-3.47	-3.43
1.39560	.02007	-1.44	3.8	4.00	-.235	.03106	.01864	9 428 1	-373.8	-.238	-8.51	-9.39	.78	.78
1.39583	.02118	-2.04	3.6	0.00	-.238	.03115	.01971	9 8 5 1	-395.8	-.238	-8.68	-9.55	.71	.71
1.39587	.01902	-1.84	3.6	0.00	-.229	.03098	.01764	9 8 6 1	-393.4	-.229	-8.35	-9.58	.68	.68
1.39584	.01918	-8.06	-85.2	27.08	-.181	.03090	.01742	9 8 7 3	-444.8	-.126	28.48	22.84	27.42	27.46
1.39534	.01936	4.45	92.8	-27.72	-.117	.03138	.01791	9 8 8 3	-269.7	-.179	-31.98	-34.89	-27.37	-27.18
1.39574	.03517	-5.61	5.1	0.00	-.326	.03385	.05295	9 8 9 1	-1032.9	-.326	-18.86	-14.24	.96	.99
1.39577	.03523	-24.35	-211.5	47.46	-.381	.03158	.04926	9 810 4	-1300.6	-.182	34.74	43.88	48.99	47.77
1.39580	.03523	10.62	227.4	-44.54	-.184	.03963	.05371	9 811 3	-811.8	-.388	-48.88	-61.88	-44.23	-43.37
1.39584	.03523	-27.43	-305.3	49.92	-.387	.03154	.04890	9 812 4	-1345.1	-.896	36.99	45.72	51.86	50.21
1.39583	.03528	16.27	316.3	-53.55	-.659	.03128	.05397	9 813 3	-724.0	-.486	-83.83	-71.38	-83.37	-82.32
1.39593	.03533	3.77	138.7	-34.88	-.159	.03884	.05368	9 814 3	-983.0	-.377	-39.96	-51.16	-34.19	-33.52
1.39583	.03516	-5.61	5.0	0.00	-.326	.03386	.05288	9 816 1	-1032.8	-.326	-18.89	-14.27	.96	.99
1.39585	.03515	-14.94	-124.3	33.45	-.371	.03212	.05063	9 817 4	-1166.2	-.170	21.88	26.02	34.55	33.97
1.39584	.03521	1.27	132.9	-24.89	-.186	.03728	.05349	9 818 3	-936.2	-.373	-36.88	-46.17	-29.33	-28.74
1.39583	.03525	-12.47	-92.5	28.33	-.368	.03224	.05109	9 819 4	-1132.5	-.196	16.84	19.72	29.38	28.89
1.39583	.03525	17.11	324.1	0.00	-.327	.03385	.05298	9 9 1 1	-711.6	-.327	-18.91	-14.32	.97	.99
1.39578	.03513	-5.59	5.2	0.00	-.327	.03383	.05286	9 9 2 1	-1032.0	-.327	-18.92	-14.31	.97	.99
1.39577	.03511	-5.53	5.3	0.00	-.327	.03377	.05284	9 9 3 1	-1031.7	-.327	-18.92	-14.31	.97	.99
1.39574	.03547	-10.24	-61.6	24.32	-.367	.03253	.05122	9 9 4 1	-1095.8	-.220	12.89	14.69	25.40	24.98
1.39573	.03543	-.92	71.7	-23.44	-.218	.03654	.05318	9 9 5 1	-961.7	-.363	-38.71	-39.29	-22.88	-22.34
1.39496	.03542	-5.45	5.4	0.00	-.323	.03374	.05198	9 911 1	-1011.3	-.323	-18.84	-14.15	.95	.98
1.39494	.03542	-4.59	-39.0	28.32	-.362	.03253	.05080	9 912 1	-1055.9	-.240	8.19	9.88	21.39	21.05
1.39495	.03531	-2.34	58.0	-19.88	-.239	.03593	.05253	9 913 1	-968.3	-.355	-27.89	-34.62	-18.38	-18.01
1.39499	.03531	-5.46	5.6	0.00	-.324	.03379	.05207	9 914 1	-1012.8	-.324	-18.88	-14.21	.96	.98
1.39443	.03532	-7.85	-25.5	17.64	-.363	.03250	.05102	9 915 1	-1044.2	-.257	5.47	6.38	18.72	18.42
1.39499	.03534	-3.27	36.7	-15.98	-.255	.03557	.05251	9 916 1	-982.2	-.352	-24.54	-31.41	-15.23	-14.92
1.39501	.03535	-7.02	-16.6	15.59	-.362	.03260	.05118	9 917 1	-1035.9	-.268	3.45	3.84	16.66	16.40
1.39504	.03535	-3.93	27.8	-12.91	-.270	.03517	.05251	9 918 1	-991.5	-.343	-21.96	-28.16	-12.11	-11.86
1.39505	.03537	-5.45	5.6	0.00	-.325	.03379	.05211	9 919 1	-1014.3	-.325	-18.90	-14.24	.96	.98
1.39504	.03533	-6.40	-7.8	12.07	-.357	.03271	.05141	9 920 1	-1026.9	-.284	.10	-.37	13.12	12.93
1.39507	.03537	-4.53	19.0	-8.56	-.290	.03471	.05245	9 921 1	-1000.9	-.342	-18.30	-23.56	-7.70	-7.53
1.39505	.03537	-6.15	-4.2	9.92	-.351	.03298	.05159	9 922 1	-1024.0	-.292	-1.87	-2.86	10.96	10.80
1.39508	.03539	-4.79	15.4	-6.65	-.300	.03445	.05241	9 923 1	-1004.8	-.340	-16.71	-21.55	-5.77	-5.62
1.39566	.03539	-5.48	5.5	0.00	-.325	.03378	.05213	9 924 1	-1014.7	-.325	-18.89	-14.22	.96	.98
1.39509	.03540	-5.95	-1.2	7.21	-.343	.03389	.05176	9 925 1	-1021.7	-.381	-4.29	-5.91	8.23	8.12
1.39513	.03539	-5.01	12.2	-4.86	-.388	.03426	.05237	9 926 1	-1008.4	-.337	-15.17	-19.62	-3.95	-3.84
1.39511	.03541	-5.79	1.1	4.98	-.337	.03323	.05188	9 927 1	-1019.8	-.387	-6.32	-8.46	5.97	5.90
1.39513	.03541	-5.16	18.6	-3.61	-.314	.03415	.05232	9 928 1	-1010.9	-.336	-14.13	-18.30	-2.68	-2.59

Appendix I (continued). Experimental Data.

TIME (K)	DT (K)	DZ (CM)	DP (PA)	V (CM/S)	Q2 (W/CM2)	DT08 (K)	DT18 (K)	DATEHMO	ROMU (PA)	Q1 (W/CM2)	VM2 (CM/S)	VM1 (CM/S)	VS2 (CM/S)	VS1 (CM/S)
1.39512	.05443	-5.43	5.3	0.00	-.325	.00379	.05217	9 929 1	-1015.0	-.325	-10.00	-14.22	.96	.90
1.39531	.01924	-1.79	4.0	0.00	-.231	.00194	.01903	915 8 1	-357.2	-.231	-0.41	-9.25	.69	.69
1.39533	.01917	-4.91	-0.5	10.95	-.206	.00120	.01041	915 9 1	-400.4	-.167	11.43	12.26	19.56	19.40
1.39529	.01918	1.34	40.4	-10.46	-.150	.00199	.01954	91510 1	-311.0	-.190	-24.22	-26.41	-17.99	-17.07
1.39344	.00120	-.04	1.3	0.00	-.093	.00040	.00214	91512 1	-22.5	-.093	-3.50	-3.61	.20	.20
1.39343	.00125	3.00	45.7	-10.04	-.003	.00050	.00215	91513 1	22.4	-.006	-10.21	-10.34	-10.00	-10.07
1.39346	.00120	-.05	1.1	0.00	-.093	.00005	.00105	91516 1	-22.7	-.093	-3.57	-3.60	.20	.20
1.39347	.00120	10.70	207.7	-40.00	.019	.00014	.00102	91517 3	244.0	-.001	-40.17	-40.93	-40.94	-40.00
1.39349	.00130	12.44	170.9	-39.35	.014	.00003	.00091	91518 3	154.7	.001	-30.03	-39.31	-39.39	-39.00
1.39349	.00127	-.05	1.2	0.00	-.095	-.00003	.00000	91519 1	-22.4	-.095	-3.65	-3.67	.20	.20
1.39349	.00123	-.05	1.1	0.00	-.093	.00034	.00101	916 5 1	-21.0	-.093	-3.50	-3.61	.20	.20
1.39350	.00124	-1.02	-21.1	12.10	-.033	.00031	.00160	916 6 1	-44.9	-.032	10.03	10.00	12.20	12.10
1.39352	.00124	1.51	23.3	-12.52	-.017	.00045	.00203	916 7 1	.2	-.019	-13.19	-13.27	-12.47	-12.67
1.39351	.00123	-.05	1.1	0.00	-.093	.00034	.00170	916 8 1	-21.0	-.093	-3.50	-3.61	.20	.20
1.39347	.00123	-.49	-12.2	0.79	-.057	.00037	.00167	916 9 1	-35.1	-.056	6.59	6.62	0.96	0.96
1.39351	.00123	.39	14.4	-9.01	-.047	.00037	.00175	91610 1	-0.4	-.040	-10.00	-10.07	-0.07	-0.06
1.39340	.00110	-.74	-0.7	7.24	-.065	.00036	.00170	91611 1	-30.0	-.064	4.76	4.77	7.43	7.43
1.39340	.00115	.63	10.0	-7.34	-.054	.00041	.00177	91612 1	-10.6	-.055	-9.43	-9.40	-7.10	-7.17
1.39346	.00109	-.00	1.0	0.00	-.090	.00035	.00163	91613 1	-19.3	-.090	-3.44	-3.46	.27	.27
1.39349	.00125	-.05	1.1	0.00	-.093	.00034	.00175	91616 1	-22.2	-.093	-3.57	-3.59	.20	.20
1.39349	.00121	-.74	-0.7	7.40	-.065	.00036	.00171	91617 1	-31.3	-.064	4.90	5.00	7.65	7.65
1.39340	.00121	.63	10.0	-7.26	-.057	.00035	.00171	91610 1	-11.5	-.050	-9.44	-9.49	-7.10	-7.09
1.39353	.00110	-.37	-3.4	4.04	-.077	.00039	.00172	91619 1	-25.4	-.076	1.90	1.91	5.07	5.07
1.39349	.00114	.25	5.5	-3.36	-.076	.00034	.00171	91620 1	-16.6	-.077	-6.09	-6.92	-3.73	-3.73
1.39351	.00114	-.04	1.1	0.00	-.091	.00032	.00160	91621 1	-20.1	-.091	-3.49	-3.51	.27	.27
1.39352	.00119	-.35	-3.3	4.04	-.076	.00036	.00167	91622 1	-25.5	-.076	1.91	1.92	5.06	5.06
1.39349	.00114	.27	5.0	-4.05	-.075	.00033	.00165	91623 1	-15.7	-.075	-6.92	-6.96	-3.52	-3.02
1.39353	.00115	-.51	-5.5	5.04	-.071	.00036	.00166	91624 1	-27.0	-.071	3.14	3.15	6.09	6.09
1.39356	.00119	.43	4.9	-5.54	-.067	.00037	.00171	91625 1	-14.4	-.060	-0.13	-0.17	-5.34	-5.33
1.39355	.00116	-.04	1.1	0.00	-.092	.00030	.00166	91626 1	-20.5	-.092	-3.54	-3.56	.20	.20
1.39347	.00117	-.06	1.0	0.00	-.092	-.00010	.00072	10 330 1	-20.9	-.092	-3.53	-3.55	.27	.27
1.39375	.00141	24.95	306.9	-50.61	.013	.00016	.00107	10 331 3	330.6	-.010	-55.09	-57.00	-56.67	-56.50
1.39392	.00141	0.32	39.1	-20.92	.006	-.00009	.00094	10 332 3	72.7	-.001	-20.09	-20.97	-20.93	-20.91
1.39307	.00144	9.32	134.0	-34.10	.010	-.00005	.00103	10 333 3	107.0	-.000	-33.79	-34.10	-34.19	-34.16
1.39394	.00140	-.05	1.4	0.00	-.099	-.00010	.00090	10 334 3	-25.9	-.099	-3.01	-3.04	.30	.30
1.39349	.00134	-.00	1.5	0.00	-.096	-.00009	.00007	10 5 3 1	-23.5	-.096	-3.67	-3.70	.29	.29
1.39357	.00127	-.04	1.4	0.00	-.094	-.00010	.00079	10 5 4 1	-22.3	-.094	-3.61	-3.63	.20	.20
1.39360	.00125	24.97	306.9	-50.67	.019	.00013	.00009	10 5 5 3	333.7	-.009	-55.92	-57.00	-56.73	-56.64
1.39357	.00121	15.59	223.5	-44.13	.015	-.00003	.00079	10 5 6 3	200.9	-.001	-43.57	-44.17	-44.10	-44.13
1.39357	.00124	9.34	134.7	-33.06	.009	-.00006	.00079	10 5 7 3	111.5	-.000	-32.72	-33.06	-33.00	-33.06
1.39362	.00120	9.34	134.7	-33.93	.010	-.00000	.00077	10 5 8 3	110.9	.001	-33.54	-33.90	-33.96	-33.93
1.39360	.00120	0.44	39.2	-20.03	.007	-.00010	.00079	10 5 9 3	75.3	.000	-20.55	-20.01	-20.05	-20.03
1.39361	.00125	2.15	32.5	-15.04	-.011	-.00009	.00077	10 510 1	9.1	-.013	-15.45	-15.55	-15.00	-15.00
1.39364	.00120	-.04	1.3	0.00	-.094	-.00009	.00077	10 511 1	-22.2	-.094	-3.61	-3.63	.20	.20
1.39515	.01910	-1.70	3.5	0.00	-.231	.00095	.01771	10 514 1	-354.5	-.231	-0.42	-9.25	.69	.69
1.39519	.01924	-3.35	-10.1	10.50	-.222	.00009	.01765	10 515 1	-379.3	-.193	5.70	6.06	14.46	14.30
1.39515	.01925	-.22	26.3	-12.00	-.100	.00110	.01700	10 516 1	-334.9	-.216	-15.75	-21.55	-12.32	-12.24
1.39522	.01920	-2.72	-9.3	10.09	-.229	.00000	.01765	10 517 1	-369.7	-.206	2.65	2.76	11.67	11.61
1.39519	.01923	-.05	17.4	-0.00	-.207	.00112	.01703	10 518 1	-347.6	-.226	-10.35	-17.00	-0.10	-0.12
1.39510	.01917	-1.00	3.0	0.00	-.232	.00090	.01776	10 519 1	-356.0	-.232	-0.44	-9.20	.69	.69
1.39510	.01920	-2.27	-2.0	0.12	-.234	.00092	.01770	10 520 1	-353.2	-.217	-.60	-.56	0.02	0.77

Appendix 1 (continued). Experimental Data.

TIME AN (K)	DT (K)	DZ (CM)	JP (PA)	V (CM/S)	U2 (W/CM2)	DT08 (K)	DT18 (K)	DATENMC	RDMU (PA)	U1 (W/CM2)	VN2 (CM/S)	VN1 (CM/S)	V52 (CM/S)	V51 (CM/S)
1.39514	.01920	-1.33	10.5	-4.07	-.219	.00104	.01783	10 521 1	-349.9	-.230	-12.07	-14.00	-4.22	-4.10
1.39517	.01918	-1.35	-10.4	13.00	-.222	-.11624	.01755	10 522 1	-378.3	-.192	5.79	6.16	14.94	14.45
1.39516	.01909	-1.79	3.0	0.00	-.231	.00095	.01766	10 523 1	-354.6	-.231	-0.42	-9.25	.69	.69
1.40459	-.00002	-.01	-.1	0.00	0.000	-.00051	-.00067	9 3 2 1	.3	0.000	0.00	0.00	0.00	0.00
1.39974	.00010	-.01	.1	0.00	0.000	-.00031	-.00049	9 3 3 1	-1.9	0.000	0.00	0.00	0.00	0.00
1.39487	-.00000	-.01	-.1	0.00	0.000	-.00012	-.00041	9 3 4 1	-.1	0.000	0.00	0.00	0.00	0.00
1.39015	.00001	-.00	-.00	0.00	0.000	-.00003	-.00033	9 3 5 1	-.2	0.000	0.00	0.00	0.00	0.00
1.38553	-.00003	-.00	-.1	0.00	0.000	-.00007	-.00044	9 3 6 1	.5	0.000	0.00	0.00	0.00	0.00
1.41403	-.00003	-.00	-.1	0.00	0.000	-.00051	-.00064	9 3 7 1	.5	0.000	0.00	0.00	0.00	0.00
1.38561	.00001	.01	.1	0.00	0.000	-.00004	-.00040	9 4 1 1	-.1	0.000	0.00	0.00	0.00	0.00
1.40497	-.00004	.03	.0	0.00	0.000	-.00053	-.00070	9 4 1 1	1.1	0.000	0.00	0.00	0.00	0.00
1.38561	.00000	-.01	-.1	0.00	0.000	-.00003	-.00040	9 4 2 1	-.2	0.000	0.00	0.00	0.00	0.00
1.40404	.00004	-.02	-.3	0.00	0.000	-.00054	-.00070	9 8 1 1	-1.0	0.000	0.00	0.00	0.00	0.00
1.38556	.00004	-.02	-.2	0.00	0.000	-.00003	-.00045	9 8 2 1	-.9	0.000	0.00	0.00	0.00	0.00
1.38776	.00000	-.02	-.1	0.00	0.000	.00003	-.00065	9 8 3 1	-1.1	0.000	0.00	0.00	0.00	0.00
1.42105	-.00000	-.02	-.3	0.00	0.000	-.00054	-.00045	9 8 4 1	-.3	0.000	0.00	0.00	0.00	0.00
1.38031	-.00002	.00	.0	0.00	0.000	.00001	-.00062	9 9 6 1	.3	0.000	0.00	0.00	0.00	0.00
1.42113	.00001	-.00	-.00	0.00	0.000	-.00053	-.00050	9 9 7 1	-.1	0.000	0.00	0.00	0.00	0.00
1.40405	.00001	0.00	.0	0.00	0.000	-.00051	-.00065	9 9 8 1	-.2	0.000	0.00	0.00	0.00	0.00
1.38561	.00000	.00	.1	0.00	0.000	-.00003	-.00040	9 9 9 1	-.8	0.000	0.00	0.00	0.00	0.00
1.38765	.00002	.00	.1	0.00	0.000	.00004	-.00061	9 9 10 .	-.2	0.000	0.00	0.00	0.00	0.00
1.40407	-.00001	.03	.0	0.00	0.000	-.00003	-.00021	9 15 1 1	.3	0.000	0.00	0.00	0.00	0.00
1.40009	.00013	.03	.3	0.00	0.000	-.00002	.00018	9 15 2 1	-2.3	0.000	0.00	0.00	0.00	0.00
1.39519	.00000	.01	.1	0.00	0.000	.00027	.00062	9 15 3 1	.0	0.000	0.00	0.00	0.00	0.00
1.39520	-.00002	.01	.1	0.00	0.000	.00047	.00120	9 15 4 1	.4	0.000	0.00	0.00	0.00	0.00
1.39057	.00001	.01	.1	0.00	0.000	.00062	.00130	9 15 5 1	-.0	0.000	0.00	0.00	0.00	0.00
1.38500	.00005	.01	.2	0.00	0.000	.00050	.00112	9 15 6 1	-.7	0.000	0.00	0.00	0.00	0.00
1.39504	-.00000	.01	.1	0.00	0.000	.00049	.00093	9 15 7 1	.2	0.000	0.00	0.00	0.00	0.00
1.39276	.00003	.01	.2	0.00	0.000	.00047	.00093	9 15 11 1	-.4	0.000	0.00	0.00	0.00	0.00
1.39212	.00000	536.02	7620.2	0.00	0.000	.00000	.00016	9 15 14 1	7619.0	0.000	0.00	0.00	0.00	0.00
1.39202	-.00000	0.00	-.0	0.00	0.000	.00003	-.00009	9 15 15 1	.0	0.000	0.00	0.00	0.00	0.00
1.39206	-.00002	-.01	-.1	0.00	0.000	.00034	.00071	9 16 1 1	.3	0.000	0.00	0.00	0.00	0.00
1.39374	-.00001	-.01	-.1	0.00	0.000	.00031	.00072	9 16 2 1	.0	0.000	0.00	0.00	0.00	0.00
1.39667	.00001	-.01	-.1	0.00	0.000	.00030	.00071	9 16 3 1	-.2	0.000	0.00	0.00	0.00	0.00
1.39293	.00000	-.00	-.0	0.00	0.000	.00028	.00065	9 16 4 1	-.1	0.000	0.00	0.00	0.00	0.00
1.39293	.00001	-.00	-.0	0.00	0.000	.00027	.00057	9 16 14 1	-.3	0.000	0.00	0.00	0.00	0.00
1.39203	-.00001	-.00	-.1	0.00	0.000	.00029	.00059	9 16 15 1	.1	0.000	0.00	0.00	0.00	0.00
1.39291	-.00001	0.00	-.0	0.00	0.000	.00029	.00057	9 16 27 1	.1	0.000	0.00	0.00	0.00	0.00
1.39412	-.00000	0.00	-.0	0.00	0.000	.00025	.00057	9 16 29 1	.0	0.000	0.00	0.00	0.00	0.00
1.39271	-.00002	.00	.0	0.00	0.000	-.00011	-.00042	10 3 28 1	.3	0.000	0.00	0.00	0.00	0.00

Appendix 1 (continued). Experimental Data.

DT	DF	V	Q2	DT0B	DT1B	DATENMO	RDNU	Q1	VN2	VN1	VS2	VS1
(S)	(PA)	(CM/S)	(M/CM2)	(K)	(K)		(PA)	(M/CM2)	(CM/S)	(CM/S)	(CM/S)	(CM/S)
10 329 1	0.0	0.00	0.000	-0.00014	-0.00043	10 329 1	0.6	0.000	0.00	0.00	0.00	0.00
10 5 1 1	0.0	0.00	0.000	-0.00016	-0.00042	10 5 1 1	0.6	0.000	0.00	0.00	0.00	0.00
10 5 2 1	0.0	0.00	0.000	-0.00019	-0.00040	10 5 2 1	1.1	0.000	0.00	0.00	0.00	0.00
10 512 1	0.1	0.00	0.000	-0.00057	-0.00073	10 512 1	0.7	0.000	0.00	0.00	0.00	0.00
10 513 1	0.0	0.00	0.000	-0.00012	-0.00049	10 513 1	0.4	0.000	0.00	0.00	0.00	0.00

APPENDIX 2

The purpose of this appendix is to prove the assertion that the formulas already given for the overall energy balance and energy flux -- in particular eq (36) -- are still correct when the gravitational and work terms are taken into account. Our procedure is as before, i.e., equating the change in energy calculated by two different methods.

In the first method, we calculate the change in the total energy E of the helium contained within the control volume (the inside vessel), due to the increment in its mass, when the temperature is held constant. It is

$$dE = dU + dE_{\text{grav}} \quad (\text{A2.1})$$

where dE_{grav} is the change in the gravitational potential energy, and dU is again the change in internal energy of the helium.

We can prove that the variation of u within the liquid is negligible, by considering its variation with depth,

$$\frac{du}{dz} = \left(\frac{\partial u}{\partial T}\right)_p \frac{dT}{dz} + \left(\frac{\partial u}{\partial P}\right)_T \frac{dP}{dz} \quad (\text{A2.2})$$

For equilibrium within the control volume, with a gravitational field present, we still have $dT = 0$, but now $dP/dz = -\rho g$, i.e., the pressure varies with depth within the liquid. However, using the measured values of expansivity and compressibility for the liquid to evaluate the size of the pressure derivative, we find that

$$\frac{du}{dz} = -\rho \left(\frac{\partial u}{\partial P}\right)_T g$$

is much smaller (< 1%) than the corresponding variation of the gravitational potential energy density with depth ($= d(gz)/dz = g$), so that it can be safely neglected.

Since u everywhere within the liquid has nearly the same value that it has at the surface, we can repeat the entire argument used to eliminate from dU any explicit dependence on the vapor; we obtain the same equations [eqs (31) - (35)], as long as we realize that the pressure in eq (33) is the pressure of the vapor. Therefore, eq (35) is still valid if we evaluate the enthalpy of the liquid at the pressure of the surface, which we designate as P'_2 .

We may evaluate the change in the gravitational potential, without loss of generality, by assuming the inside space to have a constant horizontal cross-section A_1 , and by evaluating the gain or loss of liquid at the surface (altitude z_2) and at the bottom of the inside space (altitude z_b). It is

$$dE_{\text{grav}} = g(z_2 \rho A_1 dz_2 - z_b \rho A_1 dz_b) \quad (\text{A2.3})$$

We can express this differently by using eq (28) and the identities $dz_2/dt = V_1$ and $dz_b/dt = V_b$, and then combine it with the result for dU , to obtain

$$dE = \left(\rho u_2 + P'_2 - T_2 \left(\frac{\partial P}{\partial T} \right)_{\text{svp}, T_2} \right) V A_x dt + \rho g (z_2 - z_b) V_b A_1 dt + \rho g z_2 V A_x dt \quad (\text{A2.4})$$

where, as before, T_2 is the inside temperature, and u_2 is the liquid energy density at this temperature.

The second method is to calculate the energy that passes through the boundary of the control volume. It is the sum of the electrical heat, the work done on the fluid by the walls of its container, and the energy that enters through the flow tube.

$$dE = dQ - dW + j_3 A_x dt \quad (\text{A2.5})$$

The work term is evaluated simply by the pressure-volume work done on the fluid by the top and bottom of the inside space, taking into account the hydrostatic pressure difference.

$$-dW = -P'_2 V_b A_1 dt + \left(P'_2 + g(z_2 - z_b) \right) V_b A_1 dt + g(z_2 - z_b) V_b A_1 dt \quad (\text{A2.6})$$

The total energy current j_e contains, as before, the enthalpy current and the heat current, but we must also add a gravitational potential energy current, $gz_{\text{ent}} \rho V$, where z_{ent} is the altitude at which the fluid enters the inside space. The enthalpy is to be evaluated at the pressure at which the liquid enters, which is, by continuity in the pressure, the local fluid pressure at the altitude of entry, $P'_2 + \rho g(z_2 - z_{\text{ent}})$. Collecting terms, we find that the z_{ent} terms cancel to give

$$j_e = \left(\rho u_{\text{ent}} + P'_2 + \dot{q}_{\text{ent}} + \rho g z_2 \right) V \quad (\text{A2.7})$$

Then substituting into eq (A2.5), and equating it to eq (A2.4), we find that all the remaining terms containing g cancel, and we recover eq (36).

U.S. DEPT. OF COMM. BIBLIOGRAPHIC DATA SHEET	1. PUBLICATION OR REPORT NO. NBS TN-1002	2. Gov't Accession No.	3. Recipient's Accession No.
4. TITLE AND SUBTITLE MEASUREMENTS OF COMBINED AXIAL MASS AND HEAT TRANSPORT IN He II		5. Publication Date February 1978	
7. AUTHOR(S) WARREN W. JOHNSON AND MICHAEL C. JONES		6. Performing Organization Code 275.05	
9. PERFORMING ORGANIZATION NAME AND ADDRESS NATIONAL BUREAU OF STANDARDS DEPARTMENT OF COMMERCE WASHINGTON, D.C. 20234		8. Performing Organ. Report No.	
12. Sponsoring Organization Name and Complete Address (Street, City, State, ZIP)		10. Project/Task/Work Unit No. 2750551	
15. SUPPLEMENTARY NOTES		11. Contract/Grant No.	
13. Type of Report & Period Covered		14. Sponsoring Agency Code	
16. ABSTRACT (A 200-word or less factual summary of most significant information. If document includes a significant bibliography or literature survey, mention it here.) An experiment was performed that allowed measurements of both axial mass and heat transport of He-II in a long tube. The apparatus allowed the pressure difference and the temperature difference across the flow tube to each be independently adjusted, and the resulting steady-state values of net fluid velocity and axial heat transport to be measured. For the larger Reynolds numbers, it was found that the relation between pressure difference and net fluid velocity was nearly indistinguishable from that of an ordinary fluid in turbulent flow. The axial heat transported was found to be suppressed from the values that were calculated by assuming that "mutual friction" was unchanged by the net fluid flow, but it was always found to be larger than the "enthalpy rise" value. Taking this second value as a lower limit, it is shown that a mild extrapolation of these results suggests that (in appropriate circumstances) forced convection would allow much greater heat to be transported in long cooling channels than could be transported by "natural" convection alone.			
17. KEY WORDS (six to twelve entries; alphabetical order; capitalize only the first letter of the first key word unless a proper name; separated by semicolons) Axial heat transport; forced convection; helium II; measurements; 1.4 - 2.1 K; pressure drop.			
18. AVAILABILITY <input checked="" type="checkbox"/> Unlimited <input type="checkbox"/> For Official Distribution. Do Not Release to NTIS		19. SECURITY CLASS (THIS REPORT) UNCLASSIFIED	21. NO. OF PAGES 84
<input checked="" type="checkbox"/> Order From Sup. of Doc., U.S. Government Printing Office Washington, D.C. 20402, SD Cat. No. C13.45:1002 <input type="checkbox"/> Order From National Technical Information Service (NTIS) Springfield, Virginia 22151		20. SECURITY CLASS (THIS PAGE) UNCLASSIFIED	22. Price \$2.40

NBS TECHNICAL PUBLICATIONS

PERIODICALS

JOURNAL OF RESEARCH—The Journal of Research of the National Bureau of Standards reports NBS research and development in those disciplines of the physical and engineering sciences in which the Bureau is active. These include physics, chemistry, engineering, mathematics, and computer sciences. Papers cover a broad range of subjects, with major emphasis on measurement methodology, and the basic technology underlying standardization. Also included from time to time are survey articles on topics closely related to the Bureau's technical and scientific programs. As a special service to subscribers each issue contains complete citations to all recent NBS publications in NBS and non-NBS media. Issued six times a year. Annual subscription: domestic \$17.00; foreign \$21.25. Single copy, \$3.00 domestic; \$3.75 foreign.

Note: The Journal was formerly published in two sections: Section A "Physics and Chemistry" and Section B "Mathematical Sciences."

DIMENSIONS/NBS

This monthly magazine is published to inform scientists, engineers, businessmen, industry, teachers, students, and consumers of the latest advances in science and technology, with primary emphasis on the work at NBS. The magazine highlights and reviews such issues as energy research, fire protection, building technology, metric conversion, pollution abatement, health and safety, and consumer product performance. In addition, it reports the results of Bureau programs in measurement standards and techniques, properties of matter and materials, engineering standards and services, instrumentation, and automatic data processing.

Annual subscription: Domestic, \$12.50; Foreign \$15.65.

NONPERIODICALS

Monographs—Major contributions to the technical literature on various subjects related to the Bureau's scientific and technical activities.

Handbooks—Recommended codes of engineering and industrial practice (including safety codes) developed in cooperation with interested industries, professional organizations, and regulatory bodies.

Special Publications—Include proceedings of conferences sponsored by NBS, NBS annual reports, and other special publications appropriate to this grouping such as wall charts, pocket cards, and bibliographies.

Applied Mathematics Series—Mathematical tables, manuals, and studies of special interest to physicists, engineers, chemists, biologists, mathematicians, computer programmers, and others engaged in scientific and technical work.

National Standard Reference Data Series—Provides quantitative data on the physical and chemical properties of materials, compiled from the world's literature and critically evaluated. Developed under a world-wide program coordinated by NBS. Program under authority of National Standard Data Act (Public Law 90-396).

NOTE: At present the principal publication outlet for these data is the Journal of Physical and Chemical Reference Data (IPCRD) published quarterly for NBS by the American Chemical Society (ACS) and the American Institute of Physics (AIP). Subscriptions, reprints, and supplements available from ACS, 1155 Sixteenth St. N.W., Wash., D.C. 20056.

Building Science Series—Disseminates technical information developed at the Bureau on building materials, components, systems, and whole structures. The series presents research results, test methods, and performance criteria related to the structural and environmental functions and the durability and safety characteristics of building elements and systems.

Technical Notes—Studies or reports which are complete in themselves but restrictive in their treatment of a subject. Analogous to monographs but not so comprehensive in scope or definitive in treatment of the subject area. Often serve as a vehicle for final reports of work performed at NBS under the sponsorship of other government agencies.

Voluntary Product Standards—Developed under procedures published by the Department of Commerce in Part 10, Title 15, of the Code of Federal Regulations. The purpose of the standards is to establish nationally recognized requirements for products and to provide all concerned interests with a basis for common understanding of the characteristics of the products. NBS administers this program as a supplement to the activities of the private sector standardizing organizations.

Consumer Information Series—Practical information, based on NBS research and experience, covering areas of interest to the consumer. Easily understandable language and illustrations provide useful background knowledge for shopping in today's technological marketplace.

Order above NBS publications from: Superintendent of Documents, Government Printing Office, Washington, D.C. 20402.

Order following NBS publications—NBSIR's and FIPS from the National Technical Information Services, Springfield, Va. 22161.

Federal Information Processing Standards Publications (FIPS PUB)—Publications in this series collectively constitute the Federal Information Processing Standards Register. Register serves as the official source of information in the Federal Government regarding standards issued by NBS pursuant to the Federal Property and Administrative Services Act of 1949 as amended, Public Law 89-306 (79 Stat. 1127), and as implemented by Executive Order 11717 (38 FR 12315, dated May 11, 1973) and Part 6 of Title 15 CFR (Code of Federal Regulations).

NBS Interagency Reports (NBSIR)—A special series of interim or final reports on work performed by NBS for outside sponsors (both government and non-government). In general, initial distribution is handled by the sponsor; public distribution is by the National Technical Information Services (Springfield, Va. 22161) in paper copy or microfiche form.

BIBLIOGRAPHIC SUBSCRIPTION SERVICES

The following current-awareness and literature-survey bibliographies are issued periodically by the Bureau:

Cryogenic Data Center Current Awareness Service. A literature survey issued biweekly. Annual subscription: Domestic, \$25.00; Foreign, \$30.00.

Liquefied Natural Gas. A literature survey issued quarterly. Annual subscription: \$20.00.

Superconducting Devices and Materials. A literature survey issued quarterly. Annual subscription: \$30.00. Send subscription orders and remittances for the preceding bibliographic services to National Bureau of Standards, Cryogenic Data Center (275.02) Boulder, Colorado 80302.